SYMPOSIUM ON DIFFUSION IN OCEANS AND FRESH WATERS

AUGUST 31—SEPTEMBER 2, 1964

SYMPOSIUM ON DIFFUSION IN OCEANS AND FRESH WATERS

at

Lamont Hall

Lamont Geological Observatory of Columbia University

Palisades, New York

on

August 31 through September 2, 1964

Editor: Takashi Ichiye

Published by Lamont Geological Observatory of Columbia University Palisades, New York under sponsorship of the U. S. Atomic Energy Commission and the Office of Naval Research.

December, 1965

Preface

Oceanographers have long been aware of the importance of mixing processes on different scales in different parts of the ocean. In natural water bodies, mixing processes are augmented manifoldly by stirring of the water by irregular motion or turbulence. Therefore, in oceanography the concept of eddy diffusion has been adopted since the turn of the century and widely used to explain distributions of temperature, salinity, dissolved oxygen and chemical components in the ocean. However, it was during the late forties that oceanographers started to utilize artificial tracers, including turnips, mimeograph papers, organic dye and isotope, in order to do controlled experiments on diffusion in the sea. This sudden flourish in diffusion experiments in oceanography was stimulated partly from a practical reason, that is, by the necessity for determining diffusion behaviors of water contaminated by atomic bomb tests and partly from an academic reason - the development in statistical theory of turbulence.

Initially, eddy diffusion in a medium, like ocean and atmosphere, was treated by the Fickian equation which is based on the similarity to the molecular diffusion. However, in order to explain diffusion of various quantities in a field of different scales of time and space, the diffusion coefficient or diffusivity in this equation must be taken as not only dependent on time and space but also variable in magnitude by almost ten orders. This rather embarrassing state was partially relieved by Richardson's introduction of neighboring diffusivity in 1926 which replaces the eddy diffusivity in the Fickian equation. This concept gave a heuristic explanation on dependence of diffusivity on a scale of phenomenon. In the early forties, Kolmogoroff introduced a hypothesis of statistical equilibrium of the small-scale components of the turbulence. His work was the starting point for subsequent research on statistical theories of isotropic turbulence in the late forties, which gave a deductive explanation on the scale effect of eddy or neighboring diffusivity. This development in theory stimulated the diffusion experiments in the ocean in the late forties, as mentioned above.

During the fifties there was an apparent pause in activity in field experiments of diffusion in the ocean, except for research on large-scale mixing by measuring radioactivity in the ocean from fission products, mostly by Japanese oceanographers, and from natural radioisotopes by groups of geochemists of the Lamont Geological Observatory and Scripps Institution of Oceanography. In the late fifties, Pritchard and his co-workers at the Johns Hopkins University developed a tracer technique using harmless organic dye which can be traced with a shipborne fluorometer with concentration sensitivity comparable to the radioactive tracer. A group at Lamont Observatory has fully utilized this technique in various parts of the ocean other than estuaries for which the technique was originally developed, and it is now in the process of modifying the technique for use in the deep ocean. More recently, a national program for conservation of natural resources stimulated studies of pollution of the seas and fresh waters around the country and the dye technique has been extensively utilized in various areas by different organizations. The main purposes of the present symposium were to exchange information on field techniques for measuring diffusion in natural water bodies, to discuss the interpretation of the data, to develop mathematical models of diffusion in oceans, lakes and rivers, and to coordinate and promote further studies undertaken in various institutions.

The first announcement of a proposal to have a symposium was distributed to potential participants on May 6, 1964 and was warmly received by a number of workers in oceanography, hydraulic engineering, meteorology and related fields. On May 17th, two and one-half day sessions were tentatively scheduled from August 26 to 28, which was later postponed from August 31 to September 2, owing to conflicts with other meetings. The sessions were held at Lamont Hall of the Observatory and were attended by fifty-seven participants from thirty organizations. Besides regular sessions during the day, a dinner party was held on the evening of September 1st, where a pre-dinner talk by Dr. Pochapsky was a great joy to all attendants. There was an exhibition of instruments produced by Braincon Corporation, Geodyne Corporation, G. K. Turner Associates, and Industrial Instruments, Inc.

The discussions were very active not only during the sessions but also during the inter and after sessions.

Outlines of major papers presented at the symposium have been reported by G. B. Dowling and F. C. W. Olson (Science, 146, 3650 p. 1492-1493, December 1964). Since some authors could not send in complete manuscripts, abstracts of these papers - based on notes taken by Dowling during the symposium - are included. Discussions of each paper presented at the proceedings are based on his notes. The convener is greatly indebted to Mr. Dowling for permission to use his notes.

All contributors and participants to the meeting are thanked for their enthusiastic cooperation. I am also greatly indebted to Mrs. J. Stolz who typed all manuscripts for offset printing. The publication of the proceedings is supported by the Atomic Energy Commission under Contract AT (30-1) 2663 and by the Office of Naval Research under Contract Nonr 266 (48).

Lamont Geological Observatory
of Columbia University
Palisades, New York

Takashi Ichiye

TABLE OF CONTENTS

		Page
Preface	T. Ichiye	i
Program of Symposium		v
Contributions and Discussions		
Potomac River Time of Travel Measurements	J. F. Wilson, Jr. W. E. Forrest	1
Near-Surface Oceanic Diffusion from a Continuous Point Source	R. Reinert	19
Dye Studies in the Ohio River	C. C. Kisiel	28
Limitations of Rhodamine B and Pontacyl Brilliant Pink B as Tracers in Estuary Waters (Abstract)........................	C. G. Gunnerson C. A. McCullough	53
Diffusion Experiments in Coastal Waters Using Dye Techniques....................	T. Ichiye	54
On Dye Experiments in Bahama Banks (Summary)	J. Michael Costin	68
Multi-Dimensional Aspects of Eddy Diffusion Determined by Dye Diffusion Experiments in Coastal Waters......................	J. E. Foxworthy R. B. Tibby G. Barson	71
A Theoretical Model of Diffusion of Dye Patches (Summary)....................	A. Okubo	74
The Solution of the Continuity Equation in Cylindrical Co-ordinates with Dispersion and Advection for an Instantaneous Release	D. J. O'Connor D. M. Di Toro	80
On the Use of the Rayleigh-Ritz Method for Calculating the Eddy Diffusivity............	D. Kirwan	86
Preliminary Studies of Momentum Flux in Ocean Waves	D. H. Shonting	93

TABLE OF CONTENTS (continued)

		Page
Diffusion Process vs. Oceanic Microstructure.	M. D. Wennekens	108
Diffusion Particles in the Deep Ocean	T. E. Pochapsky	114
The Application of Natural Radon to Problems in Ocean Circulation	W. S. Broecker	116
Summaries of Some Papers Prepared from Notes by G. B. Dowling:		
On Dye Diffusion Techniques Used in Chesapeake Bay Institute	D. W. Pritchard	146
The "Navi-Therm" - a New Device Measuring Sub-Surface Temperature Underway.......	E. C. Brainard, III	148
Ocean Wave Boundary Layers...............	C. E. Grosch S. J. Lucasik	149
Atmospheric Diffusion	H. E. Cramer	151
Turbulent Diffusion in Sodium Vapor Trails in the Upper Atmosphere.................	O. R. Coté	153
Correspondence and Addenda		154
List of Participants		160
Index of Authors		162
Subject Index		163

PROGRAM

of

SYMPOSIUM ON DIFFUSION IN OCEANS AND FRESH WATERS

Place: Lamont Hall, Lamont Geological Observatory, Palisades, N.Y.

Schedule:

August 31, 1964 at 9:30 A.M.

Opening speech by Dr. C. L. Drake of Lamont Observatory

"Potomac River Time of Travel Studies," by J. F. Wilson, Jr. and W. E. Forest of the U. S. Geological Survey Water Resources Division

"Surface Diffusion from a Continuous Point Source," by R. Reinert of the Department of Oceanography, New York University.

"Diffusion Experiments in Coastal Waters Using Dye Techniques," by Dr. T. Ichiye of Lamont Observatory.

"Limitations of Rhodamine B Dye as Estuarine Tracer", by C. G. Gunnerson, Public Health Service, Division of Water Supply and Pollution Control, Cincinnati, Ohio

"Three-and-Two-Dimension Aspects of Eddy Diffusion Determined by Dye Diffusion Experiments in Coastal Waters," by Dr. J. E. Foxworthy of the Allan Hancock Foundation, University of Southern California

Afternoon - 1:30 P. M.

"The Navi-Therm - A New Device Measuring Sub-Surface Temperature Underway," by E. C. Brainard, III of Braincon Corp.

"Diffusing Particles in the Deep Ocean," by Dr. T. E. Pochapsky of Hudson Laboratories.

Reports and Discussions on Techniques of Measuring Diffusion:

Moderator: C. G. Gunnerson

Reporters: Prof. C. C. Kisiel, Department of Civil Engineering, University of Pittsburgh "On Dye Experiments on Ohio River"

Dr. D. Pritchard, Department of Oceanography, Johns Hopkins University "On Dye Diffusion Techniques Used in Chesapeake Bay Institute"

J. Michael Costin, Lamont Geological Observatory, "On Dye Experiments in Various Parts of the Ocean"

September 1st - 9:30 A.M.

Discussion on "Theoretical Models of Diffusion of Dye Patches," by Dr. A. Okubo, Department of Oceanography, Johns Hopkins University.

"Variational Principle for Mixing Processes," by D. Kirwan, Department of Oceanography, New York University.

"Dispersion of Pollutant in the Estuary," by Dr. D. O'Connor, Civil Engineering Department, Manhattan College.

"Observations of Momentum Flux in Ocean Waves," D. H. Shonting, U. S. Navy Underwater Ordnance Station, Newport, R. I.

Afternoon - 1:30 P.M.

Special Lecture - "Atmospheric Diffusion," by Dr. H. E. Cramer Round Hill Field Station, Department of Meteorology, Massachusetts Institute of Technology.

Discussions on "Analysis of Diffusion Data," and "Theoretical Models of Diffusion".

Moderator: Dr. F.C. W. Olson, U. S. Navy Mine Defense Laboratory, Panama City, Florida.

Reporters: Dr. M. Pat Wennekens, San Francisco Branch of the Office of Naval Research, on "Influences of Ocean Microstructure on Ocean Pollutant Diffusion"

Dr. R. B. Tibby and Dr. J. E. Foxworthy, Allan Hancock Foundation, University of Southern California on "Diffusion Process in Ocean Coastal Waters"

Dr. O. R. Coté, Geophysics Corporation of America, on "Turbulent Diffusion of Sodium Vapor Trails in the Upper Atmosphere"

During the day, guided tours of Lamont Geological Observatory

In the evening from about 6:00 P.M. dinner at the '76 House, Tappan, New York.

Pre-dinner speech by Dr. T. E. Pochapsky of Hudson Laboratories on "Oceanographers in Moving Ocean".

September 2nd - 9:30 A. M.

Special Lectures: Dr. M. Ewing of the Lamont Geological Observatory - Welcoming speech.

Dr. W. Broecker of the Lamont Geological Observatory - "Large-scale Oceanic Diffusion Determined by Radiochemical Methods"

Dr. S. Lukasik, Stevens Institute of Technology, on "Ocean Wave Boundary Layers".

POTOMAC RIVER TIME-OF-TRAVEL MEASUREMENTS

James F. Wilson, Jr. and William E. Forrest
Engineers, U.S. Geological Survey, Water Resources Division
Washington, D.C. and College Park, Md.

Introduction

The principal objective of time-of-travel measurements is to be able to predict accurately the downstream movement of dissolved or suspended material. To many users of water from streams, travel time and dispersion information are equally important. Since time-of-travel and dispersion studies complement each other, they may be combined through the use of tracers.

The U. S. Geological Survey has been studying turbulent dispersion in streams for several years. (Godfrey and Frederick, 1963; Glover, 1964). Most tracers, such as radioisotopes, used in small-scale studies are not suitable for large-scale use in time-of-travel measurements.

Lacking a suitable tracer, hydrologists in the past computed time of travel from estimated average velocities. Average velocities in a given reach were obtained either by dividing the discharge by the average cross-sectional area, as done by Steacy (1961), or by averaging the velocities from current meter measurements, as done by Searcy and Davis (1961).

It is difficult to determine dispersion information from travel times computed from estimated average velocities. It is also nearly impossible to determine the representativeness of the data used even when special effort has been made to collect representative data. Therefore, computed travel times may or may not be "better than nothing".

Pritchard and Carpenter (1960) introduced Rhodamine B dye and a highly sensitive fluorometer to hydrologic tracing. Wright and Collings (1964) have discussed some of the applications to hydrologic studies - dispersion studies, rate-of-flow (discharge) measurements, and time-of-travel measurements. Using tracers, hydrologists can overcome both of the disadvantages of computed time of travel. The travel time of the tracer is actually measured; the observed dispersion patterns reflect the effects of natural and man-made variations in channel geometry (to the extent the dye sampling plan is properly designed to do this).

The U. S. Geological Survey, as a part of its program of collection and interpretation of hydrologic data, has made time-of-travel measurements with fluorescent dyes in seventeen states. Measurements are being planned in several other states. Many local, state, and federal agencies involved with the problems of managing our nation's streams have clearly indicated the need for these measurements by their enthusiastic support.

The principal applications of time-of-travel information are in downstream warning and planning in the event of accidental spills of harmful contaminants, and in the determination of a stream's capacity to assimilate wastes.

Buchanan (1964) has described the Survey's activities in the field of time of travel. Such field studies of dispersion tend to be empirical in nature and are not directly connected with the more scientific studies of dispersion carried out by research elements of the Survey.

To illustrate the preparations, field operations, and results of a time-of-travel measurement, the remainder of this paper will be used to describe the recent study of the Potomac River.

The Potomac River Basin (see Figure 1) has a drainage area of about 14,500 square miles above the mouth at Chesapeake Bay. Included in the basin are parts of West Virginia, Virginia, Pennsylvania, Maryland, and the District of Columbia. The river is tide-affected about 100 miles upstream, to a point between Key Bridge and Chain Bridge in Washington. Drainage area above that point is about 11,600 square miles.

Because of its relationship to the Nation's capital, the Potomac has been the subject of many studies: water supply potential, flood control, pollution abatement, and recreation potential. The river is the source of water for many communities and industries along its banks. It is also used for waste disposal and is subject to occasional accidental spill of harmful chemicals. Potomac water users are well aware of the usefulness of time-of-travel information.

Searcy and Davis (1961) computed the time of travel of Potomac water from discharge measurements. Travel times for a wide range of discharge were computed and referenced to the discharge at the gage above Chain Bridge. The continuous-stage recorder there may be dialed by telephone to obtain the river stage. Time of travel from any upstream location may then be interpolated from a set of curves. It had long been suspected that the computed times did not adequately reflect the effects of the several low dams in the reach, at least not at medium and low flows.

On April 17, 1964, a freight train was derailed at Orleans Crossroads,

W. Va., about 128 miles above the Washington water intake at Great Falls (between sites 2 and 3 in Figure 1). Several carloads of oil spilled down the banks and into the North Branch of the Potomac. A carload of caustic soda, believed to have spilled, later was recovered intact.

At the request of the Washington Aqueduct Division, Corps of Engineers, the agency responsible for Washington's Great Falls intakes, Geological Survey personnel estimated the arrival time of the contaminants at the Washington intakes. Based on the existing computations, the predicted travel time was 74 hours. As the oil was tracked visually, it soon became apparent that it was traveling much more slowly than had been predicted. The oil was observed in Williamsport, only 43 miles below the accident site, at about the same time it was supposed to have reached Washington, 85 miles farther downstream.

The need for more accurate travel time information was apparent, and support for a measurement with dyes was readily available. In addition to being directly beneficial to Potomac water users, the study would verify the feasibility of using fluorescent dyes to study long reaches of large rivers.

Preparations

The reach selected was that between Cumberland, Md., and Washington, D. C., the same reach studied by Searcy and Davis. This reach is the shaded portion shown in Fig. 1.

The discharge at the time of injection of the dye was expected to be about 10,000 cubic feet per second (cfs) at Washington. Such a discharge would be close to the long-term median flow and would provide a good basis for extending the results to higher or lower discharges. However, due to an unusually rapid recession of the spring run-off, the flow had dropped to about 5,500 cfs by the day of injection. This flow is equaled or exceeded about 60% of the time.

To complete the field work in a reasonable time interval, to obtain results comparable to a steady rate of flow, and to minimize dye concentrations at principal towns, six injection sites were selected. Survey-operated gaging stations at all but the Williamsport site enabled the injections to be referenced accurately to stream discharge. Gages are also operated on all of the major tributaries and many of the minor ones, providing good definition of inflow.

The six sub-reaches varied in length from 27 to 44 miles. It was planned to track each of the six doses at least as far as the next downstream injection site, and preferably to the second downstream injection site.

Intermediate sampling sites were first selected by map reconnaissance, then accepted or rejected on a field reconnaissance. These sites, at least one per sub-reach, were selected mainly to identify significant changes in velocity and to monitor longitudinal dispersion. A total of 23 sampling sites were used during the study. At several sites accessibility was a problem.

Because the river would be visibly colored for some time after injection of the dye, public relations received a good deal of attention. All state and county health agencies bordering the river, as well as other interested local, state, and federal agencies, were notified. The Interstate Commission on the Potomac River Basin, the Maryland State Health Dept., and the Maryland Geological Survey specifically endorsed the project. No objections were raised by any agency contacted. Considerable advanced press, radio and television coverage was used to inform the general public. Again, no objections were raised.

About 35 people, representing Geological Survey offices in eight states, participated. Many were experienced in fluorescent tracing. Sampling parties were stationed at three pre-selected motels, each responsible for a reach of the river. Additional on-call sampling help was organized among personnel living in the Washington area. Needless to say, coordination and control were difficult. Motel phones provided a minimal communication network, which was supplemented by frequent automobile tours by the project leaders.

A total of five Turner Model 111 fluorometers were used. The fluorometers were equipped with high sensitivity kits mounted on standard doors, and with primary and secondary filters having peak color specifications of 546 and 590 millimicrons, respectively.

The tracer used was Dupont's Rhodamine BA Solution, 30% Rhodamine B by weight in a mixture of water and acetic acid. The specific gravity of this solution is 1.03; nothing was added before injection. In other studies the Survey has used Rhodamine B (40%), Pontacyl Brilliant Pink B, and the newly-developed Rhodamine WT (20%).

Computation of the amount of dye to be injected was based on the volume of water in each reach, estimated by multiplying the discharge by the length of reach and dividing by the estimated average velocity. Enough dye was applied to the computed volumes to provide an average of three parts per billion in the reach. The objective was to insure peak concentrations well below the minimum visible level at the end of each sub-reach, and yet obtain good definition of the time-concentration curves. While this rule-of-thumb doesn't allow for variations in velocity or variations in channel geometry, it

has proven quite accurate (with some Kentucky windage applied at times).

The dye computations were based on 10,000 cfs at Washington, and corresponding discharges at the six injection sites. A total of 185 gallons of 30 per cent solution (containing about 480 pounds of raw dye) was obtained. By the day of injection the discharge at Washington had fallen to 5,500 cfs but the entire amount of dye was used in order to assure the desired overlapping coverage. Concentrations were only slightly higher than originally planned because the lower velocities contributed to increased longitudinal dispersion within a given reach of river.

Field Operations

Two independent dosing parties made three injections each, beginning around noon on May 25th. Within four hours all of the dye was in the river. The clear, cool weather was a definite asset. Rainfall, if heavy, can greatly reduce the usefulness of time-of-travel results. Fortunately, no rain fell during the Potomac measurement.

The dye was poured from highway bridges at Point of Rocks, Williamsport, Hancock, Paw Paw, Cumberland, and from a boat below the municipal water intake at Shepherdstown. By far the largest injection was 650 lbs. of solution (about 75 gallons) at Point of Rocks, 44 miles above Washington. This was the head of the longest-sub-reach and, of course, carried the greatest discharge. At most sites the dye was poured at two or more points across the stream to reduce the length of reach required for lateral mixing.

Generally, a grab sampling technique was used at a single point in the cross section. Samples were taken from railroad and highway bridges, from boats in mid-stream, and from dam abutments. Four-ounce plastic bottles were used to retain the samples for testing. Samples at the first sites below injections were taken at intervals of 10 to 15 minutes; as the dye clouds traveled downstream the interval was lengthened accordingly. Several daus after injection of the dye, intervals of four or more hours were adequate to define the time-concentration curves. Around-the-clock sampling was necessary to get the required information as the dye cloud passed sites of interest.

The five fluorometers were strategically located to test samples initially, as a guide to sampling. Samples were retained for re-testing later in the laboratory under more standardized conditions. A continuous flow setup was established at Whites Ferry, the first sampling site below Point of Rocks. However, for time-of-travel studies, grab sampling is generally preferred over continuous-flow sampling because samples from several sites can be tested on one instrument.

Two fluorometers were taken to remote sampling sites and operated from battery converters, but with only five fluorometers it was usually more practical to take the samples to motels for testing.

As longitudinal dispersion increased, some sampling parties found they were sampling the same dye cloud at two sites, miles apart. After the first day, a man could leave the motel, collect samples at several sites, and return to the motel to test the samples within the required sampling interval.

When the field work was completed, all samples were re-tested in the office on one fluorometer equipped with a temperature-stabilizing door. Dial readings were converted to concentration. With standards and samples all at room temperature, the effect of temperature on fluorescence can be accounted for quite accurately. It is felt that this re-testing procedure gives the most consistent results.

Results

Table 1 contains a condensed summary of the results taken from the time-concentration curves. These curves are illustrated by the set for the Cumberland dose, shown in Figure 2 (See Figure 2). Curves for the other five doses are not as smooth as those for the Cumberland dose. The decrease in the areas under the curves for Paw Paw and Hancock is indicative of the dilution effects of the two principal tributaries, South Branch Potomac and Cacapon Rivers. The concentration shown in Figure 2 are not necessarily absolute, but this should not affect the relative shapes of the curves.

The time concentration curves represent one-dimensional (longitudinal) dispersion. Vertical mixing occurs shortly after injection; lateral mixing was assumed to be essentially complete at the first sampling sites. With mid-stream injections and sampling, concentrations above the site of complete mixing would not be representative of the entire cross-section, but travel times should not be significantly different. Also, loss of dye, which is usually considerable in time-of-travel measurements, should not affect the travel times.

The curves in Figure 2 show a typical positive skewness. Godfrey and Frederick (1963, p. 23-9) have shown that these curves may be fitted to the Pearson Type III statistical distribution except near the base, where the observed tails are usually longer than expected. This provides a method for estimating the standard deviation used in computing dispersion coefficients,

Table 1.--Condensed Summary of Results

Sub-Reach	Length (Miles)	Discharge at Dose Site (cfs)	Amount of Dye Injected (Pounds)	Lead Travel Time (Hours)	Peak Travel Time (Hours)	Approx. Peak Conc. (ppb)*	Approx. Passage Time (Hours)*
Cumberland to Paw Paw	28.1	400	30	43	50.3	12	30
Paw Paw to Hancock	37.9	1,010	45	45	48.6	17	40
Hancock to Williamsport	27.8	1,380	45	68.5	77.4	5.5	60
Williamsport to Shepherdstown	27.2	1,900	90	54	63.8	7.5	80
Shepherdstown to Point of Rocks	24.1	2,200	60	44.5	49.0	9	30
Point of Rocks to Washington (Chain Bridge)	43.6	4,540	195	64	69.8	12	40
Totals	188.7		465		359		

*At lower end of sub-reach.

given by

$$K = \sigma_x^2 \, (2\bar{t})^{-1}$$

and

$$\sigma_x = \bar{V} \sigma_t$$

where K is the longitudinal dispersion coefficient, in square feet per second,

σ_x is the standard deviation of the longitudinal spread, in feet,

$\bar{t}$ is the time of travel of the centroid of the dye cloud, in seconds,

$\bar{V}$ is the mean effective velocity in the reach, in ft. per sec.,

and σ_t is the standard deviation of the longitudinal spread, in seconds.

Longitudinal dispersion coefficients computed by the above method increased downstream from about 200 sq. ft. per sec. at North Branch to about 800 sq. ft. per sec. at Hancock, for the Cumberland dose. The discharge was about 400 cfs at North Branch at the time the dye cloud passed, and about 1,300 cfs when the dye reached Hancock.

At many sampling sites the concentration curves were affected by variations in channel conditions, most notably the six low dams. The backwater tended to truncate the peaks and make them uneven, and it also lengthened the tails of the curves considerably.

Other conditions which had to be recognized included bends and large tributaries. Sampling near bends was generally avoided because of the time lag for the dye on the inside of the bends. With samples taken at more than one point across the stream, incomplete lateral mixing of the Shenandoah River with the Potomac was noticeable for many miles below the confluence.

Travel times selected from the curves in Figure 2 are presented as a function of distance in Figure 3. (See Figure 3) This type of plot, for a range of discharge, might be useful to a water plant operator. The cut-off points for the trailing edges are, of course, arbitrary.

The peak concentrations of the Cumberland dose are plotted against time in Figure 4. Again there is evidence of the diluting effects of the South Branch Potomac and Cacapon Rivers. (See Figure 4)

Figure 5 shows the time required for each of the three downstream doses to pass Chain Bridge. (See Figure 5) The longitudinal spread and the flattening of the peaks illustrates the important additional information obtained from a tracer study, compared with computed travel times. Depending on the contaminant and amount injected, the cause for alarm after an accidental spill may not be as great if the dispersal capability of the river is known. A rough projection of the Cumberland dose to Chain Bridge indicates it would have taken about seven days to pass, and would have had a peak of about 0.2 ppb, or about 0.3 per cent of the peak at North Branch.

The upper line in Figure 6 shows the composite travel time from Cumberland to Washington for the six slugs of dye. (See Figure 6) The abrupt changes in the slope of this line show the effects of the several low dams in the reach. A similar effect is evident for the tide-affected portion between Chain Bridge and Key Bridge. The dashed line is an estimate of the travel time without the dams.

The lower curve in Figure 6 gives the travel time computed by the method of Searcy and Davis (1961), for the discharge observed at the time of injection. Note that the comparison of this line with the dashed line is reasonably close.

Velocities computed from travel times of the peak concentrations ranged from about 0.2 to 0.9 miles per hour. The velocities at the 19 principal sampling points are listed in Table 2. The figures are for the first slug to pass each site; peaks for the second slug traveled about twenty per cent slower, due to the recession in discharge. The cumulative travel time of the peaks was 15.6 days from Cumberland to Key Bridge in Washington.

The centroids of the concentration curves, more closely representative of the average travel time, traveled about two to ten per cent slower than the peaks. The leading edges of the dye clouds traveled about eight to sixteen per cent faster than the peak concentrations.

Although the discharge receded continuously during the study, correlations of the discharge records of the six gaging stations in the reach, made by Searcy and Davis (1961, p. 3-4), showed the equivalent discharge at Washington to be about the same for each of the injection sites. Thus, by using six simultaneous injections, near steady-flow results were obtained.

To be of interpolative value, time of travel information must be referenced to stream stage or discharge. The U. S. Geological Survey is well equipped to do this, operating about 7,700 continuously recording stream gaging stations and some 10,000 partial records stations (flood and/or low-flow) in the United States. On the Potomac River, the gage at Chain Bridge

Table 2.--Velocities of Peak Concentrations.

Site	Distance (Miles)		Travel Time of Peak (Hours)		Velocity of Peak (Miles per Hour)	
* Cumberland						
	8.7		18.6		0.47	
North Branch						
	8.7	28.1	14.2	50.3	.61	0.56
Oldtown						
	10.7		17.5		.61	
* Paw Paw						
	19.8		24.8		.80	
Doe Gully		37.9		48.6		.78
	18.1		23.8		.76	
* Hancock						
	11.5		13.6		.85	
Ft. Frederick						
	9.7	27.8	50.3	77.4	.19	.36
Dam No. 5						
	6.6		13.5		.49	
* Williamsport						
	15.5		48.3		.32	
Dam No. 4		27.2		63.8		.43
	11.7		15.5		.75	
* Shepherdstown						
	10.5		32.3		.33	
Dam No. 3						
	7.3	24.1	8.0	49.0	.91	.49
Brunswick						
	6.3		8.7		.72	
* Point of Rocks						
	12.4		13.9		.89	
Whites Ferry						
	13.2		20.0		.66	
Seneca						
	7.6	46.9	17.5	85.4	.43	.55
Great Falls Dam						
	5.5		9.2		.60	
Cabin John						
	4.9		9.2		.53	
Chain Bridge						
	3.3		15.6		.21	
Key Bridge						
Totals	192		374.5 = 15.6 days		0.51	

*Dye injection site.

was selected as the reference gage. For shorter reaches, it is better to use the discharge at the head of the reach.

The results of measurements on other streams indicate the existence of a relationship between time of travel (i.e., mean velocity) and discharge, which can be defined with tracer measurements at two or more different discharges. Another measurement on the Potomac would be valuable in defining such a relationship. Two or three more measurements would be better - for example, during high spring runoff, at mean annual flow, and during late summer low flow. These discharges might be 50,000, 12, 000 and 1,500 cfs, respectively, at Chain Bridge. However, the greatest demand seems to be for low-flow information.

At the mouths of the South Branch Potomac and Shenandoah Rivers, the main stem discharge was approximately doubled by the inflow. However, no significant change in travel time occurred. This conforms to results of measurements on other streams.

Conclusion

The Potomac River study showed that the use of fluorescent dyes for time-of-travel measurements in large rivers is feasible, and that it is probably the best way to obtain the required information to a reliable degree of accuracy. With reliable time-of-travel information and some knowledge of expected dispersion patterns in a stream, those responsible for managing the stream may plan more confidently.

There is much to be learned about the effects of channel geometry and of low dams on dispersion and travel time in natural streams. With the results of many measurements, on a variety of streams, hydrologists may learn how to compute the needed information accurately, eliminating the need for tracers. In the mean time, the popularity of time-of-travel measurements made with fluorescent dyes is expected to increase.

References

Buchanan, T. J. (1964) Time of travel of soluble contaminants in streams; Am. Soc. Civil Engineers Proc., v. 90, no. SA3, Paper 3932, 12 p.

Glover, R. E. (1964) Dispersion of dissolved or suspended materials in flowing streams; U. S. Geol. Survey Prof. Paper 433-B, 32 p.

Godfrey, R. G., and B. J. Frederick (1963) Dispersion in natural streams; U.S. Geol. Survey open file report, 75 p.

Pritchard, D. W., and Carpenter, J. H. (1960) Measurements of turbulent diffusion in estuarine and inshore waters: Internat. Assoc. of Scientific Hydrology Bull., no. 20, p. 37-50

Searcy, J. K. and L. C. Davis (1961) Time of travel of water in the Potomac River, Cumberland to Washington: U. S. Geol. Survey Circ. 438, 12 p.

Steacy, R. E., (1961) Time of travel of water in the Ohio River, Pittsburgh to Cincinnati; U. S. Geol. Survey Circ. 439, 14 p.

Wright, R. R. and M. R. Collings, (1964) Fluorescent tracing techniques and applications to hydrologic studies; Am. Water Works Assoc. Jour., v. 56, no. 6, p. 748-54

Discussion after Wilson and Forest's paper

Comments: Pritchard - Rubber, tygon and copper tubings should not be used for intake of Rhodamine B dye to a Turner fluorometer. One can achieve one part per billion sentitivity in full scale with the Turner fluorometer by carefully adjusting and calibrating the instrument and thus can reduce significantly the amount of dye used in experiments.

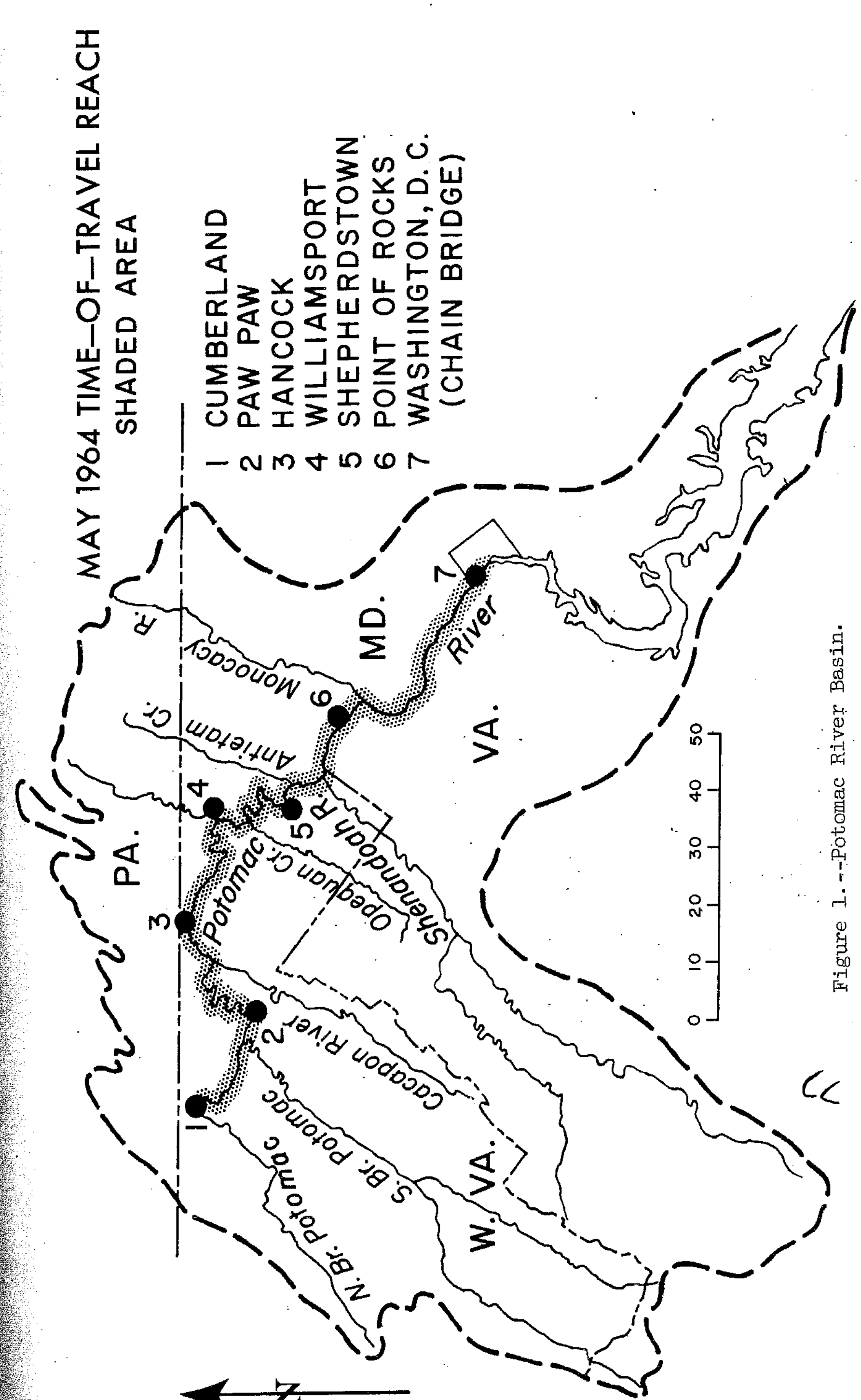

Figure 1.--Potomac River Basin.

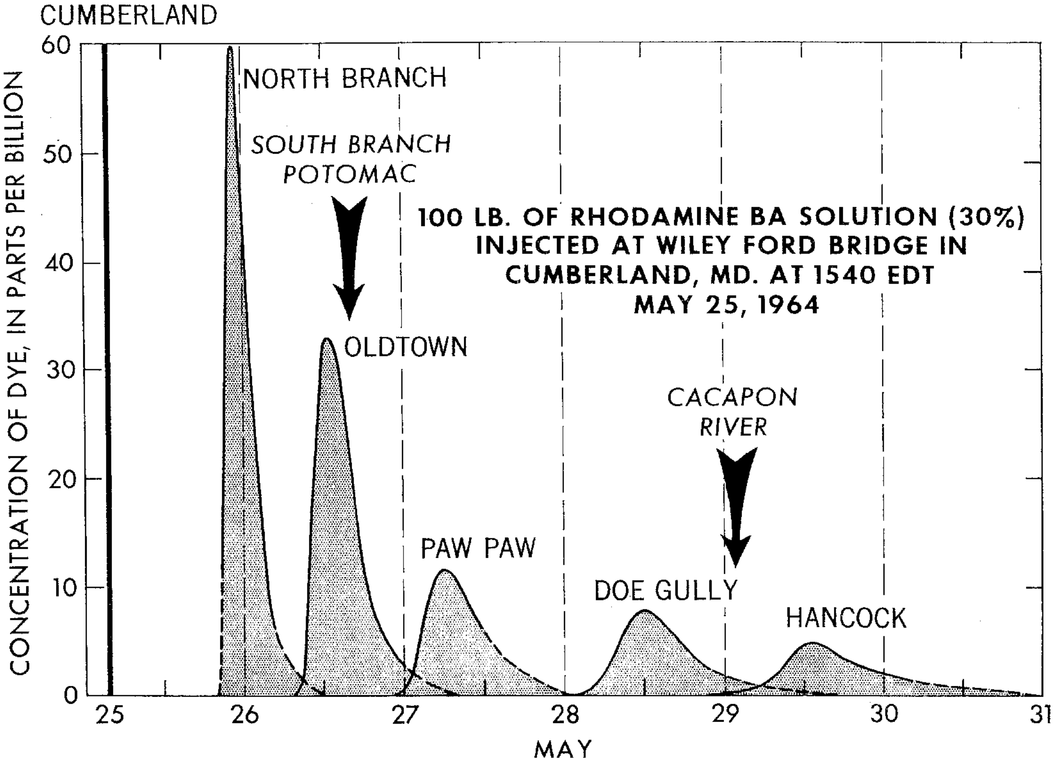

Figure 2.--Time-Concentration Curves, Cumberland Dose.

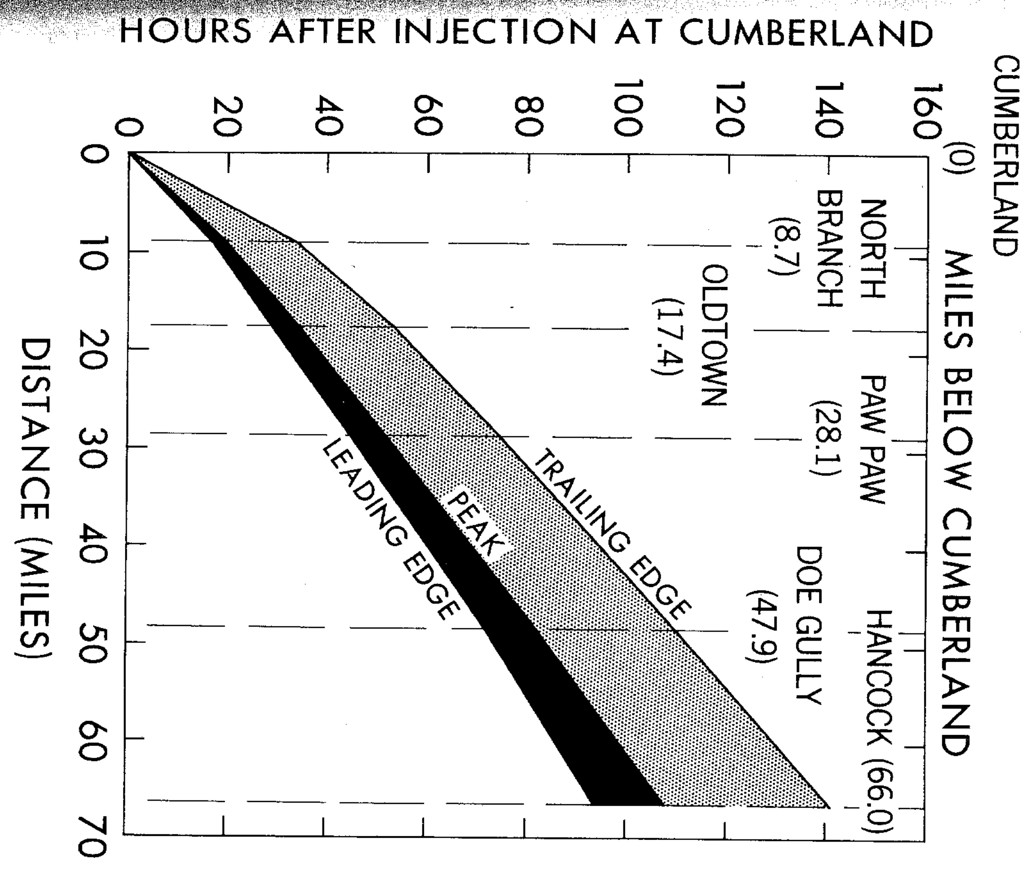

Figure 3.--Travel Times, Cumberland Dose.

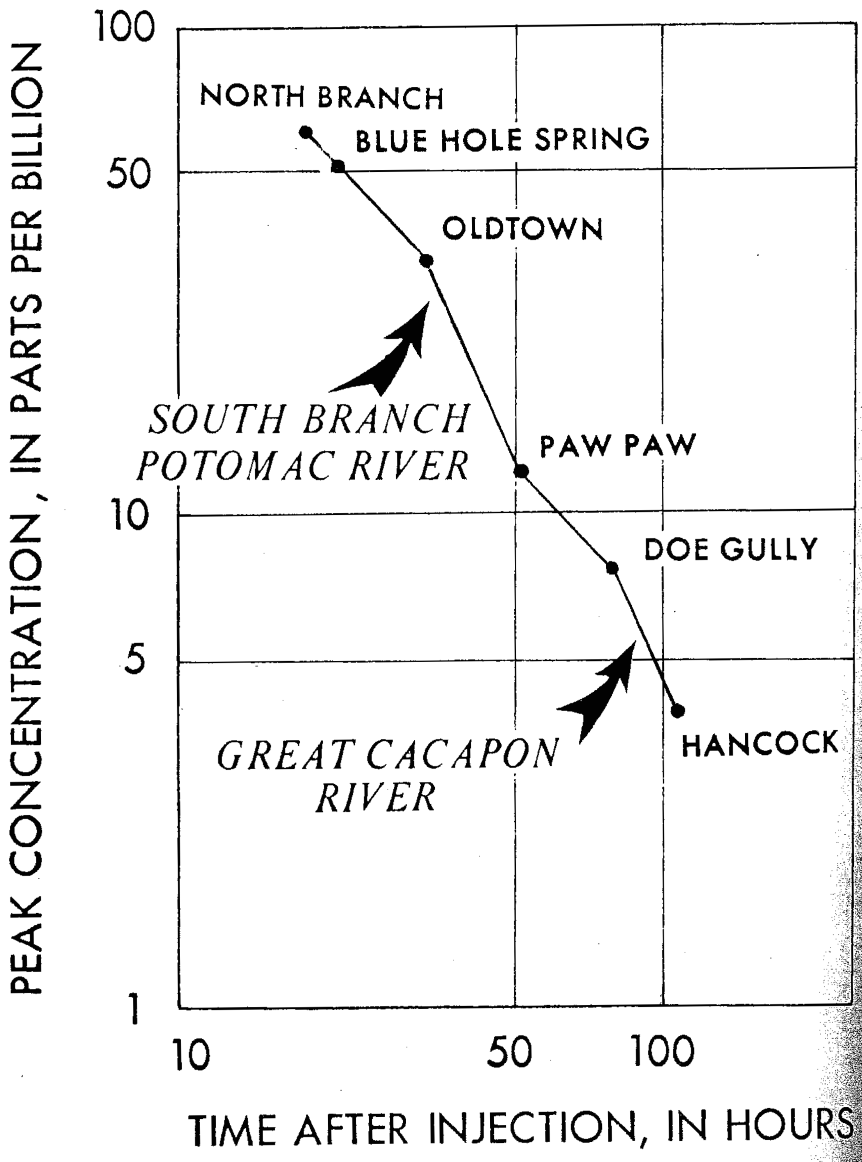

Figure 4.--Decrease in Peak Concentration with Time.

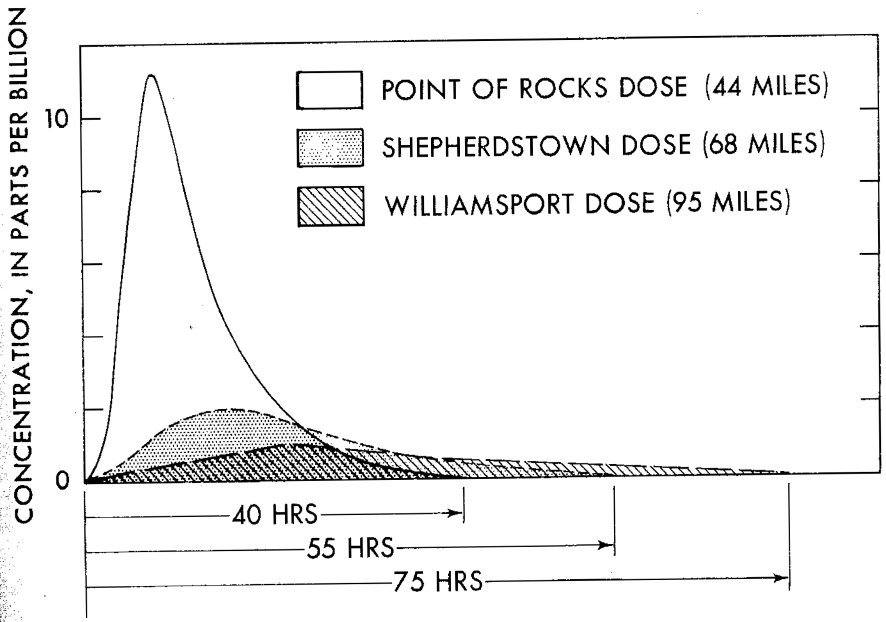

Figure 5.--Passage Time of Three Dye Clouds at Washington (Chain Bridge).

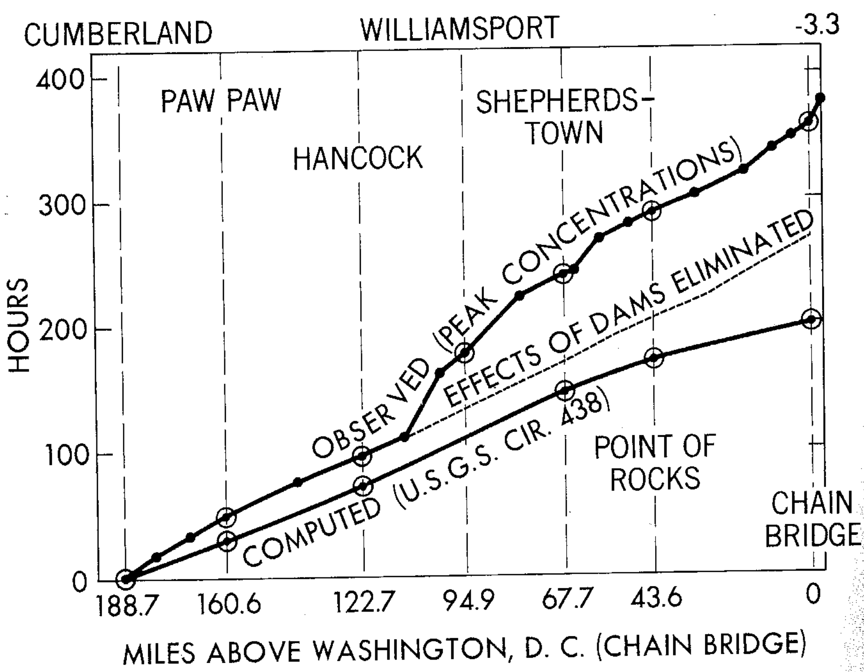

Figure 6.--Potomac Time of Travel, May 1964.

NEAR-SURFACE OCEANIC DIFFUSION FROM A CONTINUOUS POINT SOURCE*

Richard L. Reinert
Department of Meteorology and Oceanography, New York University
Bronx, New York

Abstract

Results and discussion of a dye experiment in Long Island Sound are presented. Special attention is paid to conditions that affect small scale diffusion. The experiment is performed during a time of constant tidal current and steady winds. Cross-plume concentration data and aerial photographs are included. These data show interesting patterns thought to be due to the effects of wind and waves.

Introduction

The initial interest in diffusion experiments at N Y U might best be described as micro-oceanography. Whereas previous diffusion experiments often dealt with diffusion times in terms of days, the results presented here have diffusion times ranging from thirty minutes to three hours. These data show some interesting micro-scale effects usually lost in oceanic dye diffusion experiments. This is partly due to the fact that most experiments done thus far have used instantaneous volume sources. In an experiment of this nature the dye patch is relatively large as diffusion begins, thereby masking small scale detail that would be observed if the patch had begun as a true point source. Also, in order to use the data to verify point source theory, it is customary to wait a "long" time after introduction of the dye before beginning measurements. It is during this waiting time that the effect of the high frequency component of the turbulence can be seen in the dye diffusion pattern. Any detail that might be seen in the first few hours of diffusion is eventually masked by the dominance of the low frequency component of the turbulent power spectrum, as described by Pasquill (1962).

This was one of the primary reasons for directing our efforts toward a continuous point source experiment. It is quite feasible in this case to approach the ideal point source. For instance, the hose diameter in our experiment was only one quarter of an inch.

---

* Contribution No. 32, Geophysical Sciences Laboratory of the Department of Meteorology and Oceanography, New York University.

Discussion of Experiment

The continuous point source has certain experimental advantages. Briefly they are:

1. Precise navigation. Exact navigation is made possible by the fact that the dye plume is relatively stationary so that fixed points of reference can be used. Hand buoys are placed on either side of the plume at predetermined distances from the source and runs are made between the buoys. Cross-plume distances are measured by an instrument which determines the Doppler shift of an acoustic signal reflected from the bottom. This Doppler navigator, as we call it, is permanently installed on the N Y U research vessel KYMA. One of the direct outputs of the instrument is distance traveled over the bottom.

2. Location of peak concentration. One of the necessary requirements of any dye diffusion experiment is the measurement of the peak concentration. In the instantaneous point source experiment, there is considerable uncertainty in locating the peak concentration of the patch. This is especially true in small scale experiments where gradients of dye concentration are particularly large. In the continuous point source, the uncertainty is restricted to the vertical. It is found that the maximum concentration is always within several feet of the surface. However, the vertical gradient is usually extremely large, and efforts are being made to alleviate this tracing problem.

3. A continuous point source experiment offers a good opportunity to measure the parameters that govern diffusion, and even to control these parameters in at least a gross manner. Since the experiment is confined to a relatively small area, the current field can be measured by means of current meters placed at the source and near it. There is no danger that the dye might move out of the area which is being measured. In addition, since the data is of an Eulerian nature, one is not faced with the problem of applying fixed point data to a Lagrangian experiment which is the nature of an instantaneous point source experiment.

4. Improved statistical reliability. When a vessel passes through a dye patch, the propeller turbulence mixes the dye in the vertical direction. It is impossible to erase this

effect, so that subsequent crossings through the same area of the patch will give concentration readings that have been artificially altered. This problem is not important in the continuous point source experiment, since the affected region moves away from the source after being measured. Care is taken not to measure the same part of the plume again. This experiment increases the statistical efficiency of dye sampling. Each traverse gives three statistics: plume width, peak concentration and the shape of concentration curves. It is important to make traverses at right angles to the plume axis. This can be difficult, but if the navigational buoys are carefully placed, this error is reduced. When properly done, each crossing of the plume will yield correct values of the desired statistics.

Generally the continuous point source experiment takes less time, gives more reliable data, better control, and uses relatively less amounts of dye than does the instantaneous point source experiment. Each experiment required only ten pounds of Rhodamine B.

Description of Equipment

The flotation unit for the dye source is a sailing catamaran strengthened and modified to hold a thirty-gallon barrel and a constant rate pump with a timer to determine the total pumping time. The power unit is a 12-volt automobile battery housed in an ammunition box. This battery supplies enough power for 4 to 5 one-hour experiments. The catamaran is fitted with a radar reflector and marker light on a twelve-foot mast. Horizontal motion of the catamaran is reduced by anchoring in three directions.

The tracing equipment consists of a deck pump which samples through a polyethelene hose attached to a 35-pound depressor suspended by steel cable from a small davit. The depressor is raised and lowered with a hand winch. The sample is continuously pumped on board and passed through a Turner Model 111 Fluorometer. Fluorometer readings are recorded on a portable strip chart recorder where notes concerning time, Doppler navigator readings, scale changes, and other miscellanea are jotted. The whole experiment is run from the pilot house of the KYMA, since close cooperation between the scientists and the wheelman is necessary.

Results of the Experiment

The results presented here were obtained on July 30, 1964. The experiment was performed five miles south of the Connecticut shore near New Haven in about sixty feet of water. This location was chosen because of the flat bottom and steady tidal currents in that area. Over a three hour period, the current is constant in direction and the velocity varies from 0.9 to 1.0 knots. It was hoped that nearly steady state conditions would be obtained for the duration of the experiment.

One-half hour prior to the start of the experiment, a ten-minute mean current was measured at 0.9 knots toward 270° Magnetic. The wind was from 240° Magnetic at 10-12 knots. During the experiment the wind held its direction and freshened to about 14 knots. The largest change in conditions was the sea state, building from an estimated one foot sea to approximately two feet by the end of the experiment. The dye plume axis developed at about 310° Magnetic.

The data are from crossings made at 1200, 1450, 2000, 2500 and 3000 yards from the source with the sampling inlet at a mean depth of one foot. The cross plume concentration curves shown in Figure 1 are typical curves taken from these data.

The wind direction is from right to left at an angle of about 60° from the plume axis. One should notice the windward skewness of these curves. As diffusion time or distance from source increases, the curves widen considerably and begin to lose their skewness. It is believed that the skewed character of the concentration curves indicates the combined effect of current shear and wind-driven wave action.

Figure 2 shows the width defined by zero concentration of the instantaneous plume as deduced from cross-section data. At a distance greater than 1200 yards from the source, the width is an approximate linear function of distance. The dotted lines represent extrapolation of the measured width toward the source, At this diffusion rate, the source would appear to be at about eight hundred yards from its true position. This indicates that within twelve hundred yards of the source a sudden widening of the plume occurs. This zone of transition can be seen in the photographic data as in Figure 3.

The photographs also illustrate another interesting aspect. Figure 4 shows the prevalent striations that develop in the direction of the wind. This phenomenon has been observed in dye patches and discussed by Ichiye. (Ichiye, 1962; Ichiye, et al., 1964). One of the proposed explanations is that these filaments are produced by interaction of surface waves with shear flow. This author believes that such action may be the dominant factor in early stages of the diffusion causing particle separation which subsequently amplifies with time. Figure 4 also shows the effect of the boat crossing the plume. The diagonal white streak on the picture is due to dye being brought to the surface by the propeller.

Figure 5 shows a portion of the dye plume corresponding to a diffusion time of five to ten minutes. Even at this early time, filaments of dye are being spread by the second order velocity effects of the wave field.

In Figure 6 a photograph taken from 3000 feet shows about one thousand yards of the dye plume. The development of the striations outward from the source is seen.

Also seen are low frequency periodic oscillations which can be more easily identified by placing straight edges along the plume boundaries. These oscillations have been observed in every experiment performed and have periods ranging from seven to nine minutes.

Summary and Conclusions

There are marked dissimilarities between this experiment and the comparable experiment in the atmosphere. Possibly this is primarily due to the fact that the surface layer is a region of complex anisotropic particle motion. The width of the plume is approximately a linear function of distance from the source at distances greater than twelve hundred yards. Closer to the source the width increases at a different rate. This indicates that the diffusion goes through several turbulent regimes; the high frequency components acting initially, the lower frequency dominating at later times. This increased widening of the plume would seem to be the action of turbulent mixing into deeper layers where there is greater energy at lower wave numbers.

Wind-wave tank experiments have been performed by Masch (1963) where dispersion of small particles due to wind-generated waves is studied. Masch shows that, downwind of a point source, the distribution of particles is symmetrical and parabolic in shape. This inconsistency with our results is probably due to the fact that his experiment is performed in a wave tank where the current velocity is in the direction of the wind.

Future experiments are planned which will investigate the effect of wind at various angles to the flow. It is expected, naturally, that under zero wind conditions or when the wind is parallel to the direction of flow, concentration curves will be symmetrical.

Methods are to be improved in future experiments. It is apparent from photographs that dye is mixed deeper on the windward side of the plume. Since only one fluorometer was available, simultaneous surface and subsurface cross-section measurements could not be made. In the future, sampling will be done at two depths or more.

All of the discussion in this paper is heuristic. However, theoretical work is underway which we hope will lead us to a better physical understanding of diffusion at these time and distance scales. Unfortunately, small-scale diffusion in the ocean has been largely ignored while the need for such information is particularly important. This research is sponsored by the Office of Naval Research under Contract Nonr 285(57).

References

Ichiye, T. (1962) Studies of turbulent diffusion of dye patches in the ocean. J. Geo. Res., 67, pp. 3212-3216.

Ichiye, T., H. Iida, N. B. Plutchak (1964) Analysis of diffusion of dye patches in the ocean. Tech. Rep. No. CU-8-64, Lamont Geological Observatory of Columbia University (unpublished manuscript)

Masch, F. D. (1963) Mixing and dispersion of wastes by wind and wave action. Air and Water Pollution J., Vol. 7 No. 7, p. 697.

Pasquill, F. (1962) Atmospheric Diffusion D. Van Nostrand Company Ltd. London, 297 p.

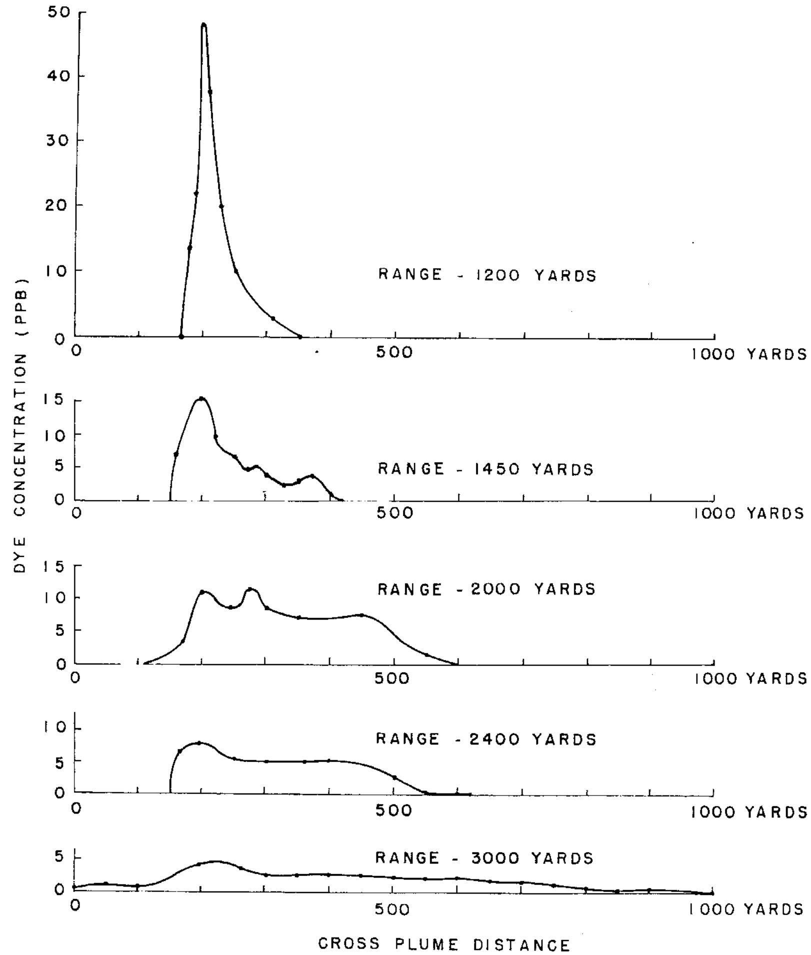

FIG. I CROSS PLUME CONCENTRATION CURVES AT VARIOUS RANGES FROM SOURCE

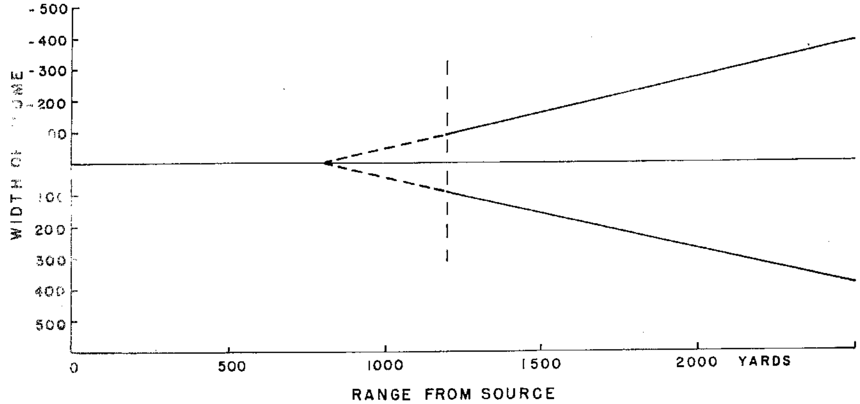

CROSS PLUME WIDTH FROM PHOTOGRAPHIC AND FLUOROMETRIC DATA

FIGURE 2

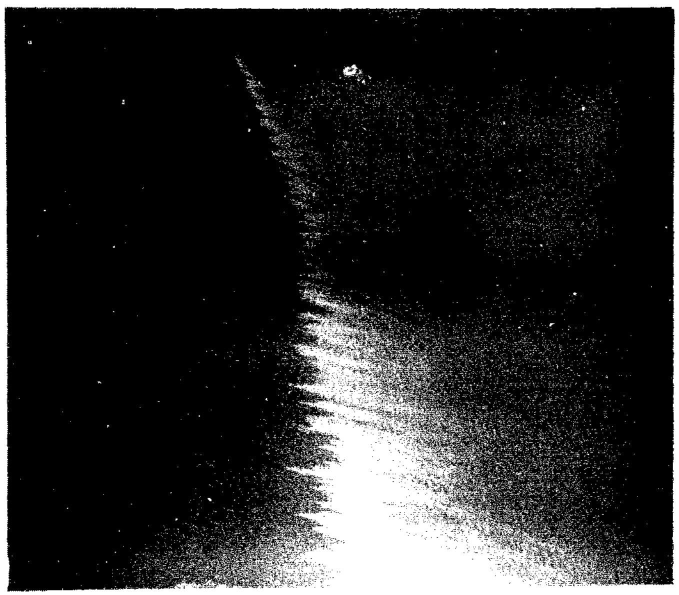

FIGURE 3

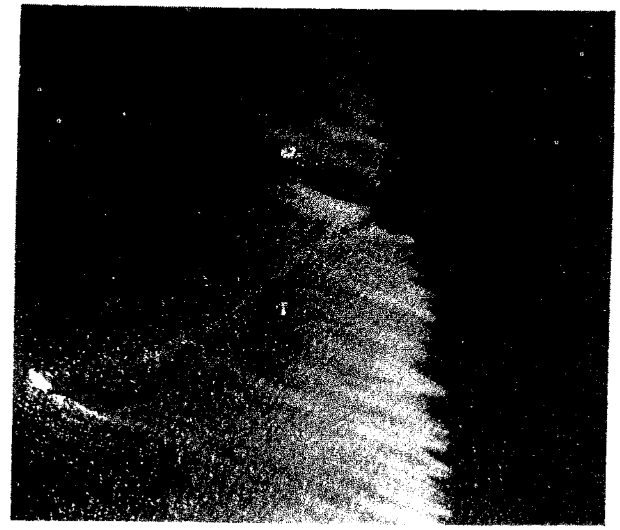

FIGURE 4

FIGURE 5

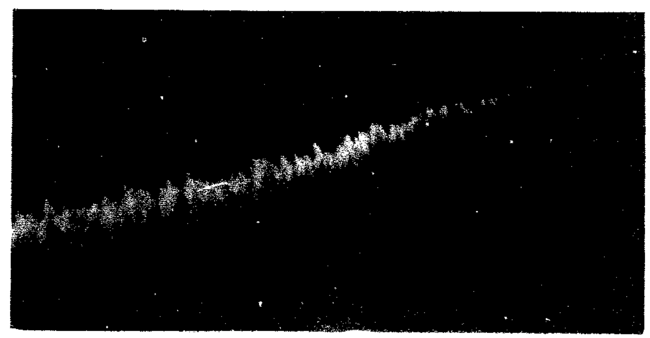

FIGURE 6

DYE STUDIES IN THE OHIO RIVER

Chester C. Kisiel
Department of Civil Engineering, University of
Pittsburgh, Pittsburgh, Pa.

General

One of the major purposes of waste treatment is to prepare the wastes for disposal by dilution in rivers. The existing dilution capacity has become increasingly taxed because of the concentration of communities and industry along many of the nation's waterways. The consequent pollution load can place a burden on downstream water users, especially when incomplete waste treatment has been provided.

The pollution load which reaches the lower reaches of a stream is dependent, in part, on the amount of dilution water available. This is particularly critical during the low-flow season. As a consequence, three alternatives arise. One would be to require more waste treatment prior to discharge into a stream so that the available dilution water remains adequate. The second approach would be to conserve the abundant water supply during rainy seasons for subsequent release during the critical low flow periods. The final alternative would be a combination of the first two. On this entire problem, Butrico and Reid (1) maintain that future pollution abatement will require a minimum dilution ratio of four parts of fresh water to one part of waste water, even with "complete" waste treatment as practiced today. Similarly, from another perspective, Schad (2) reports that by 1980 the Ohio River Basin would require about twice the 6,000,000 acre-feet of reservoir storage now available for low flow augmentation, just to provide enough streamflow to insure four parts per million of dissolved oxygen in the mixture of waste and river water. However, recognizing that waste discharges are not instantaneously mixed with the entire streamflow, Reid (3) estimates that point source loadings of the biochemical oxygen demand of a waste would require two to three times more dilution water than that necessary for uniform loading across the stream's cross-section. Thus, the effective dilution capacity of a stream becomes crucial.

The effective dilution capacity depends on the nature of the waste and its interaction with the river. Furthermore, the ability of the stream " to purify" itself to a desirable level, or to tolerate a certain amount of "insult" can vary with the stream's age, its regime, stream flow, and man-made modifications. The variety of wastes which are discharged into our watercourses

gives rise to more complex physical, chemical, and biological interactions, than would be the case with a simple "conservative" waste effluent. Conservative wastes are only affected by the action of physical mixing in the stream; chemical or biological processes do not alter a conservative waste. Our ignorance of the quantitative rates of the above interactions has led various authorities (1, 3, 4-7) to emphasize the need for more basic and applied research into the mixing process. The resulting information is essential to optimum design and operation of water resource systems wherein the water is to be cycled between the consumer, industry, waste treatment plant, river, and water treatment plant. Public health and engineering aspects of the system are emphasized, in part, by Figure 1 which illustrates the multiplicity of variables which influence the allowable waste capacity of even a small reach of stream.

The ultimate goal of studies of turbulent mixing of wastes in rivers is to predict the distributions of substances which have originated from various sources under different stream conditions. Traditionally, the Fickian mathematical model has been used to predict the distribution of substances in the ocean, atmosphere, estuaries, lakes, and pipes. Use of the model depends on an estimate of the diffusion coefficient which defines the rate at which the mixing process proceeds in the fluid. Diffusion coefficients have been estimated both by theoretical and empirical methods. The theoretical equations consider the coefficient to be a function of fluid flow variables and channel roughness; however, field work has been the most common source of estimates of diffusion coefficients in nature. Such estimates of the diffusion coefficient, coupled with a knowledge of the state of fluid motion at the time of measurement of the coefficient, are of great assistance in generalizing about the phenomenon of turbulent mixing in nature. Thus, the interplay of analytical and empirical studies should provide more reliable procedures in the future for predicting the distribution of substances in rivers.

Previous research into turbulent mixing of substances in free surface streams may be divided into three areas:

1. Theoretical prediction of diffusion coefficients by means of easily obtained hydraulic parameters (6, 9-13).

2. Experimental investigation of turbulent mixing in laboratory flumes under idealized conditions (11-12, 14-20).

3. Field observation of the rate of change of both the waste concentration and geometric shape of the waste plume with respect to time (12-13, 21-25). Such data were then used to estimate diffusion coefficients. The

Fickian mathematical model was assumed in most instances.

A review of the above research undertakings indicates that:

1. Variable channel geometry has an extensive influence on the rate of turbulent mixing. This was particularly evident over large distances on the river.

2. Longitudinal convection is the major mechanism responsible for the mixing of wastes.

3. Diffusion coefficients which were based on hydraulic parameters underestimate the rates of mixing in natural streams.

4. In general, the existing mathematical models of turbulent mixing do not adequately predict the behavior of a waste in a natural stream. The models include those for predicting diffusion coefficients and those for predicting concentration of the waste.

5. The diffusion coefficient is a function of both the scale of turbulence and the mean rate of energy dissipation under idealized flow conditions in a laboratory flume (14, 15).

   The relationship is the well-known 4/3 power law, based on Kolmogoroff's theory of local isotropy, which has been used to describe initial and later phases of the mixing process in both the atmosphere and the sea. This power law has not been tested in natural streams.

6. There have been no reported studies of the initial phases of horizontal mixing of instantaneous sources in a natural stream. From a practical standpoint, such information would be important in the design of waste outfall structures.

7. There have been no investigations of the difference in behavior of plumes which have been released from various points in one transverse section of a stream.

Objectives

In the fall of 1961, a series of experiments were conducted in a small reach of the upper Ohio River, with the following objectives:

1. To investigate the initial phases of the horizontal mixing process for instantaneous sources. Implicit in this objective were the commitments to observe the time rate of change of tracer concentration and plume geometry, and to compare the results with the statistical theory of turbulent mixing (26-28).

2. To compare the downstream behavior of tracer plumes which have been released as instanteneous sources in the same transverse section of the research channel.

Such information would be of value in the design and location of waste effluent structures.

Methodology

In any river investigation, sampling of the waste plume has been a major problem. In the previously reported studies on turbulent mixing in streams, samples were collected for subsequent analysis in the laboratory. In the past few years, the direct observation of turbulent mixing in streams has become more feasible with a continuous underway monitoring system (in situ system) first reported by Carpenter (29, 30) of the Chesapeake Bay Institute, using Rhodamine-B as the conservative tracer.

With the aid of the continuous underway monitoring system, direct observations were made of changes in geometry and concentration of Rhodamine-B of four types of tracer efflunts in a two-mile reach of the river. The experiments included two shoreline discharges, two instantaneous horizontal line sources, a vertical line source at midstream and three instantenous point sources in succession at midstream. The experiments near the shore and at midstream were designed to permit evaluation of the rate of transverse diffusion. The mixing of the horizontal line was observed for rate of longitudinal spread of the source. The three instantaneous point sources were applied in order to observe the effect of a variable volume of dye on the mixing patterns at midstream.

The location of the research channel is shown in Figures 2 and 3. This site was chosen because it is relatively straight and virtually free from towboat traffic. The topography of the channel was mapped by means of a recording fathometer (See Figures 4 and 5).

The system for tracer detection from a moving boat consisted of a submersible pump, portable fluorometer adapted to monitor the tracer cloud continuously, and a recorder. Position of the craft with respect to the south shore was fixed by sighting on shore baselines with a sextant. This permitted establishing spatial profiles of tracer concentration by sampling at various depths transversely and longitudinally. Protocol for the six experiments reported here is outlined in Table I.

In the experiments of Runs 9 and 12, the dye was fed continuously at constant depth as the boat progressed from the south to the north shore. This procedure approximated a horizontal line source. The vertical line source of Run 10 was approximated by discharging the tracer continuously from an anchored boat as the feed pipe was raised from the stream bed to the surface. In Run 11, three volumes, with equal weights of dye but with volumes of one-half, five, and twenty liters, were released instantaneously at twenty-minute intervals. For Runs 8 and 13, the dye was fed as a point source from a boat anchored near the south shore.

In addition to the tracer data, velocity profiles were obtained at various cross-sections and turbulent velocity fluctuations were obtained with a current meter at three river stations (31).

Results

Figure 6 illustrates the transverse spread of the tracer clouds downstream for the shoreline discharges of Runs 8 and 13. The spread of the cloud was less at the higher stream flow of Run 13 than in Run 8. In both experiments the cloud widened linearly, but the rate was 3.6 times greater at the lower flow of Run 8 because of the greater diffusion time available. In Run 8 the linearity held down to Station 4000. Beyond this station the influence of channel widening, particularly at Station 6000, became apparent. In Run 13 this influence was not observed, probably because of the flooding of the land projection at Station 5500.

The horizontal lines (Runs 9 and 12) were visibly bowed downstream several minutes after injection of the dye. Between Stations 3000 and 5000 the central portion of the line was sheared away from the slower moving legs near the shore.

The vertical line of Run 10 was initially bent in the form of a typical vertical velocity profile from surface to stream bed. As the line moved downstream, forty-five transverse profiles of tracer concentration were

Table 1

Protocol of Tracer Experiments

Tracer Run	Date	Nature of experiment	Streamflow cu.ft./sec.	Point of application at Station 101	Depth of feed below water surface	Minutes for feed	Strength of dye solution	Volume of dye (liters)	Weight of dye (lbs.)
8	10-20-61	Point source	2450	20-50 feet from south shore	4.5	67	1.5%	48	1.59
9	10-23-61	Horizontal line source	4700	Entire width	1.5	5	1.6%	10	0.35
10	10-25-61	Vertical source	3400	Midstream	---	5.6	1.6%	36	1.27
11-1	10-27-61	Instantaneous source	3000	Midstream	1.5	---	40.0%	0.5	0.44
11-2	"	"	"	"	"	---	5.0%	4.0	"
11-3	"	"	"	"	"	0.8	1.0%	20.0	"
12	12-1-61	Horizontal line source	12,400	Across entire width	1.5	4.6	1.6%	26.0	0.92
13	12-2-61	Point source	10,710	20-40 feet from south shore	1.5	8.7	1.6%	50.0	1.77

TABLE 2

PARAMETERS OF THE FUNCTION: $C_m = at^b$ or $\sigma^2 = a' t^{b'}$, WHICH DESCRIBES THE TIME-RATE OF CHANGE OF PEAK CONCENTRATION AND HORIZONTAL SPREAD OF THE TRACER

TRACER RUN	FLOW CUBIC FEET PER SECOND	b = Slope of Log-Log Plot		
		PEAK CONCENTRATION VERSUS TIME	σ_x^2 VERSUS TIME	σ_y^2 VERSUS TIME
8	2,450	-5.0	-----	2.07
9	4,700	-2.0	4.6	-----
10	3,440	-0.95	-----	2.34
11-1	3,000	-1.75	5.9	2.05
11-2	"	-1.55	-----	-----
11-3	"	-1.44	2.1	-----
12	12,400	-0.9	1.5	-----
13	10,710	-2.0	-----	1.36

NOTE: σ_x^2 = STANDARD DEVIATION OF LONGITUDINAL PROFILE SQUARED
σ_y^2 = STANDARD DEVIATION OF TRANSVERSE PROFILE SQUARED
C_m = MAXIMUM CONCENTRATION IN SPATIAL DISTRIBUTION CURVE
t = TRAVEL TIME
a,b = PARAMETERS IN THE FUNCTION

obtained. Thee-fourths of these profiles approximated a normal distribution curve. Standard deviations of the observed profiles were estimated from arithmetic-probability plots of transverse distance versus cumulative per cent of area under the distribution curve. The standard deviations were subsequently used to locate the outer edge of the cloud as it progressed downstream (Figure 7). The edge of the cloud in any transverse profile is located at plus or minus two standard deviations from the peak concentration. This graph illustrates the effects of channel widening at Stations 5000 and 6000, observed also in the shoreline experiment of Run 8.

In Run 11 the cloud with the largest initial volume of tracer (20 liters) diffused more rapidly in the horizontal plane than did the other clouds of this experiment. This may be ascribed to:

1) The larger interface between the cloud and "unpolluted" surroundings.

2) The early effectiveness of large eddies in the initial stages of mixing.

Patterson (32) obtained similar results on the Colorado River near Austin, Texas.

Theoretically, the concentration in one-, two-, and three-dimensional diffusion varies inversely with travel time to the one-half, one, and three-halves power, respectively. Since field observations indicated that uniform vertical mixing had occurred early in the diffusion process, each of the experimental clouds may be classified as undergoing either a one- or two-dimensional diffusion process. Thus, the instantaneous horizontal line eventually behaved as a vertical transverse plane which could diffuse only in the direction of stream flow, i.e., one-dimensional diffusion. Similarly the clouds which were discharged as points at midstream and shore could diffuse transversely and longitudinally, i.e., two-dimensional diffusion. It was found that for seven of the eight clouds the peak concentration decreased at a time-rate that was larger than predicted by theory. The only exception was the time-rate of change of peak concentration for Run 10, the vertical-line source experiment. Figure 8 shows a log-log plot of "instantaneous" peak concentration versus travel time. The slopes of the log-log plots for all clouds ranged between -0.9 and -5.0 in contrast with the predicted slopes of one-half, one, and three-halves, for one, two, or three dimensional mixing, respectively.

For the horizontal spread of the clouds, theory predicts that for long-term diffusion processes, the square of the standard deviation of the spatial distribution curve varies linearly with time, and that for short-term diffusion processes the standard deviation varies directly with time. However, for the research channel the time-rate of change of the horizontal spread was more rapid than predicted. Figure 9 shows a log-log plot of the square of the standard deviation versus time. The slopes of these graphs ranged between 1.3 and 5.9 (Table 2).

Analysis of the observed relationships between the standard deviation, σ, versus time, t, indicates that the dispersion patterns in these experiments were probably very significantly influenced by large scale convective eddies. These were possibly a kind of pseudo macro-turbulence, the characteristics of which depended on channel geometry which in turn varied in the x-direction. None of the current statistical theories of turbulent diffusion provide an adequate framework for interpreting such non-random phenomena as the effect of variable channel geometry.

Prediction of Peak Concentration

The accuracy of predictions of concentrations depends on the validity of theoretical assumptions. The assumptions of Taylor (9), Elder (11), and Glover (12) in the theoretical equations for channels include:

1. a broad open channel with no side effects
2. constant velocity U at all points in the stream
3. constant rate of diffusion as described by transverse and longitudinal mixing coefficients (K_x and K_y)
4. uniform turbulence in all parts of the stream
5. straight uniform channel with uniform shape throughout its length

From the behavior of the clouds it is evident that the assumptions do not hold for the research channel.

To use the models for one-and two-dimensional diffusion requires an estimate of diffusion coefficients. These may be obtained by three methods:

1. by field observation of the horizontal spread of clouds in terms of the standard deviation σ and then using the relationship, $\sigma^2 = 2Kt$.
2. by calculation, using the hydraulic radius R and shear velocity u.
   These parameters describe average conditions of flow in the stream. However, the method is limited because a straight channel is assumed.
3. by utilizing coefficients obtained on other streams for similar hydraulic conditions. Figure 10 represents the available information, including the results of our study, on longitudinal mixing coefficients for several streams in the United States.

A typical comparison of the observed with predicted peak concentrations is shown in Figure 11. In most instances, the predictions are within one order of magnitude of the observed concentrations for the test channel.

Summary and Conclusions

In this investigation a continuous monitoring system has been used in an attempt to define quantitatively the early development of tracer clouds in a stream. For the experimental channel, the following conclusions may be drawn:

1. The Fickian mathematical model does not accurately predict the peak concentration of tracer during the early stages of the mixing process. However, the models can aid the investigator to plan for more intelligent measurements on the river.
2. The rate of dilution of the tracer is more rapid than predicted by the Fickian model.
3. The use of constant diffusion coefficients as predicted independently from the equations of Taylor and Elder would eventually predict peak concentrations which would agree closely with observed values.
4. In general, the Fickian Model satisfactorily predicts the Gaussian shape of a transverse profile of concentration in the center of a stream; however, the longitudinal profiles were definitely skewed.
5. The influence of variable channel geometry is particularly pronounced at the shoreline.
6. The width of the plume at the same downstream station is inversely related to the streamflow. Although the plume is narrower and a smaller percentage of the stream's dilution capacity is effective at a higher flow, the absolute

concentration of Tracer is still lower than that observed for the lower streamflow.

7. The downstream behavior of a waste depends on the manner in which it is initially introduced into the stream and on the initial volume of waste discharged. The larger the initial volume of tracer, the more rapid the mixing process because of the earlier influence of large eddies on a large volume of tracer.

8. The horizontal line source is the most efficient method for diluting a waste since the entire dilution capacity of the stream is almost immediately available.

9. During the early stages of the mixing process in the research channel, anisotropic mixing is an important factor in diluting the tracer.
   Based on the ratio of longitudinal and transverse mixing coefficients, longitudinal mixing is 3 to 10 times faster than transverse mixing.
   Transverse mixing was more rapid than predicted from the theoretical equations of Taylor and Elder.

The research findings indicate that, even with high degrees of waste treatment, mixing must be rapid and complete in relatively short distances in order to maintain high standards of water quality in the river. More elaborate systems of waste discharge into the river are required than just placing an outfall at the shoreline. As far as the stream is concerned, percent efficiency of the treatment process is not relevant. What is pertinent is the remaining strength and volume of treated waste to be assimilated by the stream.

Finally, the research findings emphasize the many uncertainties concerning the mechanistic nature of turbulence in open channels. If accurate predictions of mixing are to be made in the future, coordinated research is needed in four areas: theoretical analyses of mixing within finite boundaries, river models, laboratory flumes and the natural stream. In the meantime, direct observation of the mixing process is necessary for the practical problems of siting waste disposal facilities along any river.

References (Numbers appearing in text appear in parenthesis at the end of each reference)

Carpenter, J. H. (1960) Tracer for circulation and mixing in natural waters. Public Works, 91, p. 110-112 (29)

Elata, C. and A. T. Ippen (1961) The dynamics of open channel flow with suspensions of neutrally buoyant particles. M.I.T. Hydro. Lab., T. R. No. 45, p. 51. (20)

Elder, J. W. (1959) The dispersion of marked fluid in turbulent shear flow. Journ. Fluid Mech. 5, pp. 544-560. (11)

Glover, R. E. (1964) Dispersion of dissolved or suspended materials in flowing streams U. S. Geol. Survey, Professional Paper 433-B. (12)

Goda, T. and S. Nambu (1959) Some considerations on river pollution mechanism. Mem. Fac. Engr. Kyoto University, 21, p. 57-69. (25)

Hanson, H. G. and B.B. Berger (1961) Where does research stand in water pollution control? Journ. of the Water Pollution Control Federation., 33, pp. 477-484. (4)

Honstead, J. F. (1954) Columbia River survey: 1951-1953, U. S. Atomic Energy Commission, Rept. HW-32506 (secret). Declassified Form: TID 10126. (21)

Ippen, A. T. and F. Reichlen (1957) Turbulence in civil engineering measurements in free surface streams. Journ. of the Hydraulics Div., Proceedings of American Society of Civil Engineers, 83. (16)

Kalinske, A. A. and C. L. Pien (1944) Eddy diffusion, Industrial and Engineering Chemistry, 36, pp. 220-222. (18)

Kalinske, A.A. and J. H. Robertson (1941) Turbulence in open channel flow, Eng. News-Record, 126 (19)

Kisiel, C., (1963) Turbulent mixing in the upper Ohio River, Sc. D. thesis, University of Pittsburgh. (31)

Kneese, Allen V. (1962) Water pollution--economic aspects and research needs. Resources for the Future, Inc., p. 55. (7)

Norton, H. T. (1957) The turbulent diffusion of river contaminants. U. S. Atomic Energy Commission Rept. HW-49195. (22)

Orlob, G. T. (1958) Eddy diffusion in open channel flow. Contrib. No. 9, Water Resources Center, Univ. of Calif., Berkeley. (14)

Orlob, G.T. (1959) Eddy diffusion in homogeneous turbulence. Proc. Amer. Soc. Civil Engr., Jour. of Hydraulics Div., 85, pp. 75-101. (15)

Parker, F. L. (1958) Radioactive tracers in hydrologic studies. Trans. Amer. Geophys. Union 39, pp. 434-439. (10)

Patterson, C. (1963) Radioactivity transport in water - the dispersion of radionuclides in open channel flow, Ph.D. thesis, Univ. of Texas, (Tech. Rept. 2, Environmental Health Engr. Res. Lab., C.E. Dept., Univ. of Texas, Austin.) (32)

Pritchard, D. W. and J. H. Carpenter (1960) Measurements of turbulent diffusion in estuarine and inshore waters. Int'l. Assn. of Scientific Hydrology, 51, 361. (30)

Pritchard, D. W. (1960) Problems related to disposal of radioactive wastes in estuarine and coastal waters. Trans. of 1959 Seminar on Biological Problems in Water Pollution, Robert A. Taft Sanitary Engineering Center, Tech. Rept. W60-3, pp. 22-32 (8)

Proceedings of the National Water Research Symposium, March 28-30, 1961 Washington D.C., Senate Document No. 35, 87th Cong., 1st session. Statement by F. Batrico and G. W. Reid, pp. 219-222. (7)

Reid, George W. (1960) Water requirements for pollution abatement U.S. Senate, Select Committee on Nat'l. Water Resources, Committee print No. 29. (3)

Robertson, J. M. (1940) Diffusion characteristics of turbulence in an open channel. M.S. Thesis, State Univ. of Iowa (17)

Schad, T. M. (1960) Activities of the Senate Select Committee on National Water Resources. Journ. of Amer. Water Works Assn., 52, pp. 965-969. (2)

Simpson, E.S., W.A. Beetem and F. R. Ruggles (1958) Radiotracer experiments in the Mohawk River, N.Y. to study sewage path and dilution. Trans. Amer. Geophys. Union 39, pp. 427-433. (24)

Taylor, G. I. (1921) Diffusion by continuous movements. Proc. London Math. Soc. 20, p. 196-211 (26)

Taylor, G.I. (1936) Statistical theory of turbulence, Parts I - V. Proc. Roy. Soc. London, 151A, 421 (1935) and 156A,307 (1936). (27)

Taylor, G.I. (1938) The spectrum of turbulence. Proc. Royal Soc. London, 164 A, 476. (28)

Taylor, G. I. (1954) Dispersion of matter in turbulent flow through a pipe. Proc. Roy. Soc. (London), 220A, pp. 446-468. (9)

Taylor, E. W. and J.A.L. Dosch (1961) Conference on water pollution problems in Europe. The Quarterly Bulletin of the International Water Supply Association, No. 4, p. 10. (5)

Thomas, H. A. Jr., (1958) Discussion of "Mixing and diffusion of wastes in streams" Proc. of Seminar on Oxygen Relationships in Streams, Robert A. Taft Sanitary Engr. Centre, Cincinnati, Ohio, p. 105. (6)

Thomas, I.E. (1958) Dispersion in open channel flow. Ph.D. Thesis, Northwestern University. (13)

Thomas, I.E., W. S. Hamilton and C. G. Bell (1959) An investigation of the fate of fission products in the Illinois Waterway System. U.S. Atomic Energy Commission, A E C U-4025. (23)

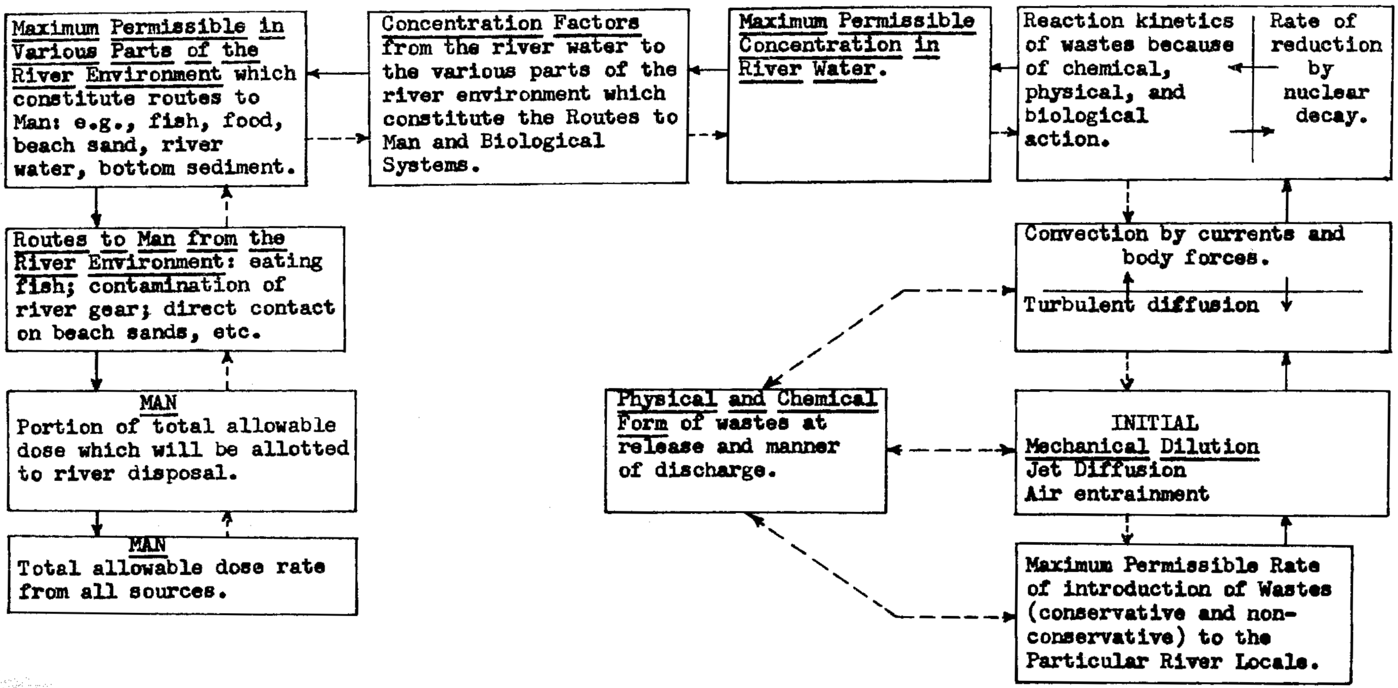

FIG. 1. SCHEMATIC PRESENTATION OF THE STEP BY STEP CONSIDERATIONS WHICH SHOULD BE MADE IN EVALUATING THE SUITABILITY OF ANY REACH OF RIVER AS A RECEIVER OF GROSS POLLUTION AND PARTLY-TREATED WASTES.*
*adapted after Pritchard(8)

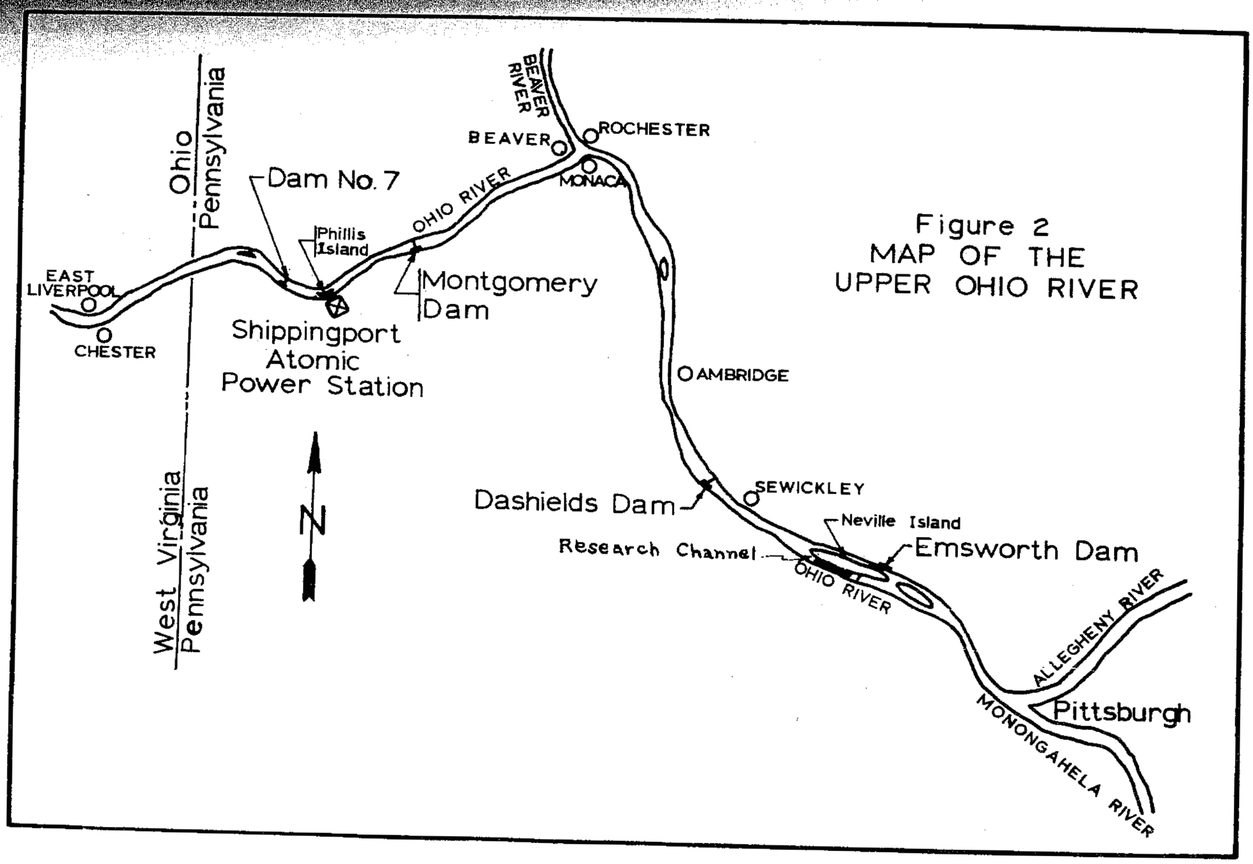

Figure 2
MAP OF THE UPPER OHIO RIVER

44

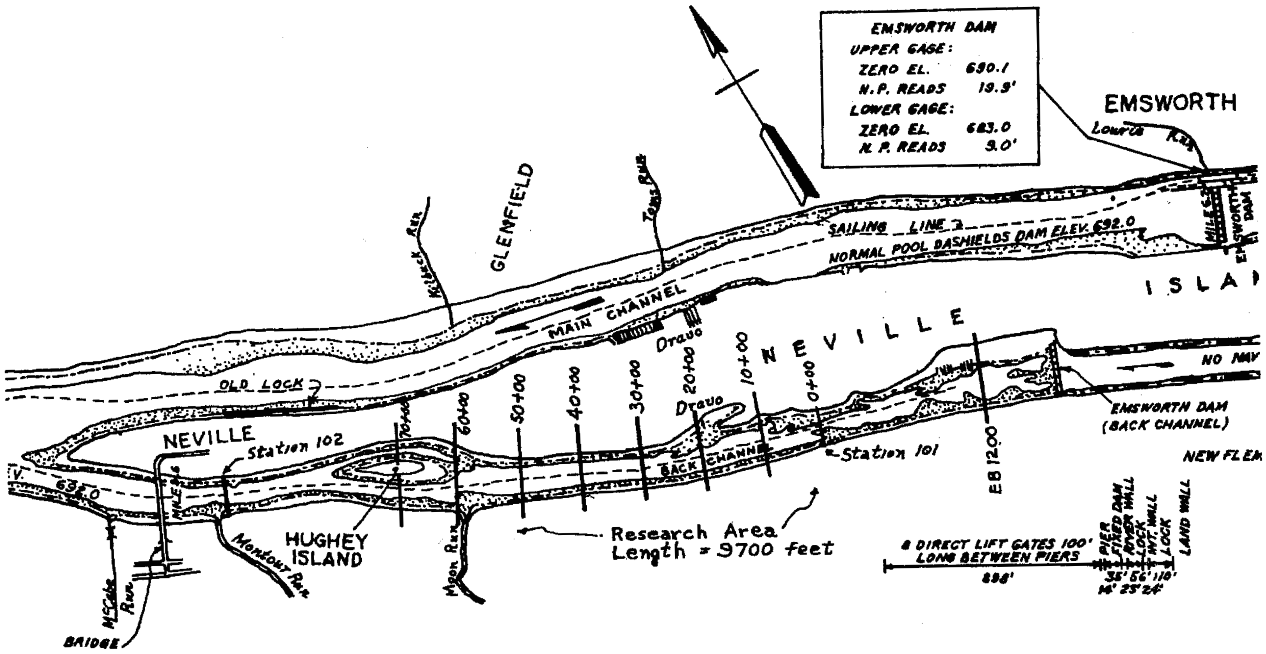

Figure 3

45

FIGURE 4

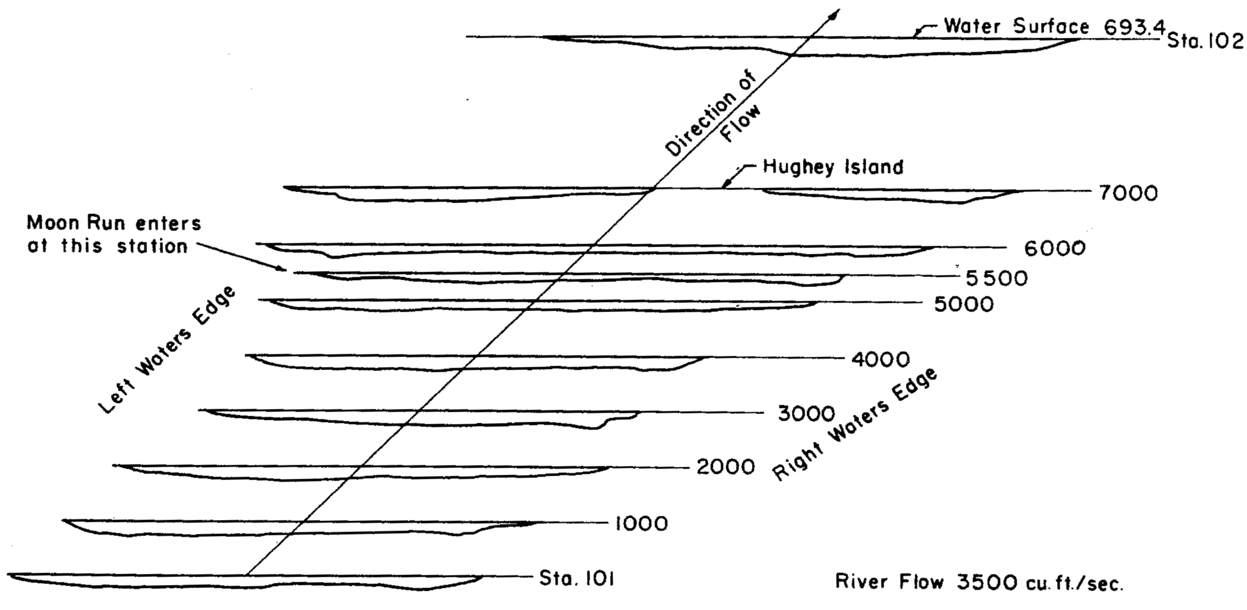

TRANSVERSE PROFILES IN BACK CHANNEL OF NEVILLE ISLAND, OHIO RIVER
BASED ON SURVEY OF 9-8-61 WITH RAYTHEON RECORDING FATHOMETER

FIGURE 5

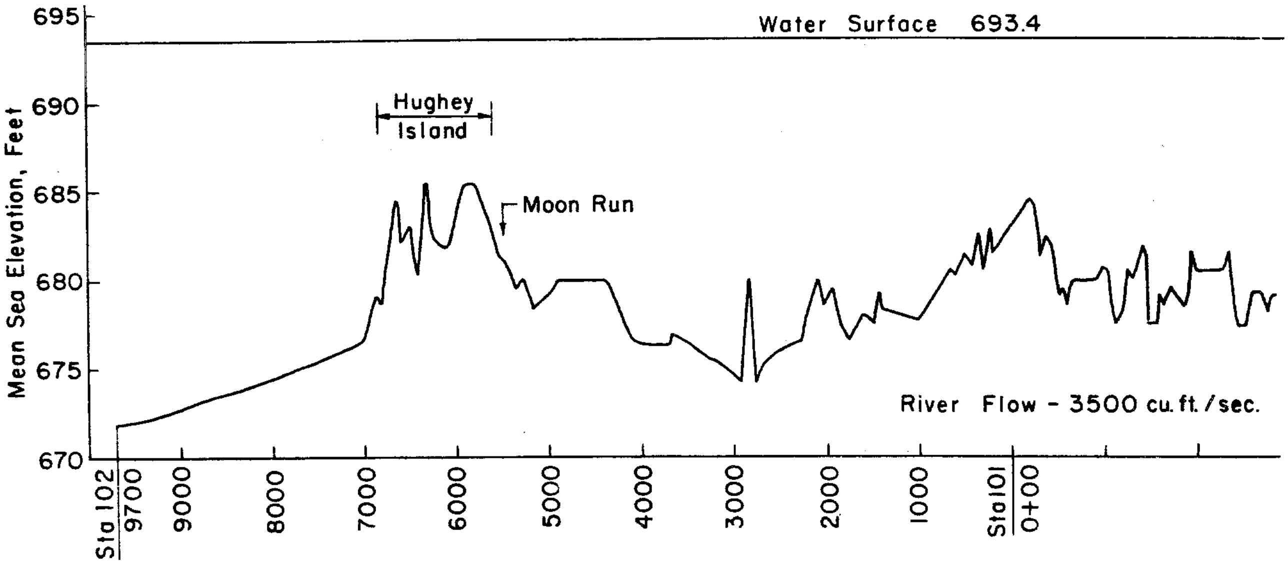

MIDSTREAM LONGITUDINAL PROFILE IN BACK CHANNEL OF NEVILLE ISLAND, OHIO RIVER BASED ON SURVEY OF 9-8-61 WITH RAYTHEON RECORDING FATHOMETER

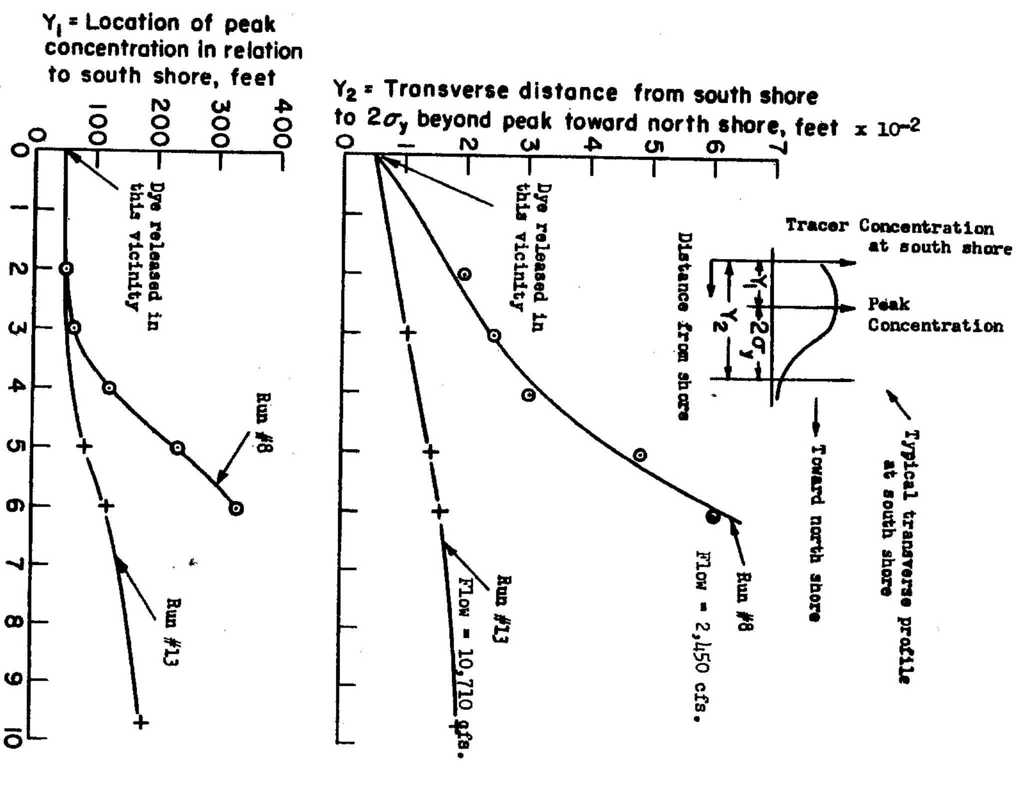

Figure 6

Transverse Mixing of the Plumes for Shoreline Discharges of Runs #8 and #13

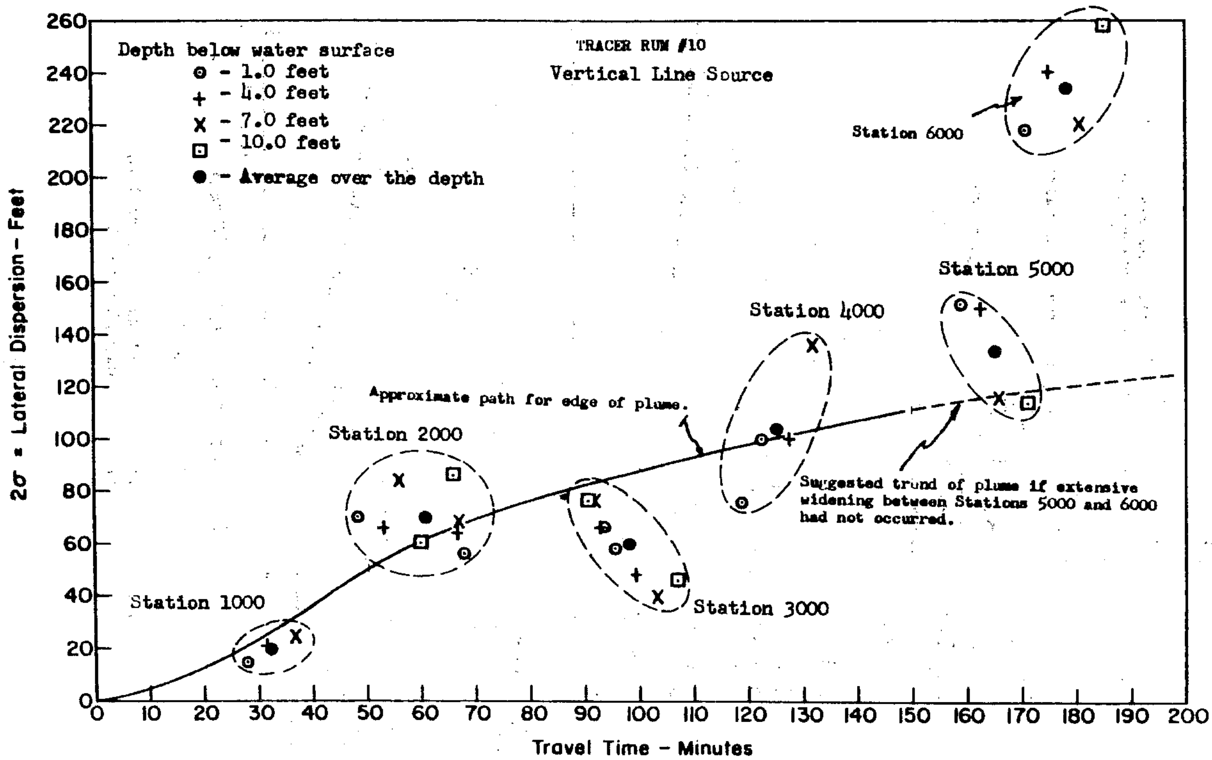

Figure 7

Lateral Dispersion Pattern for Vertical Line Source of Tracer Run #10

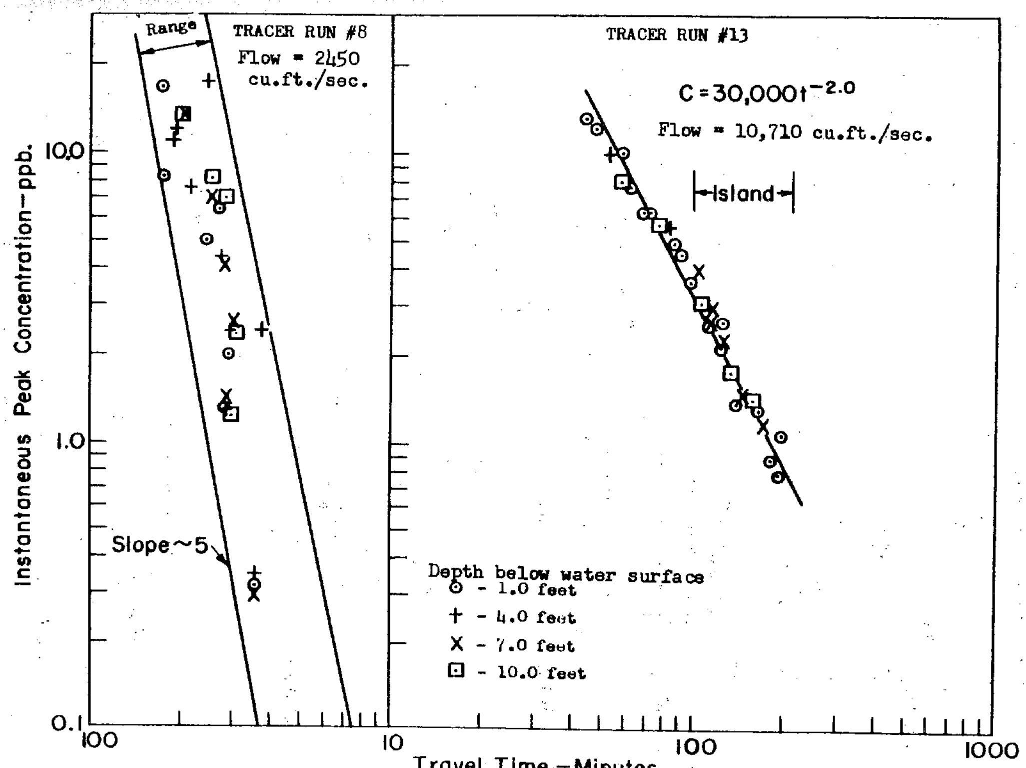

Figure 8

Variation of Peak Tracer Concentration with Respect to Time for the Shoreline Discharges of Tracer Runs #8 and #13

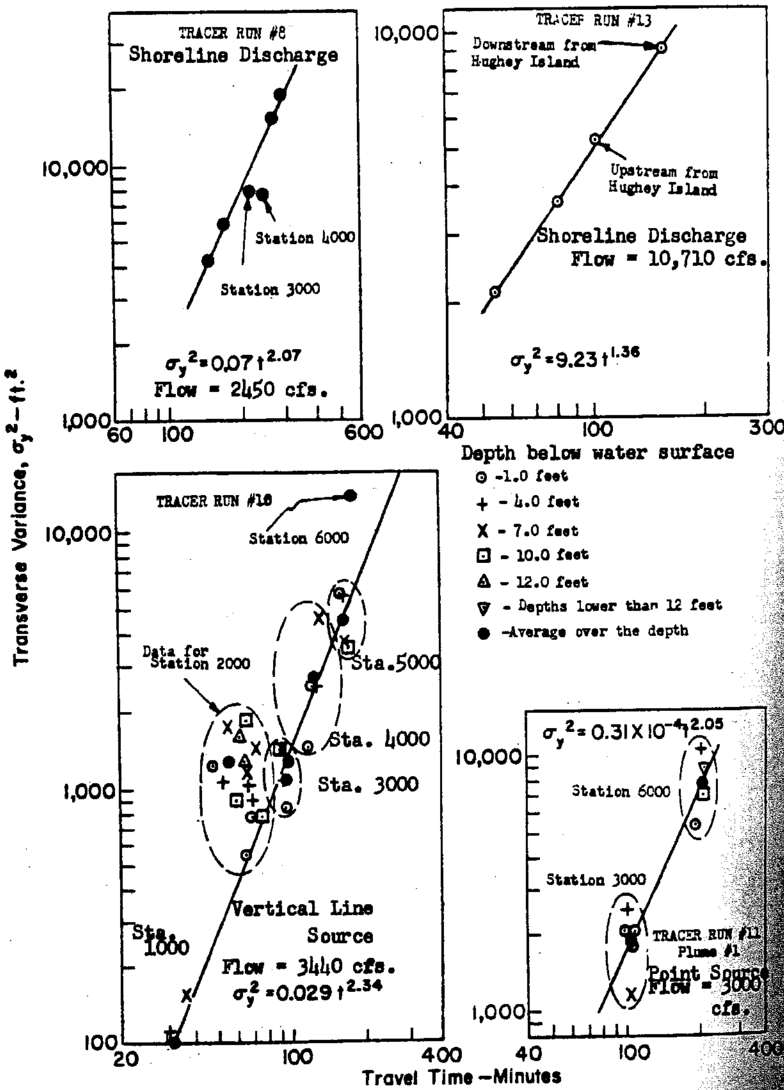

Figure 9

Transverse Variance, σ_y^2, as a Function of Time for Tracer Runs #8, #10, #11, and #13

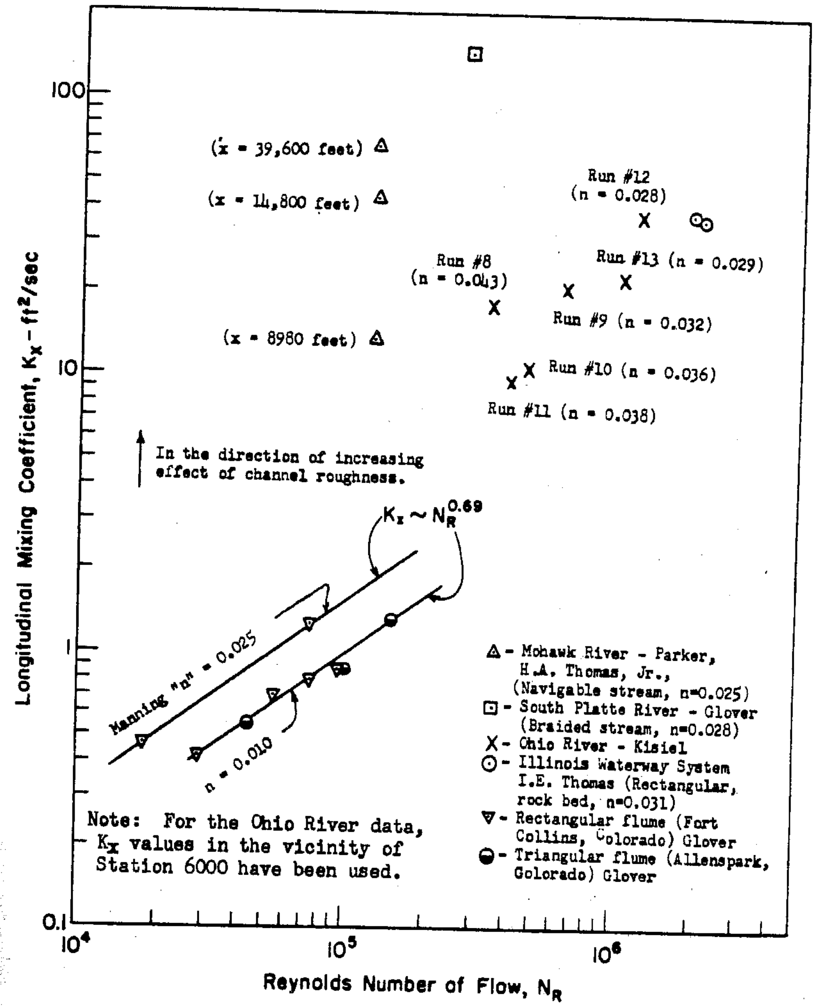

Figure 10

Longitudinal Mixing Coefficient, K_x, as a Function of Reynolds Number, N_r, for Reported River Studies

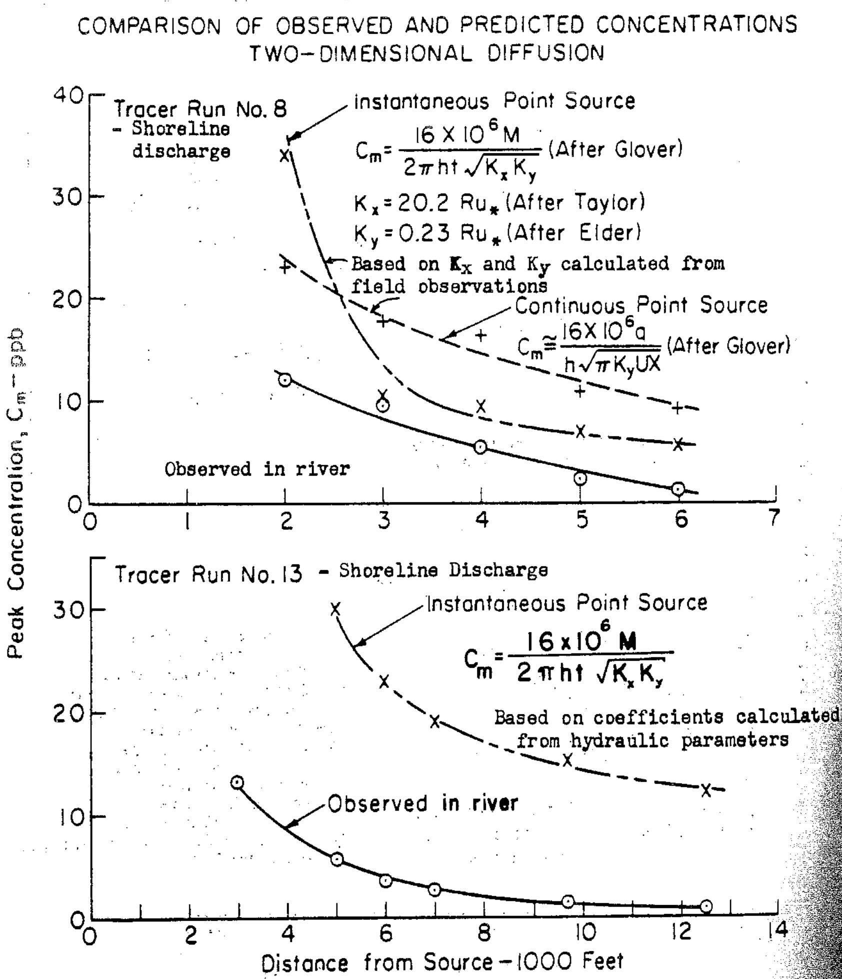

Figure 11

Comparison of Observed and Predicted Peak Concentrations for the Two-Dimensional Diffusion Processes of Tracer Runs #8 and #13

LIMITATIONS OF RHODAMINE B AND PONTACYL BRILLIANT PINK B AS TRACERS IN ESTUARINE WATERS

Charles G. Gunnerson
U. S. Public Health Service, Cincinnati, Ohio
and
Charles A. McCullough
State of California Department of Water Resources
Sacramento, California

ABSTRACT

Rate coefficients for dye losses are computed from the relationship $C_t/C_o = \exp(-kt)$ where C_o = initial concentration and C_t = concentration at time t, where t is in days. Field observations of decay rates in the Sacramento-San Joaquin Delta and Suisun Bay, California, varied from 0.041 to 0.24 day^{-1} for Rhodamine B to 0.069 to 0.36 day^{-1} for Pontacyl Brilliant Pink B. These rates are reasonably consistent with those derived from data published by other investigators of losses due to various combinations of photochemical decay, oxidation and absorption. Apparent recoveries of more dye than was released were frequent, presumably because of variable background interference which made the instrument calibrations invalid.

Definitive studies require that calibrations be made using water into which the dyes will diffuse and that tests of dye losses be made for each sub-environment. These limitations are critical in real estuaries where water quality is changing rapidly. They may be largely overcome by using hydraulic models for diffusion tests.

Discussion after Gunnerson's paper

Pritchard noted that Rhodamine B is destroyed by chlorination, thus alleviating "contamination" of drinking water by the dye. F.C.W. Olson recounted an experiment at Alligator Harbor, Florida where all of the dye used was lost by absorption of the bottom sediment.

Pritchard noted on the natural fluorescence readings that in the Severn River there are algae with pigments having spectral characteristics identical with Rhodamine B, and that the background readings there get as high as 2 ppb. He also described an experiment in which 100 lbs. of dye was reduced to 90 lbs. only after about 100 days. There was a comment from the floor regarding effects of industrial wastes as dye removers.

DIFFUSION EXPERIMENTS IN COASTAL WATERS USING DYE TECHNIQUES*

Takashi Ichiye
Lamont Geological Observatory
of
Columbia University
Palisades, New York

Abstract

The data obtained from dye experiments off New Jersey coast, on the Bahama Banks and south of Long Island since 1961 are analyzed. The areas of a visually demarcated dye patch are determined from concentration measured with fluorometers and compared with the mean square separation of a two-particle theory of diffusion, yielding t^2 and t^3 law for small and large time t respectively. The fine structures of dye patches are discussed from hydrodynamic theories. Elongation of dye patches is interpreted as vertically differential advection due to a shearing current. Striations are discussed as caused by helical vortices which may be also a cause of Langmuir circulation. The curvature of the tail part of a dye patch is attibuted to the Ekman spiral in a pure wind current, because, in most cases, curved tails were observed for moderate winds and in waters deeper than 20 m and because the curvature is clockwise from head to tail in the northern hemisphere. A modified theory of a drift current with eddy viscosity decreasing exponentially with depth is developed and compared with patterns of dye patches.

1. Introduction

Since 1961, a number of experiments using dye discharge methods were carried out by a group of Lamont Geological Observatory in the coastal waters including the coasts off New Jersey, Long Island and the Bahama Banks. The field methods consist of discharging five to fifty gallons of acetic acid solution of Rhodamine B at the surface or sub-surface, measuring dye concentration continuously with a standard Turner Model III fluorometer during crossings of the patch by a research vessel and taking aerial photographs of the patch from an airplane at a few minutes intervals (Costin and others, 1963).

The original purpose of these experiments was to determine gross features of horizontal diffusion in the ocean due to turbulence with scales less than a few hundred meters. However, various patterns of the dye patches suggest that the diffusion process in the upper layer of the ocean is deviated from predictions based on an isotropic turbulence model. Also, the fine structures of circulation which are rather difficult to be measured with conventional current meters were revealed by these patches. In this paper, the results of the experiments will be discussed in relation to both turbulent diffusion in the ocean and detailed structure of the circulation.

* Contribution No. 834

2. Two-particle model applied to dye patches

Although configuration of the dye patches in most experiments was rather complicated, the size of dye patches determined from concentration contours and aerial photographs almost always increased with time in accordance with theories of turbulent diffusion. In order to determine the rate of change of size quantitatively, the second moment of the concentration distribution α^2 is determined from the observed concentration contours by curve fitting method for a relation

$$C = C_m \exp(-A/\pi\alpha^2) \tag{1}$$

in which A is the area enclosed by a contour of the concentration C and C_m is the maximum concentration. This quantity α^2 corresponds to the area of a dye patch demarcated visually or photographically and is proportional to the mean square separation ξ^2 of two particles whose relative motion is caused by turbulence (Gifford, 1957).

Batchelor (1950) discussed the rate of change of ξ^2 from a basis of dimensional analysis. When the Reynolds number of turbulence is sufficiently large as in the ocean, there is an equilibrium between energy transfer from larger eddies to smaller ones by inertial forces and energy dissipation at the smallest eddies by viscosity. This state of turbulence is called the inertial sub-range. When the rate of energy dissipation and the average initial distance of pairs of particles are taken as ϵ and ξ_o respectively, the change of ξ^2 is given by a relation

$$d\xi^2/dt = \epsilon t^2 F(\xi_o/\sqrt{\epsilon t^3}) \tag{2}$$

from dimensional consideration of the process in the inertial sub-range where F is a universal function. In the initial stage of release of the two particles, the relative velocity remains constant and, thus, the lefthand side of (4) is proportional to t. Therefore, for sufficiently small t, the function F is a 2/3 power of its argument. Thus, Equation (2) after integration with t yields

$$\xi^2 = \text{const} \cdot t^2 (\epsilon\xi_o)^{2/3} + \xi_o^2 = \text{const}\ (t^2 + t_o^2) \tag{3}$$

where t_o is the constant which is proportional to $\epsilon^{-2/3}\xi_o^{1/3}$. When t becomes so large that the relative motion of the two particles no longer depends on the initial separation ξ_o, the function F becomes constant and

Equation (2) yields

$$\xi^2 = \text{const} \cdot \epsilon t^3 \tag{4}$$

In order to test the proposition that α^2 is proportional to ξ^2 whose change with time is predicted by (3) and (4), the values of α^2 determined from the experiments off New Jersey and on the Bahama Bank (Costin, 1963) are plotted against time in Fig. 1. Here the theoretical curves given by Equations (3) and (4) are also plotted for comparison. Since t_o in Equation (3) depends on the initial condition of dye patches, its value is different for different sets of experiments. Therefore, the curves for Equation (3) are constructed for $t_o = 0$, 200, 300 and 500 min. respectively. Although experimental data are rather scattered, it can be seen in this figure that the increase of α^2 is slow at first and obeys a t^3 - law in the later stage. The data on the South Bahama Bank is exceptional. The difference of values of α^2 between off New Jersey and the Bahama Banks indicates that the dissipation rate of turbulent energy is much larger in the former area. In fact, the Bahama Bank is so shallow that available energy for turbulence is very low.

3. Elongation and Striation of Dye Patches

In most cases, dye patches became elongated a half to one hour after dumping in the direction which was usually parallel to surface currents. Such elongation may be caused partly by anisotropic turbulence or elongation of energy containing eddies in the direction of the mean flow as verified experimentally in a shear flow (Townsend, 1958) and partly by the effect of the vertical shear of mean flow which advects dye with vertically different velocity (Ichiye and others, 1964). The second effect was obvious in many aerial photographs of dye patches which indicate the head and tail. The head has the highest concentration of dye near the surface and moves ahead, while the tail trails behind the head with dye sinking below the surface as indicated occasionally by stirring up a band of dye when a boat crossed the tail part. This effect was analytically discussed by solving the Fickian diffusion equation with constant and vertically variable horizontal current respectively (Ichiye and others). The concentration of dye in aerial photographs is expressed by the vertical integration with weight of the actual concentration. It was shown by numerical integration that the apparent concentration contours become elongated in the direction of the mean current when the advective current is variable with depth.

Another conspicuous feature observed in many dye patches is striations which, in most cases, are almost parallel to the wind direction. They have almost regular spacings of an order of 100 m when the wind is steady. Two examples of dye patches which indicate such striations are shown in Fig. 2 which is reproduced by sketching the aerial photographs taken in the

experiments made on September 11 and 12, 1963 south of Long Island at about 40° N 72.5° W (Ichiye, 1964). These striations may be produced by helical vortices whose axes are parallel to the wind as explained by Langmuir (1938) and Faller and Woodcock (1963) for the alignment of rows of Sargassum along the wind direction. There are several discussions about causes of such helical vortices but none of them is satisfactory. Welander (1962) explained that an organic surface film is accumulated along the wind. This reduces the surface roughness. Thus, the wind over the band of the film becomes faster, producing wind streaks. However, rather regular spacings, deep penetration and slow response to the wind of the striations of dye patches are contrary to Welander's theory (Ichiye, 1963). Ichiye (1964) proposed a theory in which the alternative rough and smooth surface is explained from observed "two-peaked" directional spectrum (Longuet-Higgins). Then, streamlines of cellular motion due to the periodic change of surface roughness was derived. Ichiye and others (1964) also considered an applicability of roll-type instability discovered by Faller (1963) in the rotating tank as a cause of striations. The Reynolds number of a rotating boundary layer in most dye patches exceeds the critical value of generation of instability determined by Faller.

4. Curvature of Dye Patches

The most remarkable feature of dye patterns is a pronounced curvature of the tail, as indicated by the patch of September 11 in Fig. 2. In most cases, this curvature is clockwise from the head to the tail as the patch increases its depth and it occurred in waters deeper than about 20 m and for moderate to strong winds.

Since many aerial photographs showing the curvature were taken obliquely from the sea surface, there is a possibility that the refraction at the sea surface may cause a distorted image of a submerged object. The equation of an image at the surface was derived by use of Snell's law when a submerged straight line extending from the sea surface at Point P with an angle θ to the depth is seen from above. The line of sight to P makes an angle ϕ with the sea surface. The image has a slight curvature clockwise from the surface to the depth. For instance, the computed radius of curvature of the image at the sea surface is about eighty times height of the eyesight for $\theta = 5.7°$ and $\phi = 45°$ (Ichiye and others, 1964). However, this can hardly explain a large curvature observed in dye patches whose radius of curvature is sometimes less than 1 km.

Since a dye patch becomes deeper from head to tail, the curved pattern seems to be caused by an advective current whose direction and velocity are variable with depth. Further, the predominance of clockwise curvature from head to tail in many dye patches seems to be due to the effect of vertically differential advection in the upper Ekman flow. In fact, the friction depth D for eddy viscosity of 10 cm^2 sec^{-1} is equal to 14 m from a relation $D = \pi (2K/f)^{1/2}$ where K is vertical eddy viscosity and f is Coriolis coefficient. Within this depth the vector of horizontal currents changes its direction by 180°, producing a pronounced clockwise curvature in the projection of the hodograph on the sea surface. Another evidence of the Ekman current as a cause of curved dye patches is a series of aerial photographs taken by B. Katz (1965) in the southern hemisphere off the Argentine coast. One of these pictures is shown in Fig. 3 together with one taken in the New York Bight. The two pictures indicate that the curvature of the tail is clockwise and counterclockwise in the northern or southern hemisphere respectively. The smallness of curvature may be due to shallowness and high eddy viscosity as discussed below.

It is striking that the two patches shown in Fig. 2 indicate quite different features for the first patch with a strongly curved tail and the second one with a rather straight tail although the experimental procedure and the place were almost identical. The difference in environmental situations in those two days was that the wind was 11 to 14 knots from directions of east to southeast during the experiment on September 11, while on the next day it was 20 to 30 knots from the south. Such difference in the wind speed seemed to cause the different degree of vertical mixing. The fluorometer measurements indicated that dye was diffused only above 10 meters during the first day while it penetrated deeper than 20 m the next day. The increased eddy viscosity may reduce the curvature of a dye patch in a shallow water in two ways: Firstly, the larger the eddy viscosity, the deeper becomes the Ekman layer. Since from the air only dye above a certain depth can be seen, the apparent dye patch may be in the upper portion of the Ekman spiral where the curvature is very small. Secondly, when the frictional depth becomes deeper than the actual depth, the hodograph of the wind drift becomes almost a straight line (Defant, 1961). This is indicated in the lower part of Fig. 4. Three sets of hodographs are computed from Ekman's theory of pure drift currents in the sea of 50 meter depth (h) for frictional depths (D) of 4 h, 2h and 0.8 h, corresponding to the eddy viscosities of 2×10^3, 5×10^2 and 10^2 (cm^2 sec^{-1}), respectively (Ichiye, 1964). The upper curve of Fig. 4 indicates the hodograph of the drift current for an eddy viscosity decreasing exponentially with depth as $\eta_o \exp(-\gamma z)$. In this case the equation for the vertical distribution of velocity is expressed by

$$u + iv = i2TZ\beta^{-1}(m_2 n_1 - m_1 n_2)^{-1}\left\{n_2 H_1^{(1)}(\beta Z) - n_1 H_1^{(2)}(\beta Z)\right\} \qquad (5)$$

for the boundary conditions that the wind stress τ is applied in the v-direction at the surface ($z = 0$) and that the current vanishes at $z = h$, where u and v are velocity components, $H_i^{(j)}$ is Hankel's function and

$$T = \tau(\gamma\eta_o)^{-1} \qquad \beta = (1-i)(2f/\eta_o)^{1/2}\gamma^{-1} \qquad Z = \exp(1/2 \cdot \gamma Z) \qquad (6)$$

$$m_j = H_o^{(j)}(\beta) \qquad n_j = H_1^{(j)}\left[\beta \exp(1/2 \cdot \gamma h)\right] \qquad (j = 1, 2)$$

The numerical constants for the curve of Fig. 4 are taken as $\eta_o = 25$ cm^2/sec., $\gamma = 10^{-2}$ cm^{-1} and $h = 50$ m. This functional form of the eddy viscosity corresponds to the semi-empirical formula obtained by Dobronklonsky (1947) and Shebalin (1957) for turbulence due to surface waves (Ichiye, 1962), yielding the numerical values of η_o and γ stated above for waves with length 13.6 m, height 0.5 m and period 3 sec. The important features of the velocity distribution given by (5) are that the velocity decreases quite rapidly with depth and that the curvature of the hodograph is very strong even near the surface, contrary to the case of constant eddy viscosity as seen from Fig. 4 (Ichiye, 1964).

The curvature of an image of a dye patch at the sea surface can be expressed by the vertical eddy viscosity K(z), the mean current and its shear u, v, u_z and v_z when it is assumed that the initial dye filament extending vertically downwards is horizontally advected by stationary currents corresponding to the equation of motion

$$f(-v + iu) = (d/dz)\left\{K(z)(d/dz)(u + iv)\right\} \qquad (7)$$

without horizontal diffusion (Ichiye, 1963; Ichiye and others, 1964). If we take X and Y as the coordinates of the projection of the filament after time t on the sea surface, X and Y can be expressed by

$$X + iY = (u + iv)t \qquad (8)$$

for the steady state. The radius of curvature R(z) of the projection of the filament on the surface is given by

$$R(z) = \left|X_{zz}Y_z - X_z Y_{zz}\right|^{-1}(X_z^2 + Y_z^2)^{3/2} \qquad (9)$$

Substitution of Equation (7) and (8) into (9) yields

$$R(z) = f^{-1} K(Z) t \left\{ (d/dz)(u^2 + v^2) \right\}^{-1} (u_z^2 + v_z^2)^{3/2} \tag{10}$$

Equation (10) indicates that the radius of curvature increases with the eddy viscosity and time after release of dye. It also gives an approximate value of K(z) from the curvature of aerial photographs of dye patches when vertical profiles of currents are known.

Concluding Remarks

Dye techniques may be utilized effectively in many areas either to determine the gross features of diffusion or to obtain fine structures of near surface circulation which have been difficult to measure with conventional methods. However, a number of problems which are both technical and theoretical have been brought up from many field experiences on dye techniques. Firstly, a more rapid method of measuring concentrations than the present shipborne fluorometer method is necessary to know details of turbulence and circulation. We are now testing a new field procedure in which a densitometer will be used to determine dye concentration from vertical aerial photographs which are taken simultaneously with fluorometer measurements. Secondly, in order to determine relationships between diffusion of dye patches and turbulence characteristics, currents must be measured at close intervals of space and time concurrently with dye experiments. Such data will yield information on oceanic diffusion in terms of statistical structures of turbulence. So far most conventional methods of current measurement have been found unsuitable for this purpose. Construction of an instrument similar to "turbulimeter" used by the Russian oceanographers (Kolesnikov and others, 1958; Ichiye, 1962) would be highly desirable. Thirdly, vertical structures of dye patches must be determined by measurement of concentration and/or by underwater photography in order to determine detailed structure of the upper circulation with dye techniques. Fourthly, repeated experiments at the same place using the same techniques are necessary in order to obtain statistical features of diffusion.

Acknowledgment

The research reported in this paper was supported partly by the Atomic Energy Commission through Contract AT (30-1) 2663 and partly by the Office of Naval Research through Contract Nonr 266(48).

REFERENCES

Batchelor, G. K. (1950) The application of the similarity theory of turbulence to atmospheric diffusion. Quart. J. Roy. Meteorol. Soc. 76, 133-146

Costin, J. M. (1963) Dye diffusion experiments on the Bahama Banks. Tech. Rep. No. CU-6-63, Lamont Geol. Obs. of Columbia Univ. (unpublished manuscript)

Costin, J. M., P. Davis, R. Gerard and B. Katz (1963) Dye diffusion experiments in the New York Bight. Tech. Rep. No. CU-2-63, Lamont Geol. Obs. of Columbia Univ. (Unpublished manuscript)

Defant, A. (1961) Physical Oceanography, Vol. I, Pergamon Press

Dobroklonsky, S. V. (1947) Turbulent viscosity in the surface layer of the sea and swell. Doklady Akad. Nauk. USSR 58(7)

Faller, A. J. (1963) An experimental study of the instability of the laminar Ekman boundary layer. J. Fluid. Mech. 15, 560-576.

Faller, A. J. and A. H. Woodcock (1964) The spacing of wind rows of Sargassum in the ocean. J. Mar. Res. 22(1) 22-29.

Gifford, F. (1957) Relative atmospheric diffusion of smoke puffs. J. Met. 14, 410-416.

Ichiye, T. (1962) Oceanic turbulence (Review) Tech. Paper No. 2 of Oceano. Inst. of Florida State Univ. for the Office of Naval Research, pp. 200

Ichiye, T. (1963) Some comments and prospectives on dye diffusion experiments. Tech. Note for AEC and ONR, Lamont Geol. Obs. of Columbia Univ., pp 11 (unpublished manuscript)

Ichiye, T. (1964) On a dye diffusion experiment off Long Island. Tech. Rep. No. CU-9-64 to ONR and No. CU-10-64 to AEC, pp 19 (unpublished manuscript)

Ichiye, T., H. Iida and N. B. Plutchak, (1964) Analysis of diffusion of dye patches in the ocean. Tech. Rep. No. CU-8-64 to ONR and No. CU-9-64 to AEC pp. 16 (unpublished manuscript)

Katz, B., R. Gerard and M. Costin (1965) Response of dye tracers to sea surface conditions. Tech. Rep. No. CU-22-65 to AEC pp. 16 (unpublished manuscript)

Kolensnikov, A. G. and others (1958) Equipment and methods used in recording turbulent microfluctuations of the temperature and current velocities in the sea. Izvestia Akad. Nauk USSR Ser. Geofis. 405-413

Langmuir, I., (1938) Surface motion of water induced by wind. Science 87, 119-123

Shebalin, O. D. (1957) Eddy viscosity induced by waves in a shallow sea, Trudy Akad. Nauk. USSR 116(4) 591

Townsend, A. A. (1956) The Structure of Turbulent Flow, Cambridge Univ. Press.

Welander, P. (1963) On the generation of wind streaks on the sea surface by action of surface film. Tellus 15, 33-43

EXPLANATION OF FIGURES

Figure 1 — The second moment of concentration α^2 versus time from dye experiments at Bahama Banks (BBN and BBS respectively for a northern and southern part) and off New Jersey. (Theoretical curves designated with I represent those proportional to t^2 with $t_o = 0$, 200, 300 and 500 (min) respectively for Ia, Ib, Ic and Id. The curves designated with II are proportional to t^3.

Figure 2 — Sketches of dye patches based on aerial photographs taken south of Long Island. The figures near each picture indicate the time the photograph was taken. Scales of the dye patches were determined by comparison with the research ship.

Figure 3 — Aerial photographs of two dye experiments. (The left picture was taken on May 5, 1964 in the New York Bight, 16 km from shore (about 40° N) in water 28 meters deep with wind of 4 m/sec. The right one was taken on July 27, 1964, 47 km off the Argentine Coast (about 38° S) in water 80 meters deep with wind of 5 m/sec. The arrow indicates wind direction. The scales and the time elapsed after release of the dye are different for these pictures).

Figure 4 — Hodographs of wind-driven currents. (The depth of each velocity is indicated by meters). (A) for an eddy viscosity decreasing exponentially with depth. (B) for different values of the constant eddy viscosity.

Discussion after Ichiye's paper

Comments: Pritchard showed aerial photographs of dye patches (in shallow waters off Cape Kennedy) with similar clockwise curvature, indicating the Ekman spiral effect. Ichiye referred to pictures taken off Argentina by B. Katz, which indicate reversed curvature. It was confirmed by both that the Ekman spiral can develop in shallow waters if there is stable stratification.

FIG. I

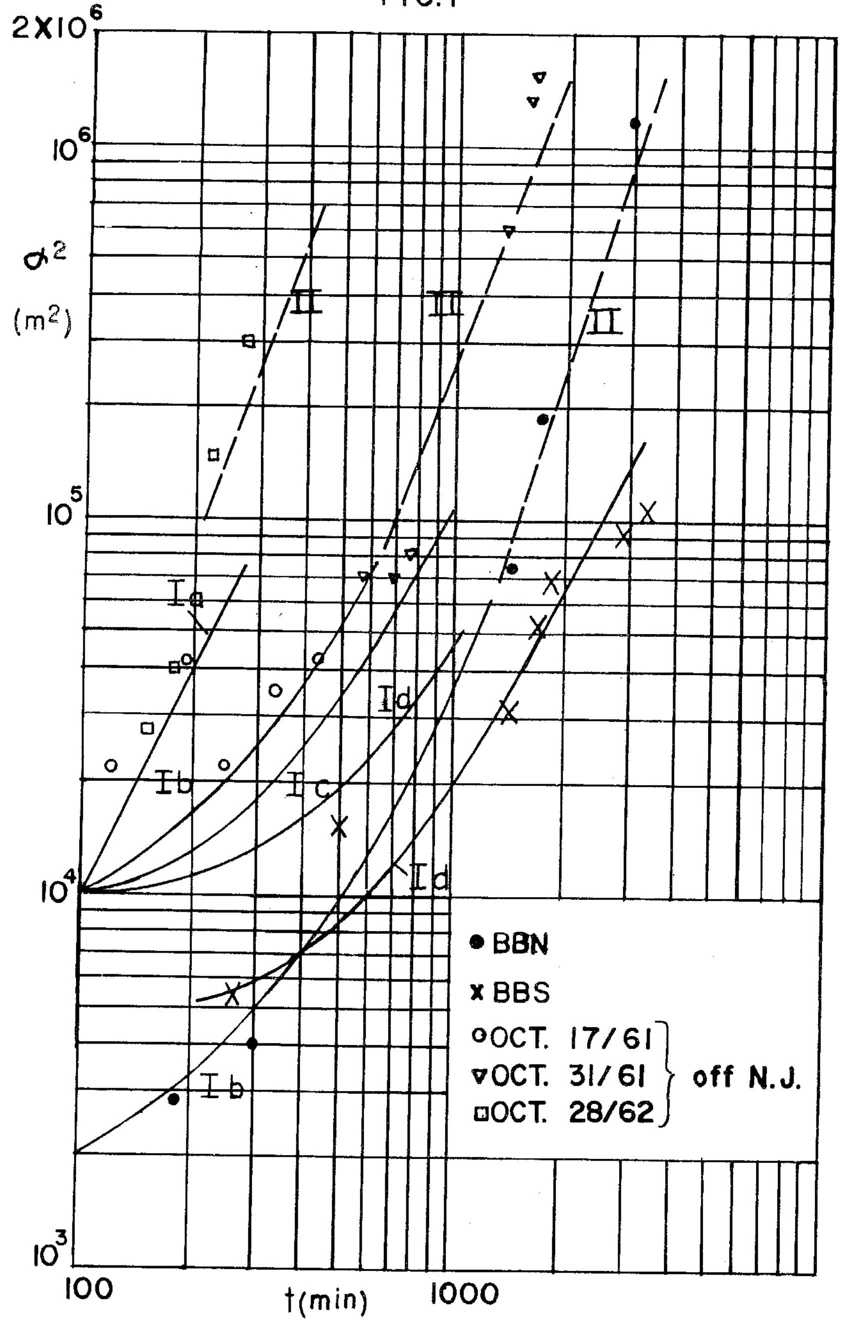

64

Fig. 2

65

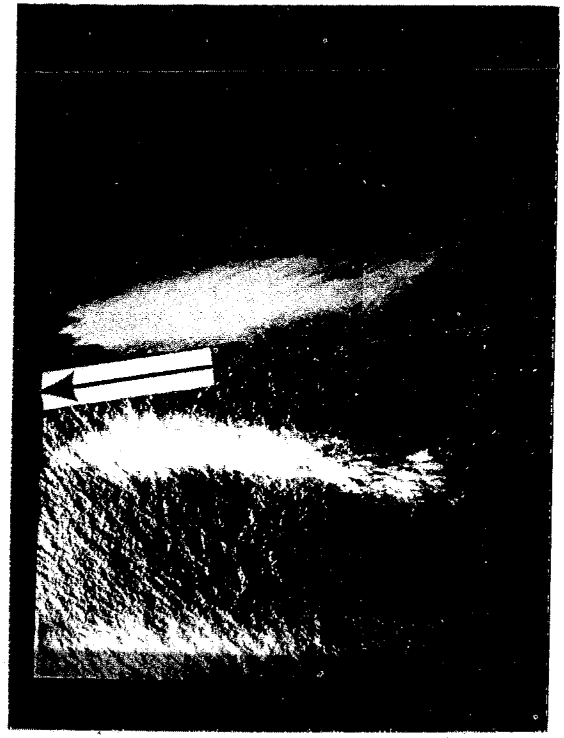

Fig. 3

FIG. 4

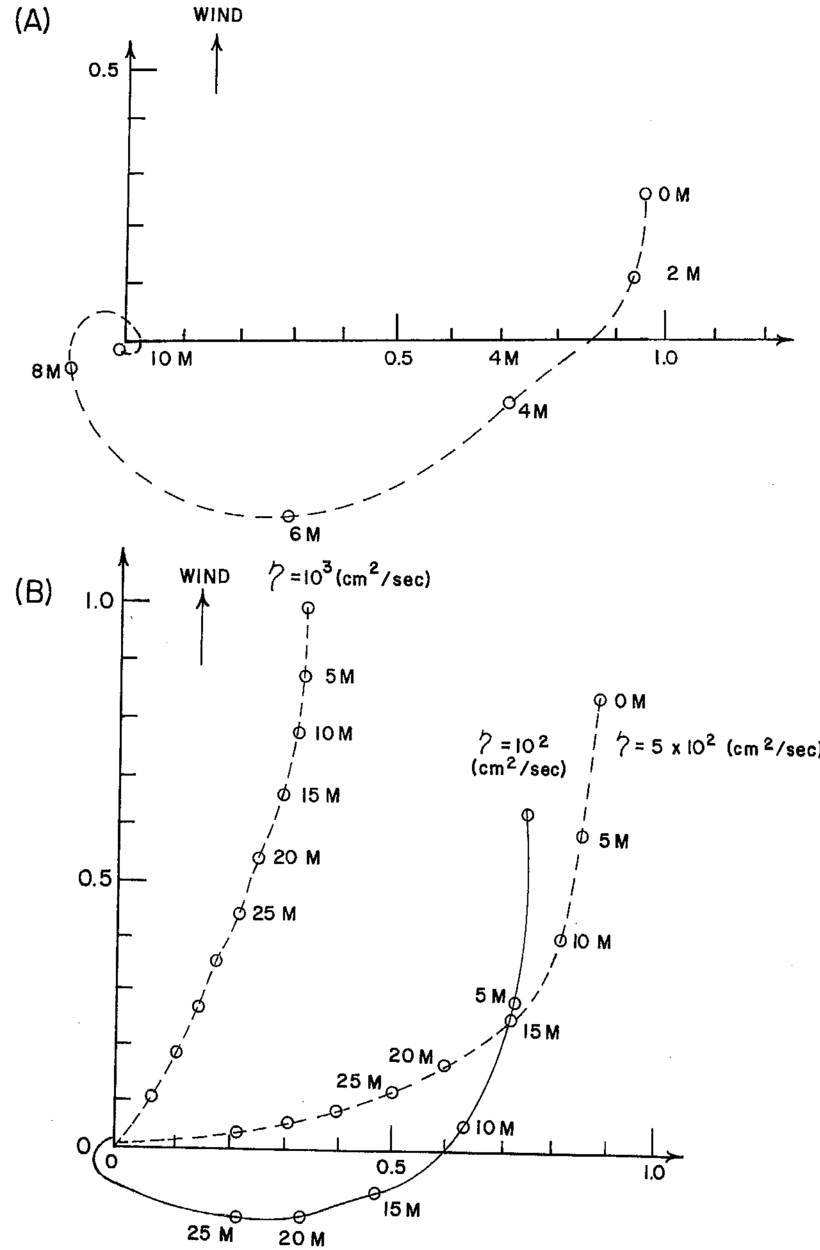
(A)
WIND
0.5
0.5
1.0
0 M
2 M
4 M
4 M
6 M
8 M
10 M
(B)
WIND
$\nu = 10^3$ (cm²/sec)
$\nu = 10^2$ (cm²/sec)
$\nu = 5 \times 10^2$ (cm²/sec)
1.0
0.5
0
0
0.5
1.0
0 M
5 M
10 M
15 M
20 M
25 M

DYE TRACER STUDIES ON THE BAHAMA BANKS*
(Summary)

J. Michael Costin
Lamont Geological Observatory of
Columbia University, Palisades, N. Y.

Dye diffusion experiments were conducted on the Great Bahama Banks in August, 1962. In two sets of experiments, 144 and 126 kilograms of Rhodamine B dye in 40 per cent acetic acid-methanol solution were introduced into the surface water northwest of Andros Island at 25° 30' N, 78° 27' E and 25° 01' N, 78° 32' E on August 10 and 13, respectively. The dye concentration at two-meter depth of each patch was monitored with a Turner fluorometer Model III for about fifty hours after dye introduction in order to determine contours of concentration at different times. Five and seven sets of transects of the patches were made on the August 10th and 13th experiment, respectively. Each set was made within a period averaging 1.9 and 1.4 hours and consisted of about 10 and 11 transects in the August 10th and 13th experiment, respectively. Aerial photographs with a 77A Wratten filter were taken frequently during the daylight hours. Since the area of the experiments is uniformly shallow with a depth of five meters and currents are weak with speed less than one-half knot, the dye patches did not show irregular patterns but elongated with the ratio of a long to short axis of 2 to 2.4 in a direction parallel to the major axis of the tidal ellipse. The areas enclosed by the contour of threshold concentration (0.05 ppb) and the maximum measured concentration are shown for different times after time of dye introduction in the following table:

Time (hrs.) after dump	7	10	25	50
Area (sq. mi.) Aug. 10th	0.1	6.4	1.5	~10
Max. Conc. (ppb)	>120	>120	50	5.2
Area (sq.mi.) Aug. 13th	0.25	0.5	1.2	2.0
Max. conc. (ppb)	>120	>120	113	49

Appendix

In order to measure dye concentration below the thermocline, a sensitive deep-towed fluorometer was developed by a group at Lamont Geological Observatory. The underwater unit consisting of fluorometer, depth and temperature transducers and associated electronics is housed in three pressure cases which, with a cast aluminum wing and tail fins, form the depressing body. The attached figure shows the underwater unit. The shipboard unit consists of a four-channel Sanborn recorder and three discriminators. The underwater unit can be towed with 3/8 inch faired cable to a depth of 200 meters or more at speeds up to eight knots.

In order to locate a thin tabular dye patch below the surface, an in-situ fluorometer has been developed by Lamont workers. The three basic units, light source, light detector and pressure transducer/pinger are interconnected but separately housed in water tight cases, each of which is about three inches in diameter and 16 inches long. The total weight is about thirty pounds. In operation, the high intensity pulsed light source illuminates the surrounding water through a circular window. The phototube controls the pulsing of a sonic pinger which increases the pinging rate whenever the phototube senses fluorescence above a pre-set level. The ship's echo sounder is used as a listening and recording device for signals from the pinger.

*(Adapted by the Editor from author's manuscript and notes prepared by R. Gerard, Lamont Geological Observatory)

LAMONT DEEP-TOWED FLUOROMETER

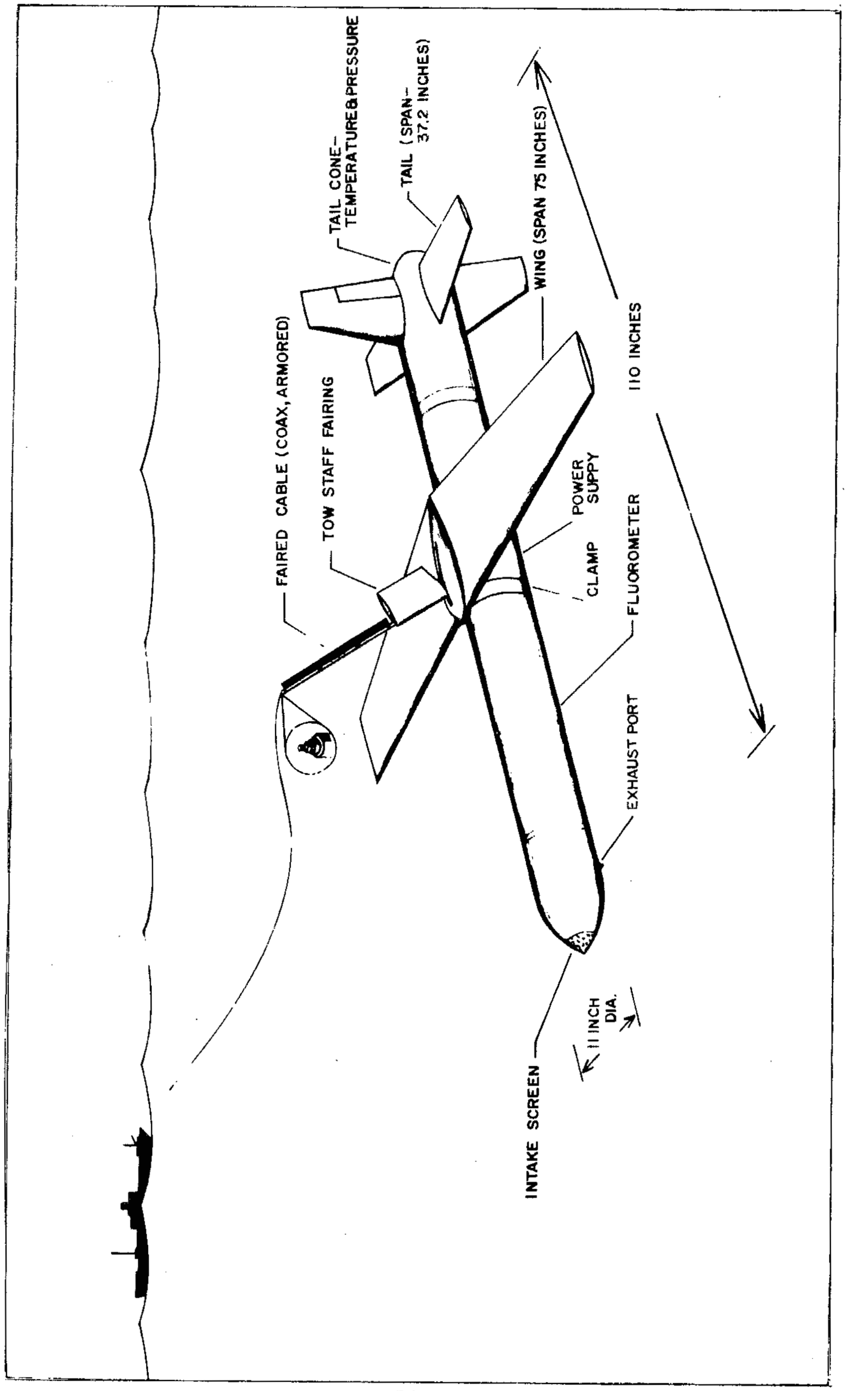

MULTI-DIMENSIONAL ASPECTS OF EDDY DIFFUSION
DETERMINED BY DYE DIFFUSION EXPERIMENTS IN COASTAL WATERS
(Summary)

James E. Foxworthy
Loyola University, Los Angeles, California
Richard B. Tibby and George Barsom
Allan Hancock Foundation, University of Southern California
Los Angeles, California

In this paper the authors present the results of a series of experiments on multi-dimensional diffusion conducted in the near shore coastal areas off Southern California. The principal objectives of those experiments were:

1. to verify some of the proposed multi-dimensional diffusion models as they pertain to the dispersion of dye discharged from instantaneous and continuous point sources in the ocean.

2. to determine the effects of wind speed and water column stability on the parameters controlling the diffusion process.

3. to determine the applicability of the point source models in item (1) to the case of diffusion of waste material from a large scale or volume source.

4. to propose, in the event the point source models did not apply, a solution for the problems of diffusion from one- and two-dimensional instantaneous and continuous volume sources in the ocean.

The first part of the paper deals with experiments on two- and three-dimensional relative diffusion of a patch of dye released from an instantaneous point source. By utilizing a continuous flow type fluorometer and specially designed underway sampling equipment, it was possible to ascertain the average spacetime distribution of fluorescent dye concentration in a diffusing patch. From these data the rates of diffusion (in terms of the mean square dispersion) were determined in the vertical and horizontal coordinate directions. It was found that the decrease in maximum dye concentration with time was proportional to the amount of dye initially released and inversely proportional to the square root of the overall rate of diffusion, as predicted by several statistical models of two- and three-dimensional relative diffusion.

The results of these experiments demonstrated the importance of the vertical component of diffusion on the decrease in maximum dye concentration with time. The rate of vertical diffusion is shown to be a function of wind speed and vertical stability of the water column. Experiments conducted on days with relatively high wind speed and/or low water column stability indicated that vertical diffusion played an important role in the overall dispersion process. For these conditions, it was found that Gifford's three-dimensional model for relative diffusion in a homogeneous and stationary turbulent field accurately described the rate of change of the maximum dye concentration. On days of relatively low wind and/or high water column stability, vertical diffusion was suppressed. For these conditions the horizontal diffusion models proposed by Joseph and Sendner, Schönfeld, and Okubo and Pritchard for the change in maximum dye concentration with time were shown to be valid.

The data from these experiments did not verify Batchelor's dimensional predictions regarding the relationship between the lateral rate of mean square diffusion. This leads to the conclusion that the so-called "four-thirds law" relating the lateral coefficient of eddy diffusion and average eddy scale does not hold at least in the particular oceanic areas investigated in these experiments.

The second part of this paper deals with one- and two-dimensional diffusion of a fluorescent dye discharged from a continuous source located in a dispersing surface waste field. The results of these experiments confirmed the findings of the experiments on relative diffusion pertaining to the influence of the vertical component of diffusion.

Experiments conducted on days of relatively high wind speed and/or low water column stability showed that Gifford's two-dimensional model for the decrease in maximum dye concentration along the center line of a steady plume in a homogeneous and stationary turbulent field was directly applicable. The results of these experiments also indicated that on days of relatively low wind speed and/or high stability, vertical diffusion is negligible, and the horizontal diffusion models proposed by Batchelor and Schönfeld give a more accurate description of the decrease in maximum dye concentration with distance (or time).

The results of a full-scale experiment in which an entire surface waste field was tagged with dye indicated that, because of differences in scale, the point source diffusion models were not directly applicable. Statistical models for multi-dimensional diffusion from instantaneous and continuous volume sources, as proposed by Gifford and extended by the authors, give a more realistic description of the observed phenomenon. These models were partially confirmed by the experimental data.

Copies of the original paper including a summary of experimental data, photographs, etc. can be obtained from the authors. A report on this work has been submitted to the California State Water Quality Control Board. The complete findings will be published as Report 29 titled "An Investigation on the Fate of Organic and Inorganic Wastes Discharged into the Marine Environment".

Discussions after Foxworthy's paper

Question: Can the sewage discharge itself be used as a tracer instead of dye?

Foxworthy: There are no substances in it that we know how to detect sensitively enough, although each of three outfalls discharges sewage of about 3×10^6 gal/day.

Pritchard noted that a mathematical model for sewage discharge must be treated as a problem of multiple point sources. He commented that mathematical theories based on point or line sources predict lower power dispersions than actually found in sewage field data whose sources are finite in size. This follows, because in point source theories effects of eddies with sizes smaller than the actual sources are eliminated from the start. He pointed out that the solution for volume sources may be obtained by integrating the point source solution. Foxworthy noted that Gifford's volume source solution may be applicable to his data.

A THEORETICAL MODEL OF DIFFUSION OF DYE PATCHES
(Summary)

Akira Okubo
Chesapeake Bay Institute, The Johns Hopkins University, Baltimore, Md.

We have noticed in dye-release experiments from instantaneous sources that dye patches are more or less elongated. In particular, dye patches show a tendency to elongate in the direction of mean flow. Apart from apparent effects due to boundaries, there seems to be two possible causes for such elongation. One cause may be anisotropy of the small-scale eddies responsible for diffusion of the patches; in other words, the turbulence is more intense in the direction of the mean current than across the mean current. The other cause may be the existence of large-scale eddies which provide a non-uniform velocity field on a scale larger than the size of the dye patches.

In this paper, the author analyzes the latter cause in some detail. A simplified model of dye diffusion is proposed in which the large-scale eddies are taken to be in quasi-steady state while the small-scale eddies are supposed to be random and statistically isotropic.

The two-dimensional transport equation for the present model is written as

$$\frac{\partial S}{\partial t} + \left(\alpha x + \frac{h-\eta}{2} y\right)\frac{\partial S}{\partial x} + \left(\frac{h+\eta}{2} x - \alpha y\right)\frac{\partial S}{\partial y} = K\left(\frac{\partial^2 S}{\partial x^2} + \frac{\partial^2 S}{\partial y^2}\right)$$

where S is the concentration of dye, t is time, x and y are coordinates relative to a certain point in the diffusing patch, and K is eddy diffusivity. Quantities α, h and η are stretching deformation, shearing deformation and vorticity, respectively at $x = y = 0$. They are expressed by

$$\alpha \equiv (\partial\bar{u}/\partial x) = -(\partial\bar{v}/\partial y) \qquad h \equiv (\partial\bar{v}/\partial x + \partial\bar{u}/\partial y) \qquad \eta \equiv (\partial\bar{v}/\partial x - \partial\bar{u}/\partial y)$$

The quantities K, α, h and η are taken as functions of t only.

The solution obtained, subject to an appropriate initial condition, e.g., point-source release ($S(o, x, y) = \Omega\,\delta(x)\,\delta(y)$) is

$$S(t,x,y) = \frac{Q}{4\pi P(t)} \exp\left\{-\frac{a(t)x^2 - 2b(t)xy + c(t)y^2}{4P^2(t)}\right\} \tag{1}$$

where $P(t)$, $a(t)$, $b(t)$ and $c(t)$ are somewhat complicated functions of t.

This solution, having a quadratic form in x and y, suggests that the contours of the concentration are a set of ellipses with common principal axes, the orientation of which changes with time. In addition to this, the total spread of the dye patch is determined by the combined effect of diffusion due to the smaller eddies and of convection due to the larger eddies.

In special cases where K, α, h and η are constant, Equation (1) is reduced to forms already found. For example, when α and h are zero but η is a non-vanishing constant, we have

$$S = Q(4\pi Kt)^{-1} \exp\left\{-(x^2+y^2)/4Kt\right\} \tag{2}$$

For the case of pure stretching deformation, in which h and η are zero and α is positive, we have (Townsend, 1951)

$$S = Q(4\pi K \sinh\alpha t/\alpha)^{-1} \exp\left\{-\frac{(x^2 e^{-\alpha t} + y^2 e^{\alpha t})}{4K \sinh\alpha t/\alpha}\right\} \tag{3}$$

For a flow with a simple shear, in which α vanishes and η equals in magnitude but opposite in sign to h, we find (Novikov, 1958)

$$S = Q\left(4\pi Kt\sqrt{1+h^2t^2/12}\right)^{-1} \exp\left\{-\frac{x^2 - ht\,xy + (1+h^2t^2/3)y^2}{4Kt(1+h^2t^2/12)}\right\} \tag{4}$$

Other characteristics of diffusion can also be deduced from Equation (1). Thus, in the case of constant parameters α, h, η and K, we can derive general diffusion characteristics for very small or very large values of time compared to t_c which is defined by $t_c = |h^2 + 4\alpha^2 - \eta^2|^{1/2}$.

When the time is very small, the principal axes of the diffusing patch are coincident with those of the strain quadric of the mean velocity. In a simple shear field, for example, the initial angle of orientation of dye patches will be forty-five degrees to the direction of the mean flow. The vorticity associated with the mean velocity has no effect on the orientation of the initial patch. In other words, the patch starts to diffuse most rapidly in the direction of the major principal axis of the strain.

We now consider the case where t is very large compared to t_c. The asymptotic behavior of the characteristics may be classified into two types depending primarily on the sign of $h^2 + 4\alpha^2 - \eta^2$. First, take the case where $h^2 + 4\alpha^2 - \eta^2 > 0$. The relative predominance of the deformation field over the rotational motion in the large-scale eddies is responsible for the eventual elongation of the dye patch. At the same time the combined effect of the non-uniform convective motion and of the small-scale diffusion tends to accelerate, to a great extent, the rate of dispersion of material. Thus, in a simple shear ($h^2 + 4\alpha^2 - \eta^2 = 0$), a very much elongated patch of dye will appear almost in the direction of the mean flow.

Now take the case where $h^2 + 4\alpha^2 - \eta^2 < 0$. The eventual shape of the patch is not necessarily very much elongated in this case. The more predominant the rotational motion over the deformation in the large-scale eddies, the more concentrated will be the shape of the patch. The apparent coefficient of diffusion attains a certain limiting value. One should note, in this case, that there is a unique and interesting relation between the angle of orientation of the patch in the initial period and that in the final period of diffusion, viz., the angle between them is $\pi/4$. No such unique relation exists in the case of $h^2 + 4\alpha^2 - \eta^2 > 0$.

In Fig. 1 we show schematically the temporal behavior of the characteristics in both cases. There exists a set of dye-release experiments which seems to support these theoretical results for the behavior of the characteristics. Costin (1963) reported two experiments carried out on the Great Bahama Bank. Judging from the movement of dye patches, we may consider that one experiment was conducted essentially under a simple shear associated with tidal currents, and the other was carried out under a rotating velocity field due to the combined effect of tidal currents and wind drift. The dye patch in the former experiment showed more elongation and a faster rate of diffusion than the patch in the latter experiment. It is seen that our model may account, at least qualitatively, for these phenomena.

Some quantitative comparisons of the theoretical results with observations were made by the author in three dye-release experiments. In each experiment dye concentration was found to be almost uniform vertically. Since there is some reason to believe that in dye-release experiments we frequently encounter a simple shear field, we selected a particular model of a constant shear in the comparison. Because of the lack of information about the mean shear in the experiments, the comparison was made as follows. From an observed value of the ratio of the semi-minor axis to the semi-major axis of a dye patch, we computed the corresponding value of shear on the basis of the theoretical model. We then calculated the corresponding angle of orientation and compared its value with that observed.

The comparisons are shown in Table 1. The agreement between θ calc and θ obs is fairly good. Furthermore, the computed values of shear Ω comp maintain a fairly constant level in each experiment, as required by the theoretical model.

The present model can be generalized to the three-dimensional case, where we must take into account the fact that the horizontal eddy diffusivity is very much larger than the vertical eddy diffusivity.

This work was supported by the U. S. Atomic Energy Commission and the Office of Naval Research.

TABLE I

Comparisons of Theoretical Results with Observations

Banana River (1964) (Chesapeake Bay Institute) (Simple Shear Model)

t (hr.)	ρ obs	θ obs(degrees)	Ω comp	θ calc (degrees)
3.9	0.8	40	3.2(x10^{-5}sec^{-1})	40
6.7	0.50	30	6.2	31
24.2	0.30	10~15	3.5	22
30.6	0.26	0~10	3.4	19
52.5	0.13	- 5~30	4.0	11

Irish Sea (Seligman, 1955)

t (hr.)	ρ obs	θobs(degrees)	Ω comp	θ calc (degrees)
3.5	0.61	55	7.9 (x10^{-5}sec^{-1})	36
7.0	0.36	35	9.7	25
12.5	0.29	25	6.9	22
15.5	0.31	15	5.2	23

Cape Canaveral (1962) (Chesapeake Bay Institute)

t (hr.)	ρ obs	θ obs (degrees)	Ω comp	θ calc (degrees)
7.7	0.31	50	1.0 (x10^{-4}sec^{-1})	23
54.0	0.09	10	4.6 (x10^{-5}sec^{-1})	9

(The Banana River and Cape Canaveral dye experiments were carried out by the Chesapeake Bay Institute.)

ρ obs : Observed value of the ratio of the semi-minor axis to the semi-major axis of the dye patch

θ obs, θ calc: Observed and calculated values of the angle of orientation of the dye patch, respectively.

Ω: Computed value of the magnitude of shear.

References

Costin, J. Michael (1963) Dye diffusion experiments on the Great Bahama Bank (unpublished) Lamont Geological Observatory Technical Report No. CU-17-65, L.G.O. of Columbia University, Palisades, N.Y.

Novikov, E. A. (1958) Concerning a turbulent diffusion in a stream with a transverse gradient of velocity. J. Appl. Math. and Mech., 22, P. 576-579 (translated from Russian) Pergamon Press, Inc., N.Y.C.

Seligman, H. (1955) The discharge of radioactive waste products into the Irish Sea. Peaceful Uses of Atomic Energy, Proc. Int'l. Conf. in Geneva, August, 1955, 9 p. 418.

Townsend, A.A. (1951) The diffusion of heat spots in isotropic turbulence. Proc. Roy. Soc. London, A 209, p. 418-430.

Discussions after Okubo's paper

Kirwan pointed out the lack of boundaries in Okubo's model noting that boundary influences are significant but often subtle in real situations and that the effects of boundaries depend on the type of differential equations used in a model.

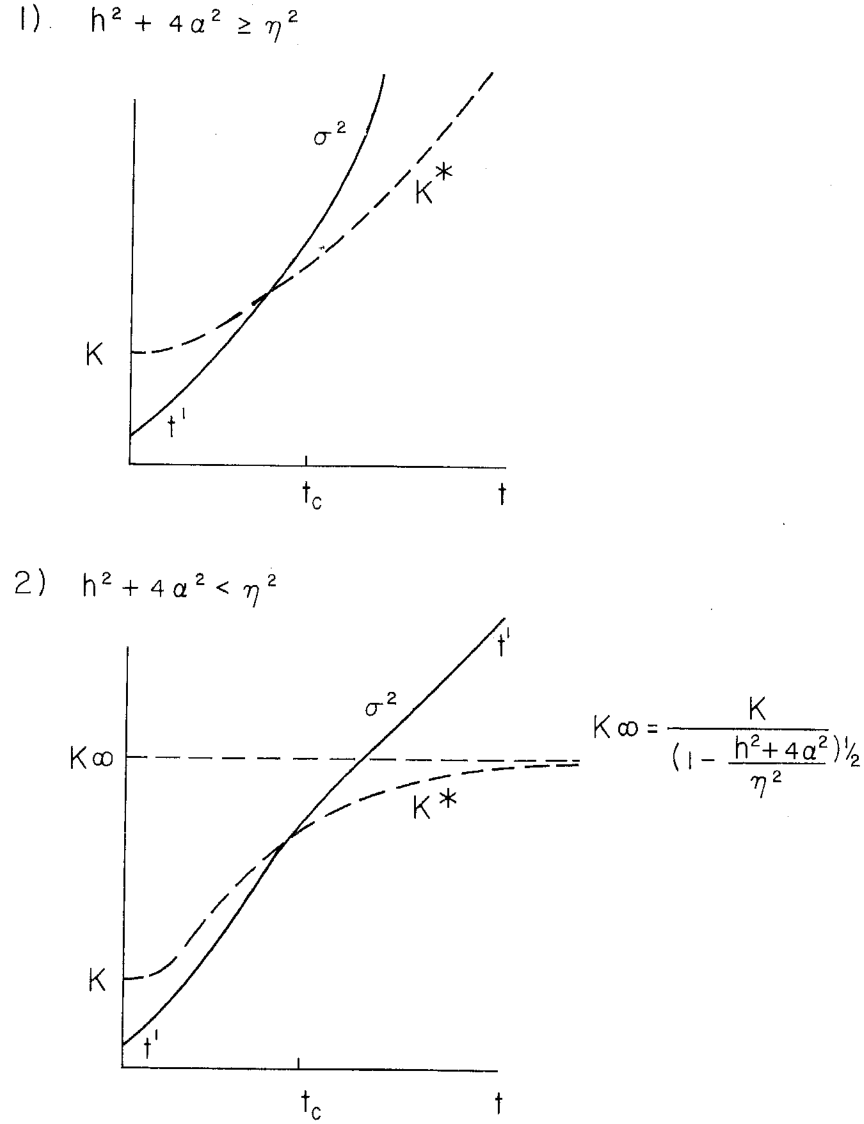

Figure 1 - Theoretical Behavior of the Characteristics of Diffusion with Time. σ^2: variance, K*: apparent coefficient of diffusion which is defined by $K^* = 1/2 \frac{d\sigma^2}{dt}$

THE SOLUTION OF THE CONTINUITY EQUATION IN CYLINDRICAL COORDINATES WITH DISPERSION AND ADVECTION FOR AN INSTANTANEOUS RELEASE

Donald J. O'Connor and Dominic M. DiToro*
Department of Civil Engineering, Manhattan College, Riverdale, N.Y.

Abstract

The continuity equation for concentration of mass is derived for a one-dimensional estuary whose cross-sectional area increases linearly with distance downstream. A solution of the equation for an instantaneous point source is obtained by use of Laplace transformation.

Fundamental Equation

The continuity equation is a mathematical statement of the principle of mass balance:

$$\nabla \cdot \vec{j} + \partial c/\partial t = 0 \tag{1}$$

where $\vec{j}$ is flux of mass, c is concentration of mass, and S is source of mass per unit time. The flux in an estuary is composed of two components: the dispersion, usually associated with tidal motion, and the advection, primarily associated with the fresh water flow. Assuming that the dispersion is proportional to the negative gradient of the concentration and that there are no sources or sinks of fluid, we obtain for Equation (1)

$$-E\nabla^2 c + \vec{U}\cdot\nabla c + \partial c/\partial t = S \tag{2}$$

The geometry of many estuaries can be represented by cylindrical coordinates, that is, the cross-sectional area increases linearly with distance downstream. Assuming the fresh water flow is radially directed in an estuary of this geometry, we rewrite Equation (2) as:

$$-(E/r)\partial(r\partial c/\partial r)/\partial r + U(r)\partial c/\partial r + \partial c/\partial t = S \tag{3}$$

The expression for $U(r)$ is obtained from the fresh water volumetric flow rate Q divided by the area at the point r. If s is the rate of increase of the cross-sectional area per unit distance downstream, and r is measured from the zero area point, then the cross-sectional area A at r is sr. Therefore, the velocity is given by

*Presently a graduate student, Dept. of Elect. Engr., Princeton Univ.

$$U(r) = Q/A = Q/sr \tag{4}$$

Since many substances are subject to a first order decay, a source which must be considered is

$$S = -Kc \tag{5}$$

where K is the first order decay coefficient.

We substitute Equations (4) and (5) into Equation (3). This yields:

$$-\frac{E}{r}\frac{\partial}{\partial r}\left(r\frac{\partial c}{\partial r}\right) + \frac{Q}{sr}\frac{\partial c}{\partial r} + \frac{\partial c}{\partial t} = -Kc \tag{6}$$

Solution for an Instantaneous Point Source

The solution obtained for an instantaneous release of mass is of fundamental importance. A boundary condition which must be satisfied for an instantaneous source of mass M released over a segment of cylindrical surface of cross-sectional area $A_o = sr_o$ at the point $r = r_o$ and time $t = 0$ is

$$\lim_{r\to r_o^-}\int_{A_1}\vec{j}\cdot\vec{n_1}\,dA + \lim_{r\to r_o^+}\int_{A_2}\vec{j}\cdot\vec{n_2}\,dA = M\delta(t) \tag{7}$$

where A_1 and A_2 bound A_o and $\vec{n}_1$ and $\vec{n}_2$ are respectively the outward directed normals. A second boundary condition is

$$\lim_{r\to r_o^-} c(r,t) = \lim_{r\to r_o^+} c(r,t) \tag{8}$$

Let us take the Laplace transform of Equations (6) and (7) with respect to time, using p as the transform variable. Then we have

$$-\frac{E}{r}\frac{d}{dr}\left(r\frac{dC}{dr}\right) + \frac{Q}{sr}\frac{dC}{dr} + pc - C(r,o) = -KC \tag{9}$$

where $C = C(r_o, r, p)$ and

$$\lim_{r \to r_0^-} \int_{A_1} \vec{J} \cdot \vec{n}_1 \, dA + \lim_{r \to r_0^+} \int_{A_2} \vec{J} \cdot \vec{n}_2 \, dA = M$$

where $\vec{J} = \vec{J}(r_o, r, p)$. From the boundary conditions we have $C(r, o) = 0$ for $r \neq r_o$ in Equation (9). Then Equation (9) can be written as

$$d^2C/dr^2 + (1-2v)\, dC/(r\,dr) - g^2 C = 0 \tag{10}$$

where $v = \Omega/(2Es)$ and $g^2 = (K + \rho)/E$.

In order to solve Equation (10) a substitution for both the dependent and independent variables will be used (McLachlan, 1961). Let $C = r^v U(Z)$ and $Z = gr$. Then Equation (10) becomes:

$$Z^2 d^2U/dZ^2 + Z\,dU/dZ - (Z^2 + v^2)U = 0 \tag{11}$$

which is the modified Bessel differential equation. (Erdelyi and others, 1963). The two linearly independent solutions are $I_v(Z)$ and $K_v(Z)$, modified Bessel functions of the first and second kind, respectively. Hence

$$C = A(p) r^v I_v(gr) + B(p) r^v K_v(gr) \tag{12}$$

where A(p) and B(p) are the arbitrary functions of p. These functions are analogous to the arbitrary constants in the solution of an ordinary differential equation. These functions are evaluated using the boundary conditions.

It is necessary that the concentration be finite within the region of interest. At both $r = 0$ where $K_v(gr) \to \infty$ and $r \to \infty$ where $I_v(gr)$ this condition is violated. The solution must, therefore, be given in two parts. For convenience, choose r_o as the dividing point. Equation (12) becomes

$$C_1 = A(p) r^v I_v(gr) \; : \; r < r_o \tag{13}$$

$$C_2 = B(p) r^v K_v(gr) \; : \; r > r_o \tag{14}$$

To express the boundary condition on the flux, let

$$\vec{J}_1 = -E(dC_1/dr)\vec{1}_r + \vec{U} C_1 \tag{15a}$$

$$\vec{J}_2 = -E(dC_2/dr)\vec{1}_r + \vec{U} C_2 \tag{15b}$$

Since $\vec{n}_1 = \vec{1}_r$ and $\vec{n}_2 = \vec{1}_r$, the boundary condition on flux becomes:

$$-\lim_{r \to r_0^-} \int_{A_1} \vec{J}_1 \cdot \vec{1}_r \, dA + \lim_{r \to r_0^+} \int_{A_2} \vec{J}_2 \cdot \vec{1}_r \, dA = M \tag{16}$$

The boundary condition on the concentration itself states that

$$\lim_{r \to r_0^-} C_1(r_0, r, p) = \lim_{r \to r_0^+} C_2(r_0, r, p)$$

That is

$$A(p) I_v(gr_0) = B(p) K_v(gr_0) \tag{17}$$

Using this condition in Equation (16), we find

$$\lim_{r \to r_0^-} \int_{A_1} \left(E \frac{dC_1}{dr}\right) dA + \lim_{r \to r_0^+} \int_{A_2} \left(-E \frac{dC_2}{dr}\right) dA = M \tag{18}$$

or

$$\lim_{r \to r_0^-} \frac{dC_1}{dr} - \lim_{r \to r_0^+} \frac{dC_2}{dr} = \frac{M}{EA_0}$$

since the integrands are constant over A_1 and A_2.

Substituting the expressions for C_1 and C_2, we obtain

$$A(p) v r_0^{v-1} I_v(gr_0) + r_0^v g I_v'(gr_0) + B(p) v r_0^{v-1} K_v(gr_0) + r_0^v g K_v'(gr_0) = M/EA_0 \tag{19}$$

where the primes denote differentiation with respect to the argument. Solving the above equations and Equation (17) for A(p) and B(p), and making use of the following relationship between modified Bessel functions (Erdelyi and others, 1953)

$$I_\nu(Z)\,K_\nu'(Z) - I_\nu'(Z)K_\nu(Z) = -1/Z \tag{20}$$

we find

$$A(p) = (Mr_0/EA_0)\,r_0^{-\nu}\,K_\nu(gr_0)$$

$$B(p) = (Mr_0/EA_0)\,r_0^{-\nu}\,I_\nu(gr_0)$$

Hence the solution is:

$$C_1 = (M/E_S)(r/r_0)^\nu K_\nu(gr_0)\,I_\nu(gr) \quad ; \quad r < r_0 \tag{21}$$

$$C_2 = (M/E_S)(r/r_0)^\nu I_\nu(gr_0)\,K_\nu(gr) \quad ; \quad r > r_0 \tag{22}$$

To find the response to an instantaneous release in the time domain, the inverse Laplace transformations of Equations (21) and (22) are needed. Using the following transform pair and the shifting theorem (Erdelyi and others, 1954)

$$\mathcal{L}\left\{\frac{1}{2t}\,e^{-(a+b)/2t}\;I_\nu\left(\frac{a-b}{2t}\right)\right\} = K_\nu(\sqrt{a}\,p + \sqrt{b}\,p)\,I_\nu(\sqrt{a}\,p - \sqrt{b}\,p)$$

$$\mathcal{L}\left\{e^{-Kt}\;f(t)\right\} = F(p+K)$$

we arrive at the solution

$$c(r_0,r,t) = \frac{M}{2Est}\left(\frac{r}{r_0}\right)^\nu \exp\left(-\frac{r^2+r_0^2}{4Et} - Kt\right) I_\nu\left(\frac{rr_0}{2Et}\right) \tag{23}$$

Acknowledgment

The work reported in this paper was supported by a research grant from the National Science Foundation. The junior author was a participant of the National Science Foundation Undergraduate Research Participation Program.

References

Erdelyi, A. (Edited by) (1953) Higher Transcendental Functions, Vol. 2, McGraw-Hill Co., New York

Erdelyi, A. (Edited by) (1954) Tables of Integral Transform, Vol. 1, McGraw-Hill Co., New York

McLachlan, N. W. (1961) Bessel Functions for Engineers, 2nd Edition, Oxford University Press, London.

(Added by the Editor to O'Connor's paper)

O'Connor discussed some applications of the theory in detail. The experimental data on the change of dye injected uniformly in the Delaware River model of Corps of Engineer Laboratory at Vicksburg indicated a good agreement with the one-dimensional theory. A dimensionless parameter $\nu = ur/2E$ was used, in which u is the water velocity, r is the distance from dye source and E is diffusion coefficient. In order to apply his theory to the East River, seventeen sources are superposed as inputs along the river. Since the theory is linear, such superposition is allowable. Thus, the theory can predict the variation of oxygen along the river in a good agreement with the experimental data. Since the East River is almost anaerobic, new sewage treatment plants will not cause drastic increase in oxygen, but they will definitely help. Also, an application to the James River was discussed. He pointed out that expense of needed sewage plants is about \$10 x 10^7 in New York City alone.

Discussion

O'Connor noted that from a practical point of view of sewage disposal, the variations of diffusion coefficients within an order of magnitude does not strongly affect outfall design and that advective effects are more crucial. Kirwan amplified on this, remarking that in some cases change of diffusion coefficients of three orders of magnitude does not outweigh advective effects and that the input pumping rate is another important factor.

Foxworthy pointed out that constant diffusion coefficients result in conservative estimates of dilution, which is good from a practical point of view.

ON THE USE OF THE RAYLEIGH-RITZ METHOD FOR CALCULATING THE EDDY DIFFUSIVITY*

A. D. Kirwan, Jr.
New York University, Bronx, New York City

Abstract

A variational equation is derived from the diffusion equation containing non-uniform mixing coefficients and fluid velocities. The space distribution of vertical and horizontal mixing coefficients in the Antarctic Intermediate Water is determined by numerically solving the equation with the Rayleigh-Ritz method. In this calculation, salinity and geostrophic velocity obtained by the METEOR Expedition are utilized. Vertical and horizontal coefficients show a minimum and maximum, respectively at the layer of high stability.

Introduction

The mathematician Von Neumann conjectured that the difficulty in solving the hydro-thermo-dynamic equations arises from the lack of a variational principle and not from their non-linear character. Variational formulations provide an extremely useful theoretical tool for understanding physical processes. Moreover, they also provide a basis for rather elaborate numerical calculations.

One area in oceanography where the numerical or practical approach may be particularly useful is in the evaluation of the eddy diffusivity. The present trend in these studies is to hypothesize some limited space or time dependency of the eddy diffusivity and then solve the resulting equations. Verification is made by comparing the concentration field predicted by the model with what was observed. Okubo (1963) has derived most of the better known approaches. The paper he presented at this symposium appears to be an interesting and valuable contribution to this method of attack.

An alternative approach would be to infer the space-time dependency of the eddy diffusivity through the characteristics of the velocity and concentration fields. The purpose of this paper is to present one such method for evaluating the diffusivity. This method utilizes a numerical technique, frequently referred to as the Rayleigh-Ritz method, which has proven to be extremely useful in solving variational problems.

Formulation of the Problem

The diffusion equation or the equation expressing the conservation of an added constituent s, neglecting molecular diffusion and in the absence

*Contribution No. 31 of the Geophysical Sciences Laboratory, Department of Meteorology and Oceanography, New York University, Bronx 53, N. Y.

of sources, can be expressed as

$$\frac{\partial}{\partial t}(\overline{\rho s}) + [\overline{\rho s}\,\overline{U}^i]_{,i} = (K^{ij}\bar{s}_{,j})_{,i} \tag{1}$$

In this equation, the overbar represents the ensemble average, ρ is the fluid density and $U^i = \overline{U}^i + u^i$ the fluid velocity. It has been assumed that the turbulent or eddy flux of s, $\overline{\rho s u^i}$ can be expressed in terms of an operator, $(K^{ij})_{,j}$ acting on the salinity gradient. Finally, the convention is employed that repeated covariant and contravariant indices imply a summation over the range of the index.

For present purposes, the left-hand side of Equation (1) and the salinity gradient term $\bar{s}_{,j}$ are regarded as known functions. The interpretation of the eddy mixing in terms of an operator, whose functional form is unknown, suggests employing the technique of Wiener (1949), or Solodovnikov (1960) for determining the optimum transfer function. This requires minimizing

$$(K^{ij}; K^{ij}_{,i}) = \left(\frac{1}{t_1 - t_0}\right)\left(\frac{1}{V}\right)\int_{t_0}^{t_1}\iiint_V \left\{\frac{\partial}{\partial t}(\overline{\rho s}) + [\overline{\rho s}\,\overline{U}^i]_{,i} - (K^{ij}\bar{s}_{,j})_{,j}\right\}^2 dV dt \tag{2}$$

Here t_0 and t_1 are convenient averaging periods and V is the volume occupied by the fluid in question.

The calculation of the variation of Equation (2) with respect to the function K^{ij} and $K^{ij}_{,j}$ is straightforward. The resulting equation is

$$\delta I = \left(\frac{1}{t_1 - t_0}\right)\left(\frac{2}{V}\right)\int_{t_0}^{t_1}\iiint_V \left\{\left[\frac{\partial}{\partial t}\overline{\rho s} + (\overline{\rho s}\,\overline{U}^i)_{,i} - (K^{ij}\bar{s}_{,j})_{,i}\right]\left[s_{,mn}\,\delta K^{mn}\right] \right. \tag{3}$$

$$\left. + \left[\frac{\partial}{\partial t}\overline{\rho s} + (\overline{\rho s}\,\overline{U}^i)_{,i}\right] s_{,m}\,\delta K^{mn}_{,n}\right\} dV dt$$

For arbitrary and independent variations of K^{mn} and $K^{mn}_{,n}$ twelve integral equations are obtained for the twelve unknown functions. If the variations of $K^{mn}_{,n}$ are not taken as independent of those of K^{mn} then the resulting number of equations and unknowns is reduced by three.

In a previous paper the writer (Kirwan, 1964) attempted to integrate numerically a drastically simplified version of Equation (3). However, the numerical integration of multiple integrals is not easy and the results were not encouraging.

From a numerical point of view a more satisfactory technique may be to construct a minimizing sequence for Equation (2). This minimizing sequence contains various parameters which can be determined by minimizing the integral. The result is an equation similar to Equation (3) except that the variations are with respect to the parameters.

Application to Antarctic Intermediate Water

The procedure outline above was used to study the mixing characteristics of a portion of the Antarctic Intermediate Water. The region studied is centered around 10° N, 25° W of the Atlantic Ocean. The analysis utilized data from METEOR Stations 212-218, 220, 260-265, and 306-310.

The numerical model of eddy diffusion incorporated three assumptions. First, the ocean was taken as incompressible. Secondly, the ensemble mean values of the velocity was taken as geostrophic. Lastly, the off diagonal terms on the mixing tensor were taken a priori as zero while the non-zero elements were taken to be at most as function of the vertical coordinate. In addition, the horizontal components of K^{ij} were assumed to be equal.

The advection and salinity gradient terms were eveluated by an objective analysis procedure described by Kirwan (1963, 1964). The computer calculations were all made in spherical coordinates. In this paper, however, the physical coordinates or local Cartesian coordinates are used. The procedure for transforming between the two coordinate system is also summarized by Kirwan (1964).

Parabolas were taken as the minimizing sequences for K^{ij}. Thus, for

$$K^{1} = K^{22} = \sum_{k=0}^{2} a_k z^k ; \quad K^{33} = \sum_{k=0}^{2} b_k z^k$$

and the assumptions indicated above, Equation (2) becomes

$$I = \frac{1}{V}\iiint\left\{ \bar{U}\frac{\partial \bar{s}}{\partial x} + \bar{V}\frac{\partial \bar{s}}{\partial y} - \left(\sum_{k=0}^{2} a_k z^k\right)\left(\frac{\partial^2 \bar{s}}{\partial x^2} + \frac{\partial^2 \bar{s}}{\partial y^2}\right) - \left(\sum_{k=0}^{2} b_k z^k\right)\left(\frac{\partial^2 \bar{s}}{\partial z^2}\right) - \left(\sum_{k=1}^{2} k b_k z^{k-1}\right)\frac{\partial \bar{s}}{\partial z}\right\}^2 dV \tag{4}$$

V in this last equation represents the volume bounded above and below by the 27.00 and 27.60 sigma-t surfaces and laterally by the region under study. In the actual calculation the integration was replaced by a summation over the stations used in the analysis.

The integral in Equation (4) is a function only of the a_k's and b_k's. The variation of this equation with respect to these parameters leads to

$$\delta I = \frac{-2}{V}\iiint\left\{ \bar{U}\frac{\partial \bar{s}}{\partial x} + \bar{V}\frac{\partial \bar{s}}{\partial y} - \left(\sum_{k=0}^{2} a_k z^k\right)\left(\frac{\partial^2 \bar{s}}{\partial x^2} + \frac{\partial^2 \bar{s}}{\partial y^2}\right) - \sum_{k=0}^{2} b_k\left(z^k \frac{\partial^2 \bar{s}}{\partial z^2} + kz^{b-1}\frac{\partial \bar{s}}{\partial z}\right)\right\}\left\{\sum_{k=0}^{2} z^k \delta a_k \left(\frac{\partial^2 \bar{s}}{\partial x^2} + \frac{\partial^2 \bar{s}}{\partial y^2}\right) \sum_{k=0}^{2} \delta b_k \left(z^k \frac{\partial^2 \bar{s}}{\partial z^2} + k z^{k-1}\frac{\partial \bar{s}}{\partial z}\right)\right\} dV \tag{5}$$

For Equation (5) to be a minimum, each coefficient of δa_k and δb_k must be zero. This leads to six equations for the unknown a_k and b_k:

$$\langle Y Z_1\rangle = a_o \langle X_1^2\rangle + a_1 \langle z X_1^2\rangle + a_2 \langle z^2 X_1^2\rangle + b_o \langle X_2 X_1\rangle + b_1 \langle X_1(X_2 z + X_3\rangle + b_2 \langle z X_1(X_2 z + 2X_3)\rangle$$

$$\langle Y X_1 z\rangle = a_o \langle z X_1^2\rangle + a_1 \langle z^2 X_1^2\rangle + a_2 \langle z^3 X_1^2\rangle + b_o \langle X_1 X_2 z\rangle + b_1 \langle z X1(X_2 z + X_3\rangle + b^2 \langle z^2 X_1(X_2 z + 2X_3)\rangle$$

$$\langle Y X_1 z^2\rangle = a_o \langle z_1^2 X_1^2\rangle + a_1 \langle z^3 X_1^2\rangle + a_2 \langle z^4 X_1^2\rangle + b_o \langle X_1 X_2 z^2\rangle + b_1 \langle z^2 X_1(X_2 z + X_3)\rangle + b_2 \langle z^3 X_1(X_2 z + 2X_3)\rangle$$

$$\langle Y X_2\rangle = a_3 \langle X_1 X_2\rangle + a_1 \langle z X_1 X_2\rangle + a_2 \langle z^2 X_1 X_2\rangle + b_o \langle X_2^2\rangle + b_1 \langle X_2(X_2 z + X_3)\rangle + b_2 \langle z X_2(X_2 z + 2X_3)\rangle$$

$$\langle Y(X_2 z + X_3)\rangle = a_o \langle X_1(X_2 z + X_3)\rangle + a_1 \langle z X_1(X_2 z + X_3)\rangle$$
$$+ a_2 \langle z^2 X_1(X_2 z + X_3)\rangle + b_o \langle X_2(X_2 z + X_3)\rangle$$
$$+ b_1 \langle (X_2 z + X_3)^2\rangle + b_2 \langle z(X_2 z + 2X_3)(X_2 z + X_3)\rangle$$

$$\langle Y z(X_2 z + 2X_3)\rangle = a_o \langle X_1 z(X_2 z + 2X_3)\rangle + a_1 \langle z^2 X_1(X_2 z + 2X_3)\rangle$$
$$+ a_2 \langle z^3 X_1(X_2 z + 2X_3)\rangle$$
$$+ b_o \langle z X_2(X_2 z + 2X_3)\rangle + b_1 \langle z(X_2 z + X_3)(X_2 z + 2X_3 z)\rangle$$
$$+ b_2 \langle z^2(X_2 z + 2X_3 z)^2\rangle . \qquad (6)$$

In these equations

$$Y = \bar{U}\frac{\partial \bar{s}}{\partial x} + \bar{V}\frac{\partial \bar{s}}{\partial y}, \quad X_1 = \frac{\partial^2 \bar{s}}{\partial x^2} + \frac{\partial^2 \bar{s}}{\partial y^2}, \quad X_2 = \frac{\partial^2 \bar{s}}{\partial z^2},$$

$$X_3 = \frac{\partial \bar{s}}{\partial z}, \quad \text{and} \quad \langle f\rangle = \frac{1}{V}\iiint f\,dV .$$

Equations (6) can be solved for the a_k's and b_k's which in turn determine K^{11} or K^{22} and K^{33}. For the region under study, the results are

$$K^{11} = K^{22} = -26.20 \cdot 10^7 + 14.0 \cdot 10^3 z - 10^{-1} z^2$$

$$K^{33} = 1.78 - 5.16 \cdot 10^{-6} z + 3.82 \cdot 10^{-11} z^2 \qquad (7)$$

for the range $2.75 \cdot 10^4$ cm $\leqslant z \leqslant 11.75 \cdot 10^4$ cm.

It is interesting to note that these last equations indicate that K^{11}, the horizontal mixing coefficient, has a maximum at 700 meters and that the vertical coefficient, K^{33}, has a minimum at 676 meters. This region of depth corresponds to the core of the Intermediate Water and thus a region of relatively stable water (Schubert, 1935). Intuitively, one would expect high stability to inhibit the vertical mixing which in turn could enhance the lateral mixing.

Equations (6) are identical to the least squares normal equations which have resulted from expression Y as a linear function of the variables X_1, zX_1, z^2X_1, X_2, $(zX_2 + X_3)$, and $z(X_2 z + 2X_3)$. This interpretation makes it possible to calculate the confidence limits on the coefficients and the efficiency of the regression scheme in explaining the variance of the divergence of advection term. It was found that the multiple regression coefficient for the complete regression was 0.682 while if only a_o and b_o were retained the coefficient was 0.300. The effect of introducing the standard error of estimate for the a_k's and b_k's in Equations (7) resulted in a maximum difference of $\pm$ 0.16 for K^{11} and 0.08 for K^{33}.

Conclusions

It appears that the method described above can produce estimates of the eddy diffusivity which are consistent in order of magnitude with those obtained by more conventional procedures. Moreover, in this particular study the results of the calculations are in qualitative agreement with the stability regime. Finally, it is apparent that the spacial variability of the eddy diffusivity is important in the distribution of salt for this region of the Antarctic Intermediate Waters.

The method of Rayleigh-Ritz as employed here has two distinct advantages over other techniques for calculating the eddy diffusivity. It permits the space distribution of both the lateral and vertical eddy diffusivity to be estimated. Through the use of standard statistical regression techniques, it is possible to obtain estimates of the accuracy of the calculations and to determine the efficiency of a particular diffusion model in predicting the spacial and/or temporal distribution of an added constituent.

Acknowledgments

Part of this research was conducted under O N R Contract Nonr 285 (57). Much of the original data was analyzed by the author at Texas A and M University under a grant from the National Science Foundation (G-13664).

References

Kirwan, A. D. Jr. (1963) Circulation of Antarctic Intermediate Water deduced through isentropic analysis. Texas A and M Department of Oceanography and Meteorology, Ref. 63-43F.

Ph.D dissertation, Texas A and M University (1964)

Okubo, A. (1962) Horizontal diffusion from an instantaneous point source due to oceanic turbulence. Chesapeake Bay Institute Tech. Report 32, Johns Hopkins University.

Schubert, O. V. (1935) Die Stabilitätsverhältnisse des Atlantische Ozeans. Deutsche Atlan. Exp. METEOR, VI, 2, 1.

Solodovnikov, V. V. (1960) Introduction to the Statistical Dynamics of Automatic Control System. Translated from Russian by J. B. Thomas and Lotfi A. Zadek, Dover Publications, New York, 309 pp.

Wiener, N. (1949) Extrapolation, Interpolation and Smoothing of Stationary Time Series. John Wiley, New York

Discussions after Kirwan's paper

Ichiye commented that attempts trying to elaborate concepts of eddy diffusivity and eddy viscosity were abandoned by most workers on turbulence about 1940 in favor of the statistical approach which seemed to offer sounder physical meanings although non-deterministic; however, the statistical approach has now been pushed to the point that some of its results become notably difficult to interpret physically and also to apply in problems of oceanography, so that perhaps now it is a good time to reawaken and revive interests in classical approaches in order to accord more solid physical meanings to concepts of eddy diffusivity or eddy viscosity.

Okubo asked about relation between K_z and stability; Kirwan answered that his results obtained from the Antarctic Intermetidate Water indicate the stability being the lowest at the depth of minimum salinity and maximum K_z, as expected from dynamic considerations.

PRELIMINARY STUDIES OF MOMENTUM FLUX IN OCEAN WAVES

D. H. Shonting
U. S. Naval Underwater Ordnance Station, Newport, Rhode Island

Abstract

This paper presents a brief review of a series of observations made of the particle velocities within the surface wind wave regime. These velocities were recorded using a ducted meter system mounted from a pier. Preliminary results of the data analysis and discussion of the instrumentation problems are presented.

Hypothetical wave motion models are given which demonstrate how orbital velocity correlations can sensibly affect eddy stresses within the wave regime. Mention is made of recent "open ocean" wave observations. It is noted how such data may allow us to explore such parameters as turbulent stress and eddy kinetic energy dissipation and how these quantities vary with depth and wind speed.

Results thus far obtained indicate that Reynolds stresses inherent in the wave motions can contribute substantially to the downward transfer of horizontal momentum supplied by the wind stress.

Introduction

The manner by which wind imparts momentum and energy to the sea surface causing wind waves and currents is not well understood. This momentum, however, must be transferred from the sea surface to the deeper layers solely by the motions of the water particles themselves. This vertical transfer of horizontal momentum results from turbulent motions although the process may be more orderly than is indicated by the term. Thus, if one considers the momentum transfer through the upper layers, it becomes apparent that one should examine the effects of the more regular quasi-oscillatory particle motions of the waves, since the waves themselves are indeed a manifestation of wind stress.

Thus, we ask what sort of orbital configuration could provide a simple mechanism for the downward transfer of wind imported horizontal momentum. One such geometry would be that of a properly titled ellipse. A particle might then acquire horizontal momentum from the wind stress at the top of its orbit and feed it downward as it moves in its trajectory. Starr (1961) has stated the probability of some such mechanism independently on other grounds. The above mechanism should be capable of representation as a Reynolds stress in terms of Eulerian hydrodynamic variables. It is of interest then to consider the problem of measuring these effects.

Narragansett Bay Measurements

The following experiments were reported by the writer (Shonting, 1964) and can be summarized as follows:

During August, 1963 measurements of the velocity components beneath ocean waves were made utilizing two adjacent ducted current meters mounted orthogonally as to sense the particle velocity components in the plane normal to the wave crests. The two cylinder ducts were about 10 cm in diameter and 20 cm long. The meter system was fixed to the end of a vertical steel beam supported rigidly at the end of a naval pier in Narragansett Bay, R. I. Jewelled-bearing and neutrally buoyant impellers mounted within the cylinders contain small iron slugs which upon rotation perturb magnetic fields of small induction coils attached to the sides of the cylinders. The output from the induction coils reflect the pulses as the impellers rotate in the fluid flow. Because of an assymetry of the magnetic fields of the induction coils, the sense of the rotation of the impellers, i.e. the direction of flow, is presented as a unique signature in the output.

A two-channel strip chart recorder was used to register the rate of flow through each of the impellers. The data was hand-converted into a continuous plot of the fluctuating velocities, U' and W' as a function of time. From this time series the sign and magnitude of the U' and W' were selected at three-second intervals and placed on punch cards for computer processing.

The horizontal flow-sensing meter was aimed normal to the crest lines of the waves and the meters were immersed about 15 cm below the trough level of the waves. The waves had been generated over an up-wind fetch of about 5 km and displayed clearly defined crests with visually estimated 1.5 second periods. The wind speed was about nine meters per second and the wave height was about 50-75 cm. The water depth below the instrument was about seven meters and it is assumed that the waves were essentially surface or deep water waves.

The covariance $\overline{U'W'}$ between the 1188 pairs of data was found to be $-7.8\ cm^2\ sec^{-2}$ providing an estimate of the magnitude and sign of the Reynolds stress (downward momentum flux). Here we define the Reynolds stress as $\tau = \rho\,\overline{U'W'}$ where ρ is the density of water (assumed constant) and U' and W' are the time variable deviations from the mean. The correlation coefficient between U' and W' was -0.21.

Spectra analysis was made of the time series data utilizing the methods described by Tukey (1949). Autocovariance spectra were made of

the time series data of the two velocity components and are shown in the upper curves of Figure 1. The spectra depicts peaks at wave periods of about 1.5 sec which was approximately the observed wave period. Both of the velocity components exhibit similarly-shaped peaks. The co-spectra component of the covariance spectra exhibits a negative peak at the dominant wave frequency. This indicates that the downward momentum flux due to the negative correlation of the velocity components occurred at frequencies equivalent to those of the waves.

The interpretation that we give to dynamics of wave measurements from this statistical analysis is critically dependent upon the sensing character of the ducted meter system. A study has and is being conducted of the response characteristics of the meters including a series of laboratory and field tests.

The meters were first calibrated for steady state flow parallel to the axis of each of the cylinders. Then the axis of the cylinders were set at arbitrary angles between 0 and 90° from the direction of steady flow to obtain the variation in instrument response to the "off angle flow". Finally a measurement of the impeller response to accelerative flow was performed.

The results indicate that the meters have essentially identical calibrations for steady flow parallel to the cylinder axis. The flow response as the meter axis is rotated with respect to the flow direction follows closely the cosine law. In other words, the component of flow varies as the cosine of the angle subtended by the cylinder axis and the mean flow direction. In order to assess the response time of the impellers, the meter system was sinusoidally oscillated vertically in a test tank and the fluctuating response of the meter recorded. These velocity variations, obtained with the calibration curve for the steady flow, were compared directly with the output of an accelerometer which was attached to the meters. The frequency response of the impellers was shown to be greater than 10 cps. This rapid response allows for accurate sensing of perturbations of the time scales of wind waves of the period from 0.5 to 8 seconds.

It is realized that there must be a limiting size of eddy or oscillatory configuration for which the volume dimensions of the meter alter or interfere with the inherent motions of the eddies. The effect of decreasing orbital size upon the flow sensing is to be determined by measuring the meter response of the ducted meters in a wave generating flume system at the Coastal Engineering Laboratory in Washington, D. C.

Three Hypothetical Wave Models

A comprehensive understanding of the analysis and synthesis of the Tukey spectral estimates is essential if we are to make correct conclusions and interpretations regarding the nature of wave motions as derived from their statistical properties. To best assess the treatment of the spectral analysis upon the two component velocity time-series data, three sets of hypothetical wave data were constructed and analyzed. These sets of data depicted three different wave models, namely, one whose particle motions are (a) quasi random with an induced bias to give $\overline{U'W'} < 0$ with no preferred frequency in the covariance spectra, (b) quasi ideal sinusoidal practical motions with no intentional bias giving $\overline{U'W'} \sim 0$ and (c) sinusoidal velocity fluctuations with a bias rendering $\overline{U'W'} < 0$ and having a preferred frequency in the covariance spectra equivalent to the frequency of the quasi-sinusoidal velocity functions. The three sets of data each contain six hundred pairs consisting of the horizontal velocity component U_n and the vertical velocity component W_n. The subscript n indicates the n^{th} data point where $n = 1, 2, 3, ---- N$. The symbol N is the total number of data pieces equally spaced at time intervals of Δt. Thus, we have for the total period of sampling of T equal to $N \Delta t$. For the three time series, T is 180 seconds. The amplitude or half range of the velocity components for all three data sets was about 10 cm sec^{-1}. Table 1 lists the pertinent statistical parameters of the three data ensembles. In the following is a description of the three models.

A. Biased Random Model (BR)

This first hypothetical wave model can be envisaged by a surface wave field where the particle motion is quasi random produced by many oscillatory progressive waves moving in many directions. The term "quasi random" is used for two reasons, namely, (1) the values of time series data were arbitrarily written down without use of tables of random numbers and (2) about 5% of actual values of data points were altered as to give a slight negative correlation function, i.e. a value of the covariance function at zero lag ($\overline{U'W'}$) less than zero. The actual value of the function is about -3.98 cm sec^{-2}. This simulated value of the stress near the water surface is thus 3.98 dynes cm^{-2}. This is of the order of magnitude of assumed mean wind stress upon the real ocean surface. This model will be referred to as Biased Random Wave Model (BR).

B. Unbiased Simple Harmonic Wave Model (USH)

The second set of data is characterized by representing the horizontal and vertical components as quasi-sinusoidal functions. Here we have assumed a simple harmonic wave model in the form of an ideal deep water progressive ocean wave as described by Lamb (1879). This model is derived

assuming an irrotational incompressible fluid in which the wave length is much less than the water depth.

The component particle velocity components are described by

$$U'(x,z,t) = \sigma A \exp(-Kz) \sin(Kx - \sigma t) \tag{1}$$

and

$$W'(x,z,t) = -\sigma A \exp(-Kz) \cos(Kx - \sigma t) \tag{2}$$

where A, K, and σ are amplitude (cm), wave number (cm^{-1}), and circular frequency (sec^{-1}) respectively. Thus, for a fixed depth Z_o and horizontal coordinate X_o we may write

$$U'(x_o, z_o, t) = U(t) = A' \sin \sigma t \tag{3}$$

and

$$W'(x_o, z_o, t) = W(t) = -A' \cos \sigma t$$

where

$$A' = \sigma A \exp(-Kz_o) = \text{const.} \tag{4}$$

We have attempted to represent this second data series given by the above equations as being simple harmonic oscillators mutually out of phase by $\pi/2$ or one quarter of a wave period. Actually, the sinusoidal functions were only approximated since they were hand drawn over a time amplitude grid having the proper frequency and amplitude. The data points were then picked off the two curves at $\Delta t = 0.3$ seconds.

It should be noted that the value of $\overline{U'W'}$ is identically zero for a long train of waves depicted by the functions (3) and (4). Since the data was only approximately sinusoidal, the value of $\overline{U'W'}$ for SHU (Table 1) is small but not zero.

C. Biased Simple Harmonic Wave Model (BSH)

The third hypothetical wave model is described as a Biased Simple Harmonic Wave function. This model is identical in every respect with USH except that the U'(t) function has been slightly increased at its positive maximum point. This intentional biasing was done for two reasons, namely, (1) to synthesize a desire negative value of $\overline{U'W'}$ for the BSH model and (2) to bias the BSH model by a simple mechanism, perhaps, not unlike that existing in natural ocean waves.

Let us examine and review the mechanism whereby momentum may be transferred from the wind through the surface waves suggested in the introduction. It is apparent that any energy and momentum within the wave must be transmitted through the actual wave surface by frictional drag and / or a form drag of the wind. Thus, the wind blows effectively horizontally across the waves and brings about an actual tractive stress on the crests of the waves and perhaps a pressure force upon the "upwind" side of the waves. Accepting this as fact, let us assume that the transfer of momentum downwards in the waves is caused simply by turbulence in the water. The wind momentum is transferred by an eddy process in which the eddies are simply the water waves themselves. Both of these forcing mechanisms could produce a sensible acceleration of the particles at the crest, i.e., when the U'(t) component is positive and maximum.

Thus, we are placing within the horizontally oscillatory component of the BSH model a biasing component which is of the frequency of the waves themselves. Hence, at a fixed point in the water column, a momentum transfer of this sort would appear as a direct coupling effect occurring at the dominant wave frequency.

Statistical Characteristics of the Hypothetical Wave Models

The three sets of data were analyzed for pertinent statistical parameters using the Tukey spectral estimate program prepared by Convair on the MIT IBM 7090 Computer.

The statistical parameters of the three pieces of data are tabulated in Table 1. It is noted that the number of pieces of data, the period of sampling, and the time spacing are identical for all three sets of data. The mean values of the horizontal and vertical velocity components are designated by U and W and in all cases do not exceed 0.5 cm sec^{-1}.

The variances $\overline{U'^2}$ and $\overline{W'^2}$ (which are equivalent to the auto-covariance function at zero lag) are shown to be about 15.16 cm^2 sec^{-2} for the BR model and between 49 and 55 cm^2 sec^{-2} for the Unbiased and Biased Simple Harmonic Wave models. This is apparent from an examination of Figures 2, 3 and 4. The covariance function for the two Biased Models BR and BSH is -3.98 and -2.57 cm^2 sec^{-2} respectively. The covariance for the ideal sinusoidal function is, of course, much smaller, i.e., -0.045 cm^2 sec^{-2}.

Table 1

SUMMARY OF STATISTICAL PARAMETERS OF HYPOTHETICAL DATA

Set	No. of Pieces of Data	Sampling Period	Sampling Interval		Max. Values	Means		Variances		Covariance	Correl. Coeff.
(1) Random Biased (BR)	600	180	0.3	10	10	+0.16	-0.27	15.43	16.41	-3.98	-0.205
(2) Ideal Sinusoidal (USH)	600	180	0.3	10	10	-0.15	+0.10	50.62	50.03	-0.045	-0.0009
(3) Biased Sinusoidal (BSH)	600	180	0.3	10	10	+0.31	-0.05	49.56	54.30	-2.57	-0.05

The correlation coefficient R_{UW} for the BR model is -0.21 and for the BSH model is -0.05. For the USH model the correlation coefficient is vanishingly small at -9×10^{-4}.

The auto-covariance and covariance spectra (which are the Fourier transforms of the respective functions) of the three sets of data are plotted in Figures 2, 3 and 4. The "in phase" or real part of the covariance spectra (termed co-spectrum) is plotted below the power spectra pairs in the figure.

The power spectra of each velocity component, i.e., Φ_U and Φ_W, are plotted as $cm^2\ sec^{-2}$ per cycle per second versus frequency (and period) on the abscissa. The values of Φ_U and Φ_W for BR are similar with each showing a dominant low frequency peak between 0.2 and 0.3 cps. This peak is well defined and drops sharply at about 0.4 cps. From 0.4 through to the limiting frequency of about 1.7 cps the Φ_W fluctuates in a similar manner as Φ_U except that the latter displays two peaks, one at 0.8 cps and one at about 1.1 cps. These oscillations of the power spectrum functions are mostly due to chance since the data was generated in a quasi random fashion.

The cross spectrum shows repeated fluctuations displaying negative peaks at 0.3, 0.8 and 1.25 cps. There is, however, no extreme peaking indicative of predominant coupling at any one frequency. The co-spectral function is, in general, negative throughout the frequency range.

The power spectra of the unbiased sinusoidal waves - USH, Fig. 3, show the expected sharply defined peaks at the 0.5 cps which is the chosen frequency of the sinusoidal velocity components.

The co-spectrum function displays only very slight values of less than 10% of the magnitude of the cross spectra of the BR at about 0.5 cps.

Turning to the power spectra of the Biased Simple Harmonic Waves (BSH), Figure 4, we see again the pronounced peaks of the velocity functions occurring at a band between 0.3 to 0.6 cps. The base of the peak for the BSH model is broader than for USH.

The co-spectrum of the BSH Model, Figure 4 (bottom), is of special interest since it displays a strong negative peak centered at 0.5 cps. It appears as almost a mirror image of the power spectrums above.

Thus, we see, by altering the magnitude of the amplitude of the U(t) component by about 5% in a cyclic fashion, the covariance function is increased by almost two orders of magnitude and the co-spectrum is completely modified to show a strong negative correlation at a frequency

associated with the waves themselves. It is of interest to note the similarity of Figure 4 and Figure 1. It is suggested that this type of simple (BSH) mechanism could be primarily responsible for the downward flux of wind imparted momentum through the water column.

Open Ocean Measurements

A series of preliminary "open ocean" observations were made with the wave meter from the Buzzards Bay Entrance Light Station situated in 20 m of water off the southern coast of Massachusetts. The wave meter was supported in a semi-rigid geometry by an array of supporting guys above it and a 50 kgm vertical damping weight suspended below it.

The measurements were made on May 11, 1964 during a period of steady wind conditions with a mean wind speed of about 6-8 m sec^{-1}. The spectral analyses of data velocity data taken at a depth of 1 meter and 4 meters below the wave trough level are shown in Figures 5 and 6.

The auto-covariance spectra of the U' and W' values at both depths indicate peaks at about 3-4 seconds which agrees with the visual estimates of the wave periods. It is noticed that there appears a strong attenuation of the U' component spectra relative to the W' at periods greater than about 1.3 seconds. This effect is apparently caused by a swinging motion in the horizontal direction which is the reaction of the meter system to the back-and-forth U' velocity component. Thus, the reaction of the meter system tends to attenuate the amplitude of the U' fluctuation component due to the gross wave motions. This effect has been largely eliminated by modifying the wire support system and using a heavier damping weight. At the time of this writing a new smaller meter system has been constructed and tested. It has about one half the cross-sectional area as the original device. Raw data from this smaller meter are strongly indicative that due to the reduction of drag the reaction to the oscillatory horizontal motions has been effectively removed.

Returning again to Figures 5 and 6, we note the effective reddening of the spectral peaks of both pairs of spectra with depth, i.e., the high frequencies are damped more effectively with depth. Measurements were made at 0 (just under the trough level), 1, 2, 3, 4 and 5 meters. This shift to more dominant low frequencies with depth is characteristic of the data.

Other than observing the gross attenuation of the frequencies above, say, 1.8 cps, the reader should be cautioned of the possible limitations of the meter in the presence of turbulent or eddy structure of the scale dimensions of the meter itself as was previously discussed. Although the impellers have a fast response character, the variations in velocity at the higher frequency bandwidths will likely be associated with smaller eddy scales of the order of the dimensions of the meter, i.e. 20 cm.

If we consider the depth variation of a particular velocity component, say, W', we find that the variance W'^2 decreases in an exponential manner. Note that the area under the spectrum curve of $\Phi_W(f)$ versus frequency is equal to the variance of the particular component caused by fluctuations occurring between the frequency ranges studied. Thus,

$$\overline{W'^2} = \int_0^{f_1} \Phi_W(f)\, df \tag{5}$$

where f_1 is the upper frequency limit determined by the sensor characteristics and sampling interval. We can define the turbulent kinetic energy by the relation.

$$E_k = 1/2\,\rho(\overline{U'^2} + \overline{W'^2}) \tag{6}$$

Thus, we see that the spectra of the velocity components are in fact literally true energy density spectra since the area under the spectral curve for a particular velocity component is equivalent to the turbulent energy contribution of the component of velocity.

The covariance spectra (bottom curves) display a negative peak at the frequencies which occur in the spectral band of the waves. The auto-covariance function at zero lag for the one meter depth was -23.3 cm^2 sec^{-2} and the linear correlation coefficient was -0.17. For the four-meter depth the covariance function was -14.1 cm^2 sec^{-2} and the correlation coefficient was 0 - 0.30. As the Narragansett Bay measurements, these covariances seem extremely large in terms of the usual empirical estimate of stresses of the order of 1 dyne cm^{-2}.

In view of the consideration of the artificial data, it appears that if the stresses in the surface regime are of the order of less than 1 dyne cm^{-2}, then only very small velocity correlations of the order of -0.05 are required to produce a Reynolds stress of this value. It is then probable that the ducted meter system will be unable to detect such small correlations because of the masking effect of relatively large scale perturbations caused by the interaction of the meter with the flow around it.

However, the results so far available indicate strong negative correlations peaking at the periods of 3-6 seconds. It is difficult to imagine that, assuming the meter system is properly mounted in the wave regime, it would artificially produce correlations at these relatively low frequencies.

It is too soon to conclude anything quantitative regarding the momentum flux mechanisms. However, we really have no prior justification for discounting the values of covariance functions obtained in them since we essentially have no previous direct measurements of stress with which to refer.

In conclusion, we may state that this method of wave particle velocity measurement allows estimate of the gross features of turbulent structure characteristic of the surface wind generated waves. It appears that the quasi-oscillatory motions due to the surface waves produce measurable downward momentum transfer due to particle velocity correlations occurring at the ambient wave frequencies.

Further studies are being made of the dynamic characteristics of the ducted meter systems and presently a miniature ducted meter system is being tested. Also, use of a drag sphere system for measuring stresses directly is under investigation.

Wave measurements in a variety of meteorological conditions are being made on Buzzards Bay Entrance Light Station. The results of these "open ocean" measurements will be reported at a later date.

It should be noted that Round Hill Field Station of MIT is being funded from NUOS to utilize and study the potential of the Buzzards Tower for making wind stress measurements. It is hoped to coordinate wind and wave momentum flux measurements to provide a better understanding of the interactions and transfer of energy between the wind and ocean.

The work reviewed is a result of studies presently being carried out by the U. S. Naval Underwater Ordnance Station, Newport, Rhode Island, and the Circulation Project of the Department of Meteorology, Massachusetts Institute of Technology, Cambridge, Massachusetts. Thanks is owed the U. S. Coast Guard and personnel aboard the Buzzards Bay Entrance Light Station for their assistance. This work is being sponsored by the Bureau of Naval Weapons, Contract RU222 FOOO/219-1/R004-03-01 for oceanographic studies.

References

Lamb, H. (1879) Hydrodynamics, Dover Publications, New York, 738 pp.

Shonting, D. H. (1964) A preliminary investigation of momentum flux in ocean waves, Pure and Appliec Geophys, Vol. 57, pps 149-152

Starr, V.P. (1961) Hydrodynamical red-shift phenomena in geophysics Pure and Applied Geophys, Vol. 48; p. 109

Tukey, J. W. (1949) The sampling theory of power spectrum estimates. Symposium on Applications of Autocorrelation Analysis to Physical Problems, Woods Hole, Massachusetts, ONR Publication 47.

Discussion after Shonting's paper

Pritchard asked about the angular response of the ducted meters. It was answered that the response was down 5 to 10% at 15° to 20° off axis. Pritchard pointed out that vectors can be resolved uniquely into u and w components only if such a meter has a sine or cosine angular response.

A question was raised as to whether the acceleration deceleration response of these meters is the same. Shonting answered that it is the same within measurement errors. Kirwan pointed out that an earlier experiment in Japan conducted in a controlled wave tank yielded similar results.

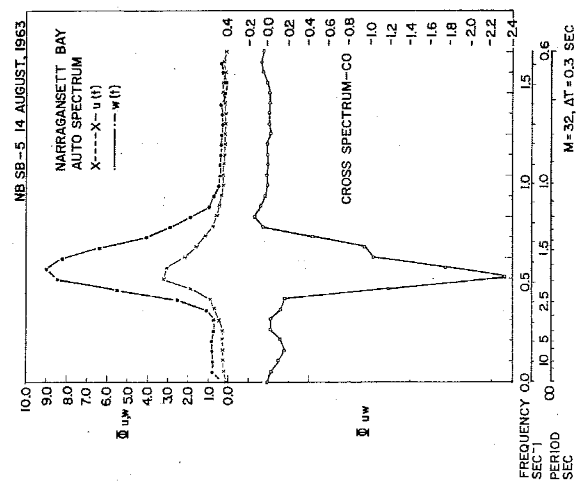

Figure 1

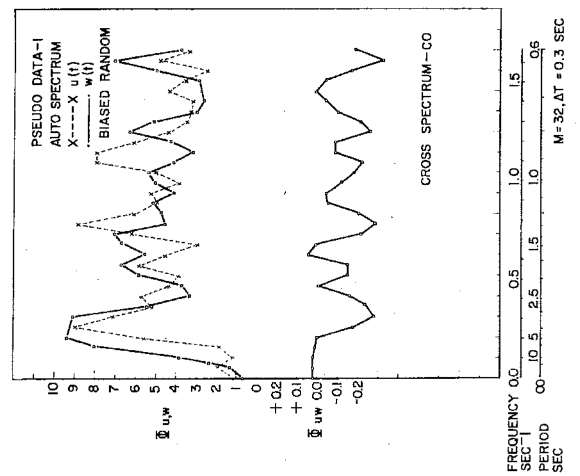

Figure 2

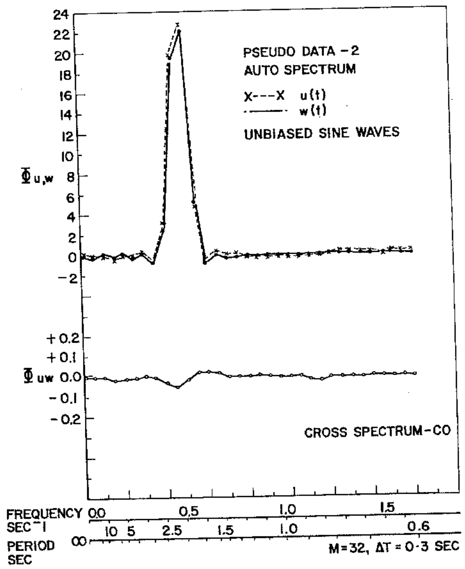

Figure 3

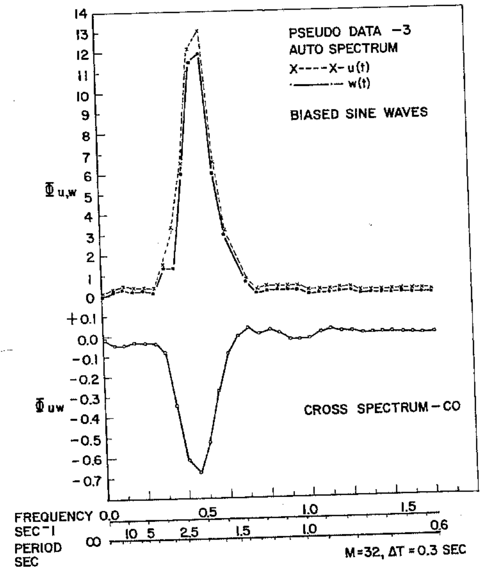

Figure 4

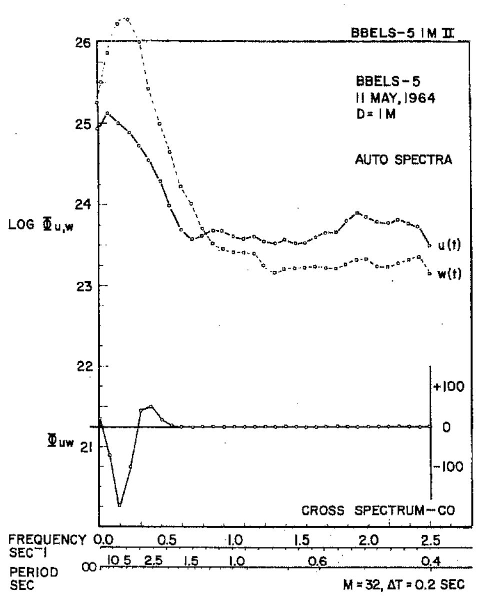

Figure 5

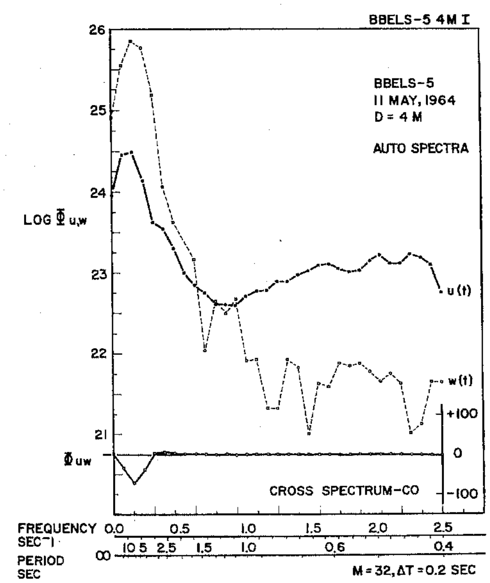

Figure 6

DIFFUSION PROCESSES VS. OCEANIC MICROSTRUCTURE

M. P. Wennekens
Office of Naval Research, San Francisco, California

Abstract

Continuous vertical profiles of sound velocity and temperature were obtained with SVTP (Sound, Velocity, Temperature, Pressure sensor) off Southern California. Vertical variances of sound velocity are most pronounced between the thermocline and 450 meters. Comparison with temperature fluctuations indicates that the water stratification is stable in this layer of large fluctuations in sound velocity.

Observations

The study of diffusion processes in the oceans can be greatly enhanced if, at the time of experimentation, a measure of the complexity and stability of the density structure can be obtained.

Recent observations acquired with instruments capable of measuring the continuous distribution with depth of such properties as temperature, salinity, sound velocity, etc., show that the oceans are less homogeneous and more variable than formerly assumed and that the occurrence of microstructure is rather widespread. The term microstructure can be defined as: any discrete sudden change in the distribution of conservative properties within small increments of depth.

Observations obtained on the West Coast, east of San Clemente Island can serve as an example. Two time studies (Fig. 1, 2) during which the entire water column was continuously and rapidly sampled for two consecutive twelve-hour periods, during the nights of 24-25 and 25-26 September, 1962, demonstrate some of the complexities of the oceanic microstructure off Southern California. The data presented pertains to direct measurement of sound velocity obtained with a U.S. Naval Ordnance Test Station SVTP (Sound Velocity, Temperature, Pressure) instrument. (Lovett and Sessions, 1961; Wennekens, 1962). Continuous in situ sound velocity measurement, integrating the combined effects of temperature, salinity and pressure, can be considered to adequately describe the density structure of the water column.

Discussion

Examination of the time studies reveals several interesting features. Firstly, there are two layers of contrasting complexity in the microstructure

below the seasonal thermocline. Between the thermocline and about 450 meters, the range of fluctuation is large, in excess of three meters per second for the larger inversion. Temperature fluctuations closely correlated with the sonic fluctuations (from about 0.5 °C to more than 1° C for the larger inversions). Of interest is the rather sharp boundary or transition zone between the layer beneath the thermocline and the deeper water. The two left curves in Fig. 2 show a very pronounced gradient; temperatures across the transition zone changed from 6.66°C at 405 meters to 6.92°C at 410 meters. Careful examination of the data indicates that temperature alone does not account for the sonic fluctuation, suggesting concurrent salinity variations. At present, no exact measure of the salinity within the inversion has been made. However, the necessary instrumentations to sample inversion layers are becoming operational and quantitative measurements on both temperature and salinity of the waters across the inversion can be expected shortly.

One should emphasize that the apparent lack of complexity in the deep water might stem from the inadequate sensitivity of the sound velocity and thermal sensors (0.3 m/sec and 0.02°C) to accurately measure smaller gradients below about 450 m.

Secondly, the vertical stability can be associated with the major and minor features of the microstructure. Examination of the data gives an impression that the larger inversions are in their proper density relationship within the water column. This means that the stratification of the water remains stable. This is especially true in the layer extending from beneath the thermocline to the transition zone. Below the transition zone, the stability of the stratification is not obvious.

Data obtained by LaFond (1963) with the NEL thermistor chain off Baja California and other observations obtained by the writer, suggest that water masses of dissimilar characteristics "interleaf" along definite density surfaces and that water parcels slide along such surfaces for considerable distances once they have acquired enough momentum. This is probably due to the eddying processes common in the area. The interleafing takes place with a minimum of disturbance in the density structure. The persistence of the features also suggests that vertical mixing is minimum, perhaps nil, and that mostly along density surfaces diffusion processes are slow.

The examples furnished here clearly emphasize that the study of diffusion processes must take into account the presence of a complex microstructure. The differences in the complexity of microstructure at various levels mean that the value of eddy diffusion coefficients will vary from layer to layer and that, to properly evaluate such coefficients, detailed and quantitative knowledge of the heterogeneity of the medium is essential.

New tools are now at hand to provide the needed information, and, through their use, more realistic assessment of eddy diffusion coefficients can be expected.

Acknowledgment

The data used in this report were obtained during research conducted under Bureau of Naval Weapons Task Assignment RE 222 E 000/ 216-1/ R 004 - 03- 01. The author gratefully acknowledges the participation of Mr. J. R. Lovett, Research Department, U. S. Naval Ordnance Test Station, China Lake, California.

References

LaFond, E. C. (1963) Detailed temperature structure of the sea off Baja California.
Limnology and Oceanography, V. 8, No. 4, pp 417-425, Oct.'63

Lovett, J. R. and S. H. Sessions (1961) An instrument for continuous deep sea measurement of velocity of sound, temperature and pressure. U. S. Naval Ordnance Test Station, China Lake, California NAVWEPS Rep. No. 7650, 9 May, 1961, 24 pp.

Wennekens, M. P. (1962) The SVTP instrument and its application to oceanography. J. Geophy. Res., Vol. 67, No. 9

(1963) NOTS Oceanographic Research. Semi-annual progress report, July-December, 1962. U. S. Naval Ordnance Test Station, China Lake, California. Tech. Note #502-1, 18 April, 1963.

Discussions and Comments on Wennekens' paper

Shonting: Can one get eddy diameter from SVTP data?

Answer: Yes, but roughly and for large features only.

Olson: What was the relative size of temperature versus sound velocity fluctuations?

Answer: Since the salinity gradient was smaller than the temperature gradient, sound velocity fluctuations were mostly due to temperature fluctuations and their total amplitudes are 1.5 to 4 m/sec.

Pochapsky: Then, the temperature profiles really represent density distributions and there should be small instability in some depths. This seems to be at odds with Wennekens' results.

(Note added later by Dowling)

The two problems should be considered in relation to apparent instability observed by SVTP profiles. Firstly, since the rotation of the earth provides a well-known stabilizing influence, it would be necessary to compute real stability from SVTP data including the effect of the rotation.

Secondly, H. Jeffreys (Proc. Roy. Soc. London Series A 118, 195-208, 1928) showed that vertical flows resulting from weak instabilities are transformed by shear motion into strips disposed more or less horizontally. This theory, when combined with Wennekens' microstructure observations, could account for production of blobs or lenses of water, as were often observed.

Question: Can a time series of temperature and sound velocity at a fixed depth be obtained?

Answer: Such measurements are possible, but not reliable due to problems of staying at a constant depth.

Ichiye commented that data taken by Lamont scientists in the Caribbean Sea with a continuously recording temperature and salinity probe show that fluctuations in temperature and salinity are so correlated as to yield the resulting stable gradient.

112

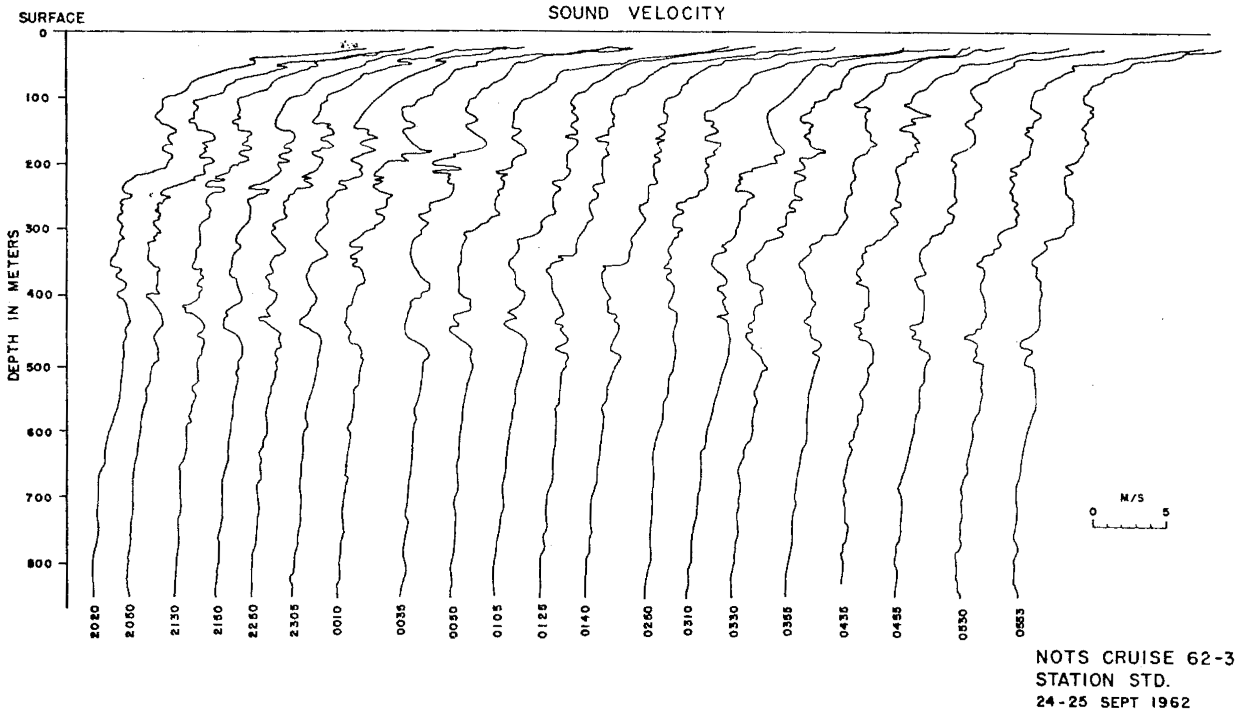

Fig. 1 - NOTS Cruise 62-3 - Station Standard (32°59.8 N, 118°29.1 W)
Time studies - 2000 24 Sept. - 0600 25 Sept. 1962

113

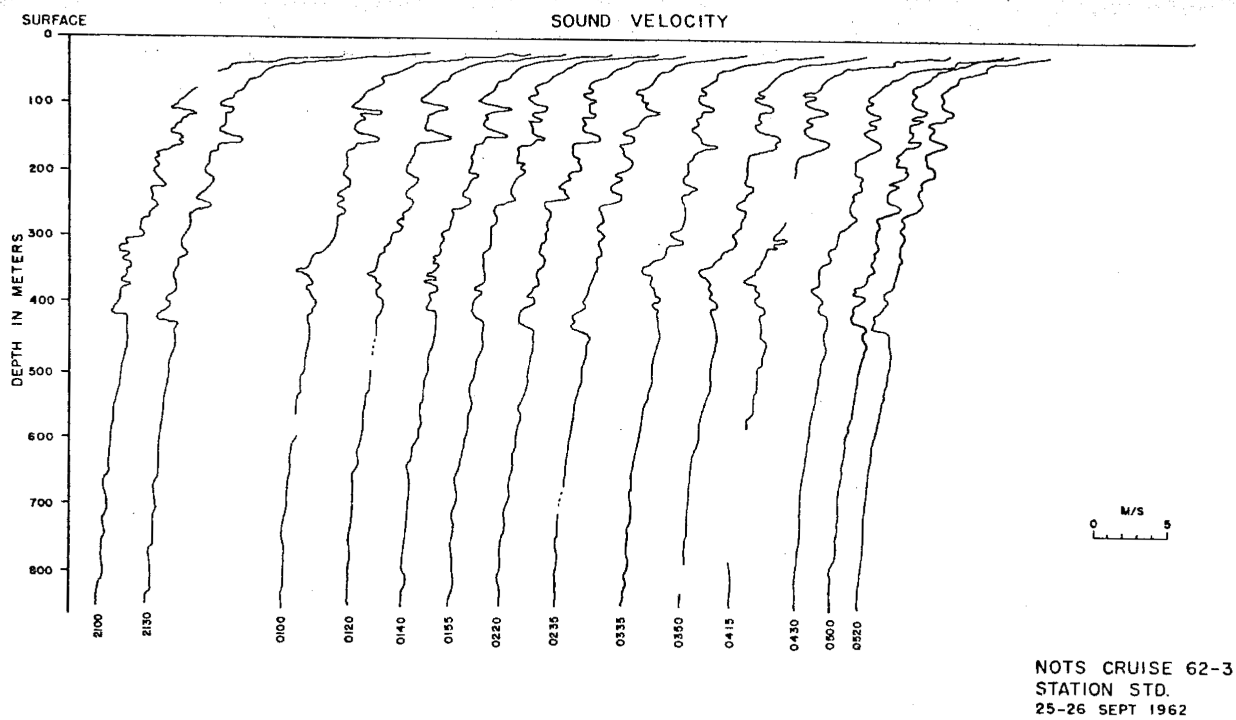

Fig. 2 - NOTS Cruise 62-3 - Station Standard (32°59.8 N, 118°29.1 W)
Time studies - 2100 25 Sept. - 0600 26 Sept. 1962

DIFFUSING PARTICLES IN THE DEEP OCEAN*

T. E. Pochapsky
Hudson Laboratories of Columbia University, Dobbs Ferry, New York

Abstract

When a quantity of dye is introduced into the ocean, the volume enclosed by the dye increases and the enclosed shape distorts. This distortion is produced by velocity gradients which take place over distance comparable with the length scale of the experiment. Repetitions of this experiment will probably show different distortions. The literature on homogeneous turbulence points out that the velocity structure is not spatially homogeneous at a given time, and so even the rate of dispersion should differ in different trials. This illustrates only one of the difficulties of obtaining data to characterize diffusion in the ocean.

A second difficulty is that of trying to measure dispersion in deep waters. To avoid this, and to simplify individual experiments so that they can be repeated more readily, neutrally-buoyant floats were used to study the velocity structure in the hope that knowledge of the velocity gradients would give insight into the mechanism of diffusion. Such floats were dropped in pairs. They transmitted data to the surface so as to establish the depths and the radial separation of the floats as a function of time. The results, so far, show the general presence of internal waves and of horizontal shear gradients. The latter are large enough to generate the turbulence required for vertical diffusion. Floats tend to come together after they separate and this pulsating behavior in combination with vertical diffusion should result in enhanced horizontal transport. Internal waves not only have a direct effect on the turbulent, or dispersive, structure of the water - they also apparently enter directly into the dispersive process.

Future work will involve studying the dispersion of a cluster of a half-dozen floats. It is hoped that diffusion coefficients can be calculated from the observed separation of pairs of floats in the cluster in the manner shown by Richardson. Surface dispersion experiments performed in this laboratory showed that such coefficients vary as the 4/3 power of the distance between dispersing particles even under conditions where the turbulence is not characterized by the presence of an inertial subrange. Experiments of this type at sea should take explicit consideration of the time as well as of the separation between particles in a pair.

This work was supported by the Office of Naval Research under Contract Nonr-266(84).

*Informal Documentation No. 48, Hudson Laboratories of Columbia University

(Editor's Note)

For the most part, the subject matter of this paper appears in three previous publications by the author: "Exploring subsurface waves with neutrally-buoyant floats" ISA Journal 8, pp. 34-37 (1961); "Some measurements with instrumented neutral floats" Deep-Sea Res. 8, pp. 269-275 (1961), and "Measurements of small-scale oceanic motions with neutrally-buoyant floats" Tellus 15, 352-362 (1963).

The author also discussed his laboratory experiment which was designed to test Ozmidov's proposition, (Ozmidov R. V., 1957; "An experimental study of turbulent diffusion in the ocean and coastal waters" Izvestia Akad. Nauk USSR, Ser. geofiz. 6, 756) determined the neighbor diffusivity F with various experiments in the Caspian Sea and in an artificial reservoir. He utilized the relation $F = \overline{[l(t) - l_o]^2} / 2t$. In this equation, $l(t)$ is a separation of a pair of particles at time t, l_o is the initial separation and the bar indicates the average of many pairs of particles. Richardson (L. F. 1926, "Atmospheric diffusion shown on a distance neighbor graph" Proc. Roy. Soc. London A 110, 709-737) and others postulated that F is proportional to $l_o^{4/3}$. However, Ozmidov found from his experiments that F is dependent also on water depth. Therefore, he concluded that although F is proportional to l_o^n, the exponent n is different from 4/3 when the water is shallow. The author made measurements of the dispersion of floating particles particularly in shallow water. He used a tank with a depth of 1 cm and a Reynolds number of 20, but he found that the neighbor diffusivity follows the 4/3 exponent theory, contrary to Ozmidov's proposition.

AN APPLICATION OF NATURAL RADON TO PROBLEMS IN OCEAN CIRCULATION*

Wallace S. Broecker
Lamont Geological Observatory of Columbia University
Palisades, New York

Abstract

Large discontinuities in radon concentration have been shown to exist at the air-sea and sea-sediment interfaces such that with respect to its parent radium measurable deficiencies of radon should exist in the surface ocean and excesses in near bottom water. Using a method allowing shipboard extraction and measurement of the small amounts of radon present in the sea, ten samples of surface water and two of near bottom water were measured establishing the existence of the predicted effects. Large excesses of radon were found in the shallow waters on the Bahama Banks. Quantitative relationships are derived which allow estimates of both the rate of ocean-atmosphere gas exchange and the rate of turbulent mixing in the surface ocean to be computed from the results of shallow profiles. Similar relationships yielding rates of turbulence in the bottom water from deep profiles are given. As vertical turbulence has proven a difficult parameter to measure in the oceans this technique should prove valuable to the understanding of mixing processes in the sea.

Introduction

Radon, the 3.85 day half-life daughter product of Ra^{226}, has been given little attention in connection with problems in oceanography. As will be shown in this paper, this inert gas isotope shows considerable promise for the study of processes taking place near the surface and near the bottom of the sea. Use of such a short-lived nuclide is possible because of the large concentration discontinuities which exist at the ocean-atmosphere and at the ocean-sediment interfaces. The distribution in bottom waters of radon which has diffused out of the sediment can yield valuable information regarding the coefficient of vertical eddy diffusion in the deep sea. The deficiency of radon in near surface water resulting from loss to the atmosphere can be used to define both the rate of vertical mixing in these waters and the rate of gas exchange between the ocean and atmosphere.

Experimental Techniques

The present study involved the determination of the concentrations of

* Contribution Number 836

Rn^{222} and Ra^{226} in water samples with activity levels as low as 0.2 dpm/liter to an accuracy of ten percent. Because of the large volumes of water analyzed (20 to 60 liters) and the short half-life of radon (3.85 days) a system for Rn^{222} measurements was developed which could be used at sea. Briefly, the method involves cycling He through the water and freezing the radon (and other condensables) out of the gas stream in traps cooled with liquid N_2. The radon is then quantitatively transferred into a scintillation chamber and its alpha activity determined. The same system could also be used for Ra^{226} analyses by allowing a second generation of radon to accumulate in the water sample over a known period of time. The details of the procedure are given below.

As aeration of the sample during collection could result in a loss of radon, sampling procedures designed to minimize this effect were developed. The technique used for the Bahama work involved direct suction of sea water into the 20-liter flint glass bottles used in the gas extraction procedure. The adaptor fitted to these bottles (standard distilled water containers) is shown in Figure 1. The bottle was first evacuated and sealed off. A length of rubber tubing was attached to the exhaust side of the adaptor. The far end was weighted and lowered into the water to the desired depth. The exhaust valve is opened and the water allowed to flow in until the desired amount was obtained. The container was then sealed, moved to the laboratory, and attached directly to the gas extraction system. In this way, near surface waters could be collected with no chance of gas loss.

A special sampler was constructed for near bottom sampling. Its main features are shown diagramatically in Figure 2. The sampler consists of a 50-liter steel cylinder fitted at either end with circular 0-ring-sealed doors pivoted along a diameter. The doors are latched in the open position during descent allowing water to freely pass through the sampler. When the foot hanging beneath the sampler hits bottom it actuates a release on the upper door latch which immediately closes under the action of a heavy spring. During its closing the upper door actuates a cable attached to the release for the lower door. Both doors close within a fraction of a second of contact with the bottom. A base covered with a coarse mesh screen prevents direct contact of the lower portion of the sampler with the sediment. As the depth at which the doors close is recorded by a special bourdon gage (identical to that described by Ewing and Gerard, 1961) malfunction can be detected.

Because pre-triggering of the sampler during descent presented a real problem, details regarding the design of the foot system are given. A rod rigidly attached to the foot hangs through two "eyes" mounted on the side of the sampler. A stop holds the rod in the desired position. This rod is connected to the release arm with two loops of heavy string. The rod is prevented from putting tension on these loops (and hence from pre-triggering the doors) by a second string tied from the rod to one of the eyes. On contact with the bottom, the second string snaps allowing the rod to actuate the release arm. After actuating the release arm, the first string also breaks allowing the sampler to fall to the bottom without damaging the triggering mechanism. This system works well.

The sealed sampler is returned to the deck and its contents are extracted into evacuated flint glass bottles (described above) through a rubber tube attached to the lower port. A small positive pressure of He is maintained on the upper port during the transfer.

Although not as foolproof as the surface sampling procedure, negligible radon is lost. During the ascent of the sampler no gas phase is present so that the radon must remain in the water. Whereas a gas phase is created during the transfer process, evasion is negligible because agitation is minimal and the entire process requires only about twenty minutes (with vigorous bubbling at least an hour is required for removal of the radon).

The flint glass bottles are attached to the extraction system shown in Figure 3. Liquid air is applied to the large traps of the evacuated system. Slightly under one atmosphere of He is introduced. The sample container is opened to the system and the pump turned on. By use of the by-pass the flow rate is adjusted to about three liters per minute. The pressures are recorded and the extraction is allowed to proceed for ninety minutes. At the end of this time the pressures are again noted (provided liquid N_2 level is returned to its initial position changes in pressure denote leaks in the system), the pump stopped, and the sampler isolated. The He is then pumped away, the system isolated and the liquid N_2 removed. After all the ice has melted the system is again filled with He. The He is circulated through the ascarite column in order to remove CO_2 and then liquid air is placed on the small U trap. Circulation of the gas through this trap is continued for five minutes at a rate of 2 liters per minute. In this way the radon is quantitatively collected in the small U trap. The pump is turned off, the He pumped away and the U tube isolated. The liquid N_2 is removed and the radon allowed to vaporize. During this period the counter is pumped. The counter is then isolated from the rest of the system and opened to the U tube. The remainder of the system is filled to one atmosphere with He. The He is allowed to expand through the U tube into the counter carrying any radon still in the U trap along with it. The counter is immediately isolated and the activity of the radon determined.

In order to make sure that the extraction was essentially complete the entire procedure is repeated and the radon counted. Generally ninety percent of the radon is recovered during the first extraction.

The sample is sealed and stored for at least seven days and the

extraction procedure is repeated. The amount of radon recovered (corrected to infinite accumulation time) is then proportional to the Ra^{226} present in the sample. The Ra^{226} growth, extraction and measurement procedure can be repeated as often as desired.

As the system is made almost entirely of metal and rubber parts and mounted on a board 2 feet high and 3 feet long, it is easily transported and not subject to breakage. The liquid N_2 required presents the main problem in shipboard use. Two or three standard Linde type 100-liter pressurized containers have proven entirely adequate for three-week periods at sea. If further work proves the value of the method, a liquid air generator will be installed on the ship. In other respects operation at sea has created no problems not encountered at Lamont.

The design of the counter is shown in Figure 4. A 2-inch diameter photomultiplier tube views an internally phosphored chamber 50 cm^3 in volume. The face of the phototube and the interior of the chamber are prepared by dusting Patterson type D actlvitated zinc sulfide phosphor over a thin coating of stopcock grease. An ionium source which acts as an internal standard is mounted on the wall of the chamber opposite the phototube. By rotating a plate the source can either be exposed to the phosphor or completely covered. The chamber is air tight and will maintain a vacuum.

The background of the counter is 0.3 cpm. The overall efficiency as determined by carrying an N.B.S. Ra^{226} standard through the entire procedure is 66 percent. The two alpha daughters of Rn are detected with the same efficiency as their parent. The Io calibration standard yields a count rate of 700 cpm. The counter has proven extremely stable, the background and calibration source counts remaining constant within the measurement error over long periods.

As the products of Rn remain behind when the gas enters the counter corrections must be applied for the extent to which equilibrium has been reestablished. Since radon itself gradually disappears during the run a correction for this decay must also be made. Figure 5a shows the count rate as a function of time for a sample containing 100 dpm of radon.

Account must also be taken of the daughter products remaining from the previous sample. Although radon itself can be entirely removed, the non-volatile products remain behind on the counter walls. The contribution of the products remaining behind after a 100 dpm radon sample is removed is also shown in Figure 5b.

The radon results are expressed in terms of equivalent Ra^{226} units (the amount of Ra^{226} having an activity equal to that of the radon).

Several special procedures were used in connection with the sediment studies. These are described below.

Direct Pore Water Analysis

Water was extracted from the pores of the sandy sediments on the Bahama Banks by driving a one half inch tube about eighteen inches into the sediment. The water is pulled in through small holes drilled in the end of the tube using a large hyperdermic-like piston device. The piston is retracted by turning a hand crank. The sampler can be easily handled by a single Scuba diver. Up to five liters of water can be obtained. The water is transferred to the evacuated extraction chamber by reversing the piston and forcing the water out.

Indirect Pore Water Analysis

A good approximation to the pore water concentration can be obtained by dispersing a known weight of the sediment in distilled water, sealing it off and allowing radon to accumulate for a period of a week or more. The sediment is then redispersed and the radon swept out by flushing the water with He. This is the only way in which estimates of the radon concentration in the pore waters of deep sea sediments and Bahama muds could be made.

Estimates of Radon Flux from Sediment to Water

Estimates of the standing crop of radon emanated from the sediment to the overlying water can be made as follows. As trigger weight cores are retained upright in the plastic liner of the core pipe, the tops are relatively undisturbed. The water above the sediment is largely removed (leaving a few millimeters) and the residual radon in the gas phase is flushed away. The tube is sealed off and the radon allowed to accumulate in the gas phase. After a week or more the gas phase is flushed out and the radon isolated.

Results and Discussion

The concentration of radon in sea water well away from the sediment and atmosphere interfaces should be controlled by the amount of Ra^{226} dissolved in the water. As shown in Table 1 the Ra^{226} concentration in sea water ranges from $5 \times 8 \times 10^{-14}$ gm per liter (hence 0.1 to 0.2 dpm per liter). The radon activity should be the same as that of its parent. The results given in Table 2 demonstrate that this is the case.

The partial pressure of radon in the atmosphere over the oceans is negligible compared to that in the water. Whereas the activity of Rn in a gas phase at equilibrium with the sea would be from 3 to 6 dpm per liter of

air, as shown in Table 3, the observed activities average only 0.013 dpm per liter.

As shown in Table 4 the concentrations of radon in the pore waters of ocean sediments are several orders of magnitude higher than those encountered in a typical ocean water sample. These very high concentrations are produced by the escape of radon from Ra^{226}-rich mineral grains. Approximately five percent radon leakage would explain each of the observed values.

These results establish that large discontinuous changes in radon concentration occur at the bottom and surface of the ocean. The next step is to consider the mechanisms controlling the transfer of radon across these interfaces.

Sediment-water Interfaces

Considerable amounts of radon should be transferred from the sediment pore water to the deep ocean creating an excess of Rn^{222} over Ra^{226} activity in near bottom waters. The concentration of excess radon at any point in the water column above the sediment will depend on 1) the influx of radon out of the sediment and 2) the rate of vertical eddy diffusion in the deep sea.

Because of the very large contrast in concentration the flux can be calculated assuming that the concentration of radon in the water immediately over the sediment is negligible compared to that below the depleted zone in the sediment. At steady state

$$-D_m \, d^2 C / dx^2 = \lambda (C_{sed} - C) \qquad (1)$$

where D_m is the molecular diffusion constant for Rn in the sediment, C is the concentration of Rn at any depth, x, in the sediment, C_{sed} is the concentration of radon below the zone depleted by upward diffusion and λ is the decay constant of Rn^{222}. For the boundary condition given above

$$C = C_{sed} \left\{ 1 - \exp \left(- \sqrt{\lambda / D_m} \, x \right) \right\} \qquad (2)$$

Hence, the flux, F, of radon through the interface (x=0) is

$$F = C_{sed} \sqrt{\lambda D_m} \qquad (3)$$

The standing crop, M, of radon in the overlying water column would be

$$M = C_{sed} \sqrt{D_m / \lambda} \tag{4}$$

If C_{sed} is assumed to be 4×10^{-13} gm/cm^3 (Ra^{226} equivalents) and D_m, 1×10^{-5} cm^2/sec, since λ is 2×10^{-6} sec^{-1}, a value of 9×10^{-13} gm/cm^2 (Ra^{226} equivalents) is predicted for M. As shown in Table 5 direct measurements of the standing crop of radon over trigger weight cores ranged from 1.5 to 160×10^{-13} gm/cm^2.

The next question is how this radon would be distributed in the bottom water. If it is assumed that the radon is spread upward into the water column by eddy diffusion then the distribution is given by

$$- D_e \, d^2 C^* / dx^2 = - \lambda C^*$$

where C^* equals the concentration of radon at any distance x above the bottom and De the rate of vertical eddy diffusion in the water column. Using the boundary condition that

$$(- D_e \, dC / dx)_{x=o} = F = M \lambda \tag{5}$$

we have

$$C = M \sqrt{\lambda / D_e} \exp (- \sqrt{\lambda / D_e} \, x) \tag{6}$$

or

$$\frac{A_{Rn}^{222}}{A_{Ra}^{222}} = \frac{C^*}{C_{H_2O}} = \frac{C_{sed}}{C_{H2O}} \sqrt{\frac{D_m}{D_e}} \exp \left(- \sqrt{\frac{\lambda}{D_e}} \, x \right)$$

where $A_{Rn}222$ and $A_{Ra}226$ are respectively the measured activities of radon and radium at any distance x above the bottom and C_{H_2O} is the concentration of radon at equilibrium with the dissolved Ra^{226} present in the water. Assuming M to be 9×10^{-13} gm/cm^2 expected Rn concentrations are given in Figure 6 (in Ra equivalents) as a function of distance above the bottom and for various eddy diffusion coefficients. Unless the rates of vertical mixing are either far more rapid or far slower than those generally predicted by oceanographers (i.e., D_e ranging from 0.1 to 10 cm^2/sec) measurable excesses of Rn should exist in deep ocean water.

The results for two such analyses made to date are given in Table 6. The first sample analyzed showed no measurable excess. Four possible explanations can be given: 1) vertical mixing is far too fast ($D_e > 100$ cm^2/sec)

2) vertical mixing is far too slow ($D_e < .01$ cm^2/sec), 3) the flux out of the sediment is far lower than predicted (standing crop of $< 1 \times 10^{-14}$ gm/cm^2) or, 4) rapid horizontal movement brings in water which has spent its recent history well off the bottom (as this sample was collected on the northern flank of the Puerto Rico trench horizontal motion could result in such a phenomenon). Of these 4) is perhaps the most likely candidate. The second sample, collected off Capetown, showed a measurable excess but again considerably smaller than might be expected. Further work is in progress to resolve these questions.

Water-Atmosphere Interface

Measurable deficiencies of radon should exist in the surface ocean as the result of loss to the atmosphere. The magnitude of the deficiency depends on the rate of gas exchange between the two phases and on the rate of vertical mixing in the surface ocean. The problem can be approximated by the model for gas exchange used by Bolin (1960). It is assumed that the atmosphere is an infinite radon sink and completely mixed to the interface. The main barrier to gaseous transfer is a tens of microns thick layer at the surface of the liquid through which gas is transferred only by molecular diffusion. The thickness of this layer (and hence the rate of gas exchange) depends on the rate of turbulent mixing in the underlying liquid. Mixing below this thin surface layer is by eddy diffusion.

In order to determine the distribution of the radon concentration C*, we consider the model as shown in Figure 7. In the surface boundary layer of a thickness z, the concentration C* increases from zero at the top to C_o at the bottom. Below the boundary layer the concentration C* at any depth x can be derived from the following general steady state equation.

$$D_e \, d^2 C^* / dx^2 - C^* \lambda + C_{H_2O} \lambda = 0 \tag{7}$$

where C_{H_2O} is that amount of radon at equilibrium with the Ra present and D_e and λ are the vertical eddy diffusivity in the water column and the decay constant of Rn^{222}. From this equation, the ratio of Rn^{222} to Ra^{226} activity can be written as

$$\frac{C^*}{C_{sed}} = \left(1 - \frac{C_o}{C_{H_2O}} \right) \left\{ 1 - \exp \left(- \sqrt{\frac{\lambda}{D_e}} \, x \right) \right\} + \frac{C_o}{C_{H_2O}} \tag{8}$$

The flux F of radon at depth x below the boundary layer is

$$F = D_e \, dC^* / dx = D_e (C_{H2O} - C_o) \sqrt{\lambda / D_e} \exp (- \sqrt{\lambda / D_e} \, x) \tag{9}$$

At the base of the boundary layer (hence at $x = 0$) this flux equals that through the boundary layer. In the boundary layer the flux is constant and equals $D_m C_0/z$, where D_m is molecular diffusion coefficient. Hence we have

$$D_m C_o / z = D_e (C_{H_2O} - C_o) \sqrt{\lambda / D_e} \quad (10)$$

Then the quantity C_0 can be expressed by

$$C_o / C_{H_2O} = (1 + D_m / z\sqrt{\lambda D_e})^{-1} \quad (11)$$

The activity ratio of Rn^{222} to Ra^{226} can be written as

$$C^* / C_{H_2O} = \left[D_m \left\{ 1 - \exp (- \sqrt{\lambda / D_e}\, z) \right\} + z \sqrt{\lambda D_e} \right] (D_m + z \sqrt{\lambda D_e})^{-1}$$

The typical depth profile of C^* is shown in Figure 7. In Figure 8 the relationship between the surface deficiency of radon (hence C_0/C_e) (expressed as fraction of the Ra^{226} activity) and the rates of gas exchange and vertical mixing are given. From this plot it is apparent that measurable radon deficiencies should exist in the surface ocean. By measuring the deficiency at several depths it should be possible to establish both the rate of gas exchange and the rate of vertical mixing in the surface ocean.

Although no profiles have been analyzed to date, the results on surface samples given in Table 7 clearly confirm the utility of this technique. The two samples showing the greatest deficiency were collected shortly after severe wind storms (winds up to 60 mph). Further analysis of samples from near surface profiles is currently in progress.

Radon in Shallow Waters

In areas where the ocean depth is less than 30 meters the water should certainly be influenced both by radon gain from the sediments and loss to the atmosphere. The shallow waters on the Bahama Banks (mean depth 4 meters) provide an excellent example of such a situation. Since the residence time for waters on the Banks ranges from several days to many weeks it is possible for steady state Rn^{222} concentrations to be established. If the Bank waters are assumed to be well mixed vertically then the steady state concentration of Rn in the water, C can be computed from the relationship

$$C_{sed} \sqrt{\lambda D_m}\; Z^{-1} + C_{H_2O}\, \lambda - c\, \lambda\, D_m\, c (z\, Z)^{-1} = 0$$

where the first term gives the flux into the water from the sediments (C_{sed} is the radon concentration in the pore water; D_m the molecular diffusion rate of radon in the pore water; Z the thickness of the water column; and λ the decay constant of radon); the second term the rate of production of

radon in the water column (C_{H_2O} is the concentration of radon at equilibrium with the radium present); the third term the rate of decay of radon in the water column; and the fourth, the rate of loss of radon to the atmosphere (z is, as above, the thickness of the stagnant layer). Thus,

$$\frac{A_{Rn}^{222}}{A_{Ra}^{226}} = \frac{C}{C_{H_2O}} = \frac{1 + (C_{sed} / C_{H_2O}) \sqrt{D_m / \lambda}\; Z^{-1}}{1 + D_m\ (\lambda\ z\ \ Z)^{-1}}$$

If we take C_{H_2O} as 5×10^{-17} gm/cm^3 equivalent Ra^{226} units (based on the Ra^{226} concentration data given for Bahama surface water samples in Table 1), C_{sed} as 2×10^{-14} gm/cm^3 Ra^{226} equivalent units (see Bahama Bank pore water Rn results given in Table 4), D_m as 1×10^{-5} cm^2/sec, Z as 400 cm and z as 1×10^{-2} cm (this choice yields suitable exchange rates for CO_2, Bolin, 1960), C^* is found to be 7×10^{-14} gms/liter equivalent Ra^{226} units. A Ra excess in the water of 2×10^{-14} gms/liter equivalent Ra^{226} units is thus predicted. Under these conditions two thirds of the radon added to the water comes from the sediment (the rest is produced in situ by the decay of Ra^{226}) and one half of the total radon added escapes to the atmosphere (the rest decays in situ). As summarized in Table 8 observed concentrations in areas with a sand bottom (pore water data is only available for sand bottoms) average about 20×10^{-14} gm/liter (Ra^{226} equivalent units). The difference between the prediction and observation could stem either from an over-estimate of the rate of loss to the atmosphere (if loss to atmosphere were reduced to zero the prediction would rise to 16×10^{-14} gm/l) or an under-estimate of the rate of discharge of radon from the sediment (doubling discharge would raise prediction to 12×10^{-14} gm/l). The combined effect of eliminating the loss and doubling influx is to raise the prediction to 27×10^{-14} gm/l. In any case the large excesses of radon observed in Bahama Bank waters confirms the importance of Rn loss from the sediments.

In conclusion Rn^{222} should be added to the ever growing list of natural radioisotopes which can be applied to problems in ocean circulation. In addition to estimates of the rate of vertical mixing near the top and bottom of the ocean, information regarding the rate of gaseous exchange between the ocean and atmosphere can be obtained from measurements of the ratio of Rn^{222} to Ra^{226} concentrations.

Acknowledgments

The author is grateful for the assistance of Dr. Taro Takahashi in carrying out these experiments and also for the help provided by Ross Horowitz. Financial support for this work was provided by the Atomic E Energy Commission grant AT (30-1)2493.

References

Bolin, B. (1960) On the exchange of carbon dioxide between the atmosphere and the sea. Tellus 12, 274-281.

Broecker, W. S. and T. Takahashi (in press) Calcium carbonate precipitation on the Bahama Banks. J. Geophys. Res.

Gerard, R. and M. Ewing (1961) A large-volume water sampler. Deep-Sea Research 8, 298-301.

Table 1. Ra^{226} Concentrations in Sea Water

Sample No.	Collection Date	Latitude	Longitude	Depth (m)	Ra^{222} 10^{-14} gm/l
		Caribbean Sea			
IN	2/10/61	19°N	82°W	3	5.7±1.0
IE	2/3 /61	20°N	84°W	11	5.2±0.5
IF	2/3 /61	20°N	84°W	11	4.2±0.7
IA	2/2 /61	21°N	83°W	200	4.6±0.4
IL	2/9 /61	18°N	83°W	200	6.0±0.6
IK	2/7 /61	17°N	84°W	400	6.0±0.4
IB	2/3 /61	20°N	84°W	600	7.0±0.4
IJ	2/7 /61	17°N	84°W	600	7.3±0.5
ID	2/3 /61	20°N	84°W	800	7.2±0.4
IH	2/7 /61	17°N	84°W	800	7.6±0.4
IG	2/7 /61	17°N	84°W	1000	8.2±0.7
II	2/7 /61	17°N	84°W	1350	7.3±0.5
IC	2/3 /61	20°N	84°W	3000	7.3±0.5
IM	2/9 /61	18°N	83°W	3000	7.0±0.5
		Eastern Pacific			
IIE	2/22/61	3°N	81°W	14	3.8±1.0
IIJ	3/6 /61	29°S	76°W	14	5.1±0.7
IID	2/22/61	3°N	81°W	200	6.0±1.5
III	3/6 /61	29°S	76°W	400	7.0±0.4
IIC	2/22/61	3°N	81°W	400	8.5±0.7
IIB	2/22/61	3°N	81°W	600	9.4±0.5
IIA	2/22/61	3°N	81°W	800	9.7±0.6
IIH	3/2 /61	16°S	83°W	1000	11.7±0.7
IIG	3/2 /61	16°S	83°W	1300	12.8±0.7

Table 2. Rn^{222}/Ra^{226} Ratios in Oceanic Samples from Intermediate Depth in Western North Atlantic

Collection Date	Sample No.	Sample Depth (m)	Water Depth (m)	Rn^{222} 10^{-14} equiv. gm Ra^{226}/L	Ra^{226} 10^{-14} gm/L	$\frac{Rn^{222}}{Ra^{226}}$
11/13/62	BWM#1	50	>1000	6.0±1.2	(5)	1.2±0.2
11/20/62	BWM#2	300	>1000	6.1±1.2	(5)	1.2±0.2
1/16/63	BWM#3	200	>1000	3.9±0.8	(5)	0.8±0.2
1/17/63	BWM#4	600	>1000	4.0±0.8	(5)	0.8±0.2
2/24/63	V19-8	~300	>4000	6.1±1.0	(5)	1.2±0.2
3/8 /63	V19-22	~600	>4000	6.5±1.0	(5)	1.3±0.2

Table 3. Rn^{222} Concentration in Oceanic Air

Sample No.	Location	Collection Date	Measured Rn^{222} 10^{-14} equiv. gm Ra/L
FHC-A	Frazer's Cay, Bahamas	6/14/62	0.7±0.4
FHC-B	Frazer's Cay, Bahamas	6/15/62	0.8±0.1
FHC-C	Frazer's Cay, Bahamas	6/24/62	0.6±0.1
V19-4	R. V. Vema - Ambrose Light Ship, N.Y. Harbor	2/22/62	2.3±0.3
V19-7	R. V. Vema - W.N. Atlantic	2/23/62	0.5±0.1
V19-19	R. V. Vema - W.N. Atlantic	3/7 /63	0.3±0.05
V19-21	R. V. Vema - W.N. Atlantic	3/8 /63	1.2±0.1
V19-23	R. V. Vema - W.N. Atlantic	3/11/63	0.6±0.1

Table 4. Rn^{222} Results on Sediment Pore Water Samples

Location	Sediment Type	Measurement Method*	Rn^{222} 10^{-14} equiv. gm Ra/L	Ra^{226} 10^{-14} gm/L
Bahamas	$CaCO_3$ sand	Direct	1700	8
Bahamas	$CaCO_3$ sand	Direct	2500	-
Bahamas	$CaCO_3$ sand	Direct	2400	-
Bahamas	$CaCO_3$ sand	Direct	2100	-
Bahamas	$CaCO_3$ sand	Direct	1700	-
	Red clay	Indirect	50,000	-
Off Cape-town	Glob. ooze	Indirect	30,000	-

*see text for description

Table 5. Estimates of Amounts of Radon Emanating Up Through the Sediment-Ocean Interface

Core	Material	Standing crop of Rn over sediment 10^{-14} equiv. gm Ra^{226}/cm^2
-	Red clay	120*
V19-6	Red clay	~ 80
V19-7	Red clay	~ 30
V19-14	Globigerina ooze	~180
V19-79	Red clay	~1600
V19-96	Globigerina ooze	~ 80
V19-110	-	~350
V19-121	-	~ 15
V19-127	-	~ 80
V19-150	Ash bearing lutite	~ 20
V19-154	Ash-bearing globigerina ooze	~ 70
V19-157	Ash-bearing globigerina ooze	~360
V19-166	Red clay	~200

* leakage measured over material sedimented in laboratory - all others are for undisturbed trigger weight cores.

Table 6. Rn^{222}-Ra^{226} Ratios in Oceanic Samples Taken Near Bottom

Collection Date	Latitude and Longitude	Bottom Depth (m)	Distance off Bottom (m)	Rn^{222} 10^{-14} equiv. gm Ra^{226}/L	Ra^{226} 10^{-14} gm/L	Excess Rn^{222} 10^{-14} equiv. gm Ra/L
3/ 4/63	30°28'N 70°43'W	5000	180	8	(7)	<2
3/ 5/63	28°20'N 68°06'W	5500	180	4.6	(7)	<2
3/12/63	20°13'N 66°11'W	6000	1	7.1	(7)	<2
9/14/63	35°43'S 22°53'E	1800	1	19±2	8±1	11±3

Table 7. Rn^{222}-Ra^{226} Ratios in Surface Ocean Water

Sample No.	Location	Wind Velocity	Rn^{222} 10^{-14} equiv. gm Ra/L	Ra^{226} 10^{-14} gm Ra/L *	$\frac{Rn^{222}}{Ra^{226}}$
FHC-3	Tongue of the Ocean	Normal	3.3±0.3	5.1±0.5	.65±.10
FHC-4	Tongue of the Ocean	Normal	3.3±0.3	(5.1)	.65±.10
FHC-5	Tongue of the Ocean	Normal	4.8±0.5	(5.1)	.94±.10
FHC-16	Tongue of the Ocean	Normal	5.7±0.5	5.7±0.5	1.00±.10
V19-6	North Atlantic	Normal	1.9±0.2	(5)	~ 0.4
V19-9	North Atlantic	Gale Force	1.1±0.2	(5)	~ 0.2
V19-10	North Atlantic	Gale Force	1.4±0.2	(5)	~ 0.3
V19-11	North Atlantic	Normal	2.0±0.2	(5)	~ 0.4
V19-13	North Atlantic	Normal	4.4±1.0	(5)	~ 0.9
V19-18	North Atlantic	Normal	4.5±1.0	(5)	~ 0.9

* Values in ( ) are estimates based on the results for other samples (see Table 1).

Table 8. Rn^{222} and Ra^{226} Results on Bahama Bank Waters
(See Broecker and Takahashi, in press for exact locations)

Station	Sample Depth (m)	Bottom Depth (m)	Type of Sediment	Rn^{222} 10^{-14} equiv. gm Ra/L	Ra^{226} 10^{-14} gm/L	$\frac{Rn^{222}}{Ra^{226}}$	Excess Rn^{222} 10^{-14} equiv. gm Ra/cm^2
62-35	0	2	$CaCO_3$ sand	23±2	5.4±0.5	4.3±0.5	3.8±0.4
62-35	0	2	$CaCO_3$ sand	24±2	4.2±0.5	5.8±0.6	4.0±0.4
62-37	0	3	$CaCO_3$ sand	17±2	5.0±0.5	3.4±0.4	3.6±0.5
62-30	0	4	$CaCO_3$ sand	–	5.5±0.5	–	–
62-46	0	0.7	$CaCO_3$ sand	31±3	5.0±0.5	6.2±0.6	3.7±0.4
63-5	0	5	$CaCO_3$ sand	18±2	(5)	~4	~7
63-5	5	5	$CaCO_3$ sand	19±2	(5)	~4	~7
63-7	0	4	$CaCO_3$ sand	33±3	(5)	~7	~11
63-7	4	4	$CaCO_3$ sand	18±2	(5)	~4	~5
63-12	0	3	$CaCO_3$ sand	39±4	(5)	~8	~10
63-12	3	3	$CaCO_3$ sand	20±2	(5)	~4	~5
63-24	2	4**	$CaCO_3$ sand	56±6	(5)	~11	~20
62-22	0	5	$CaCO_3$ mud	6.0±0.6	6.6±0.6	0.9±0.1	<0.5
62-17	0	6	$CaCO_3$ mud	13±1	9±1	1.5±0.2	2.4±1.2
62-36	0	6	$CaCO_3$ mud	10±1	10±1	1.0±0.2	<1.2
63-13	0	4	$CaCO_3$ mud	15±1	(7)	~2	~3
63-17	0	5	$CaCO_3$ mud	31±3	(10)	~3	~10
63-18	0	5	$CaCO_3$ mud	14±2	(10)	~1.5	~2
63-19	0	5	$CaCO_3$ mud	15±2	(10)	~1.5	~2

* Values in ( ) are estimates based on the 1962 results.
** Adjacent to very shallow waters of Brown's Cay oolite bores.

Explanation of Figures

Figure 1 Disperser adaptor designed to fit standard 20-liter flint glass bottles.

Figure 2 Fifty liter sampler designed to collect near bottom water.

Figure 3 Portable vacuum system used to extract Rn from water samples.

Figure 4 Scintillation counter used for radon counting. The 30 cm^3 pillbox is totally internally phosphored.

Figure 5a Growth curves for radon daughter products.

Figure 5b Decay curves for radon daughter products.

Figure 6 Theoretical distribution of excess radon above the ocean-sediment interface as a function of the rate of vertical eddy mixing.

Figure 7 Bolin-type gas exchange model showing the distribution of radon in the stagnant boundary layer and within the underlying eddy mixed water. The distribution depends on two parameters, the thickness of the boundary layer z and eddy diffusion rate D_e.

Figure 8 Fraction of equilibrium f_s between the Rn^{222} and Ra^{226} activities in surface sea water as a function of gas exchange rate (expressed as either the thickness of the stagnant boundary layer of Bolin or as the equivalent CO_2 exchange rate) and of the rate of vertical mixing in the surface ocean (expressed either as an eddy diffusion coefficient or as the depth at which half of the surface anomaly is removed).

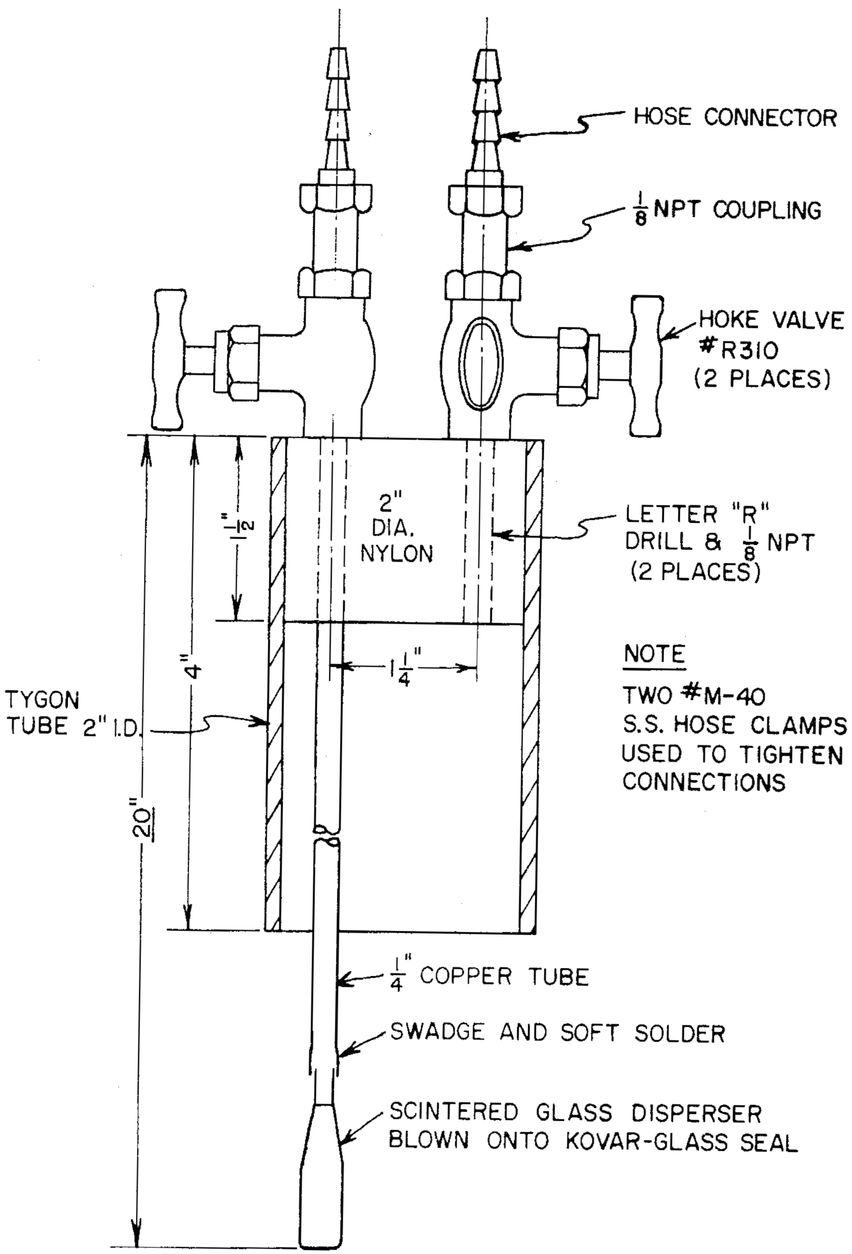

FIGURE I

136

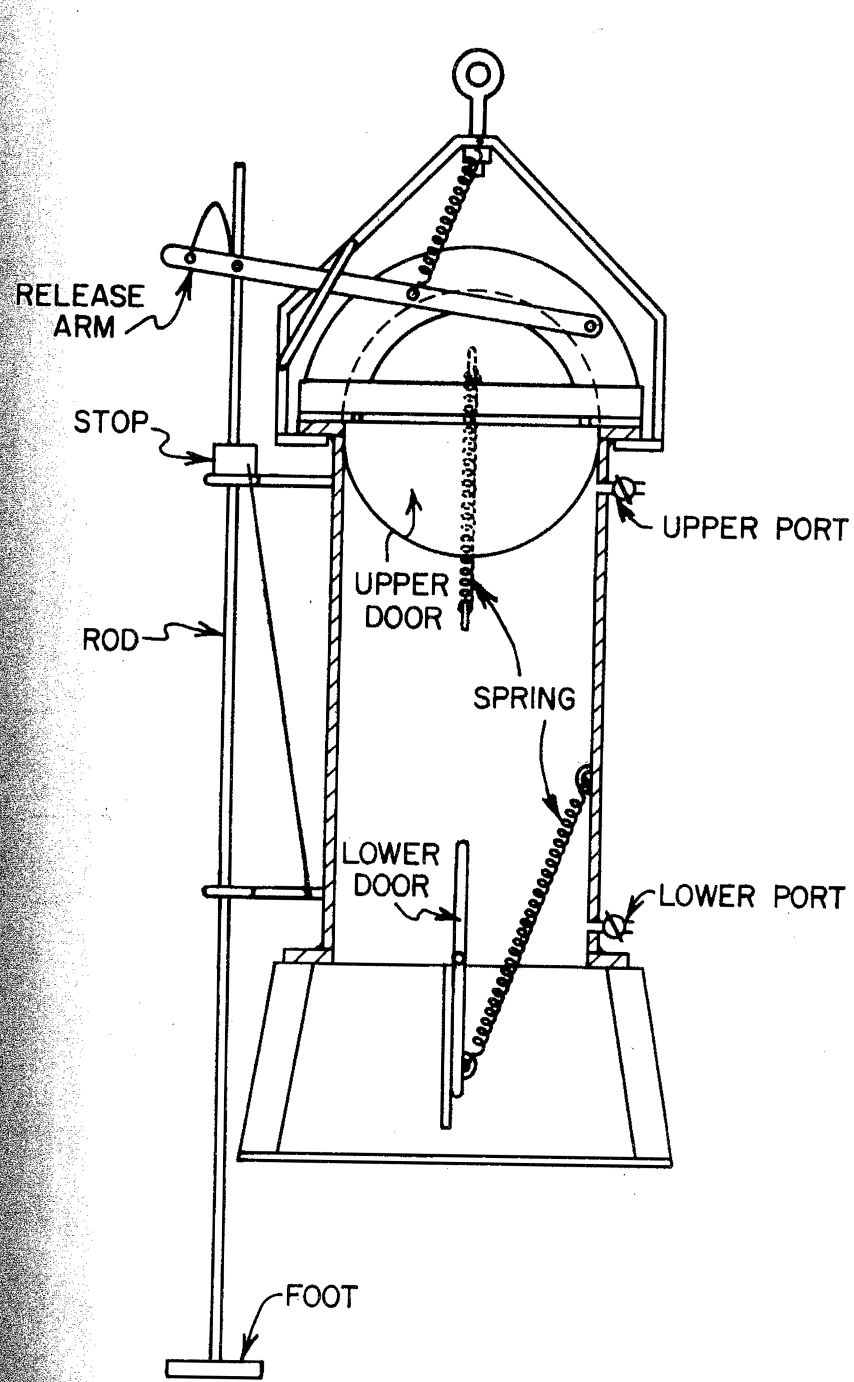

FIGURE 2

137

138

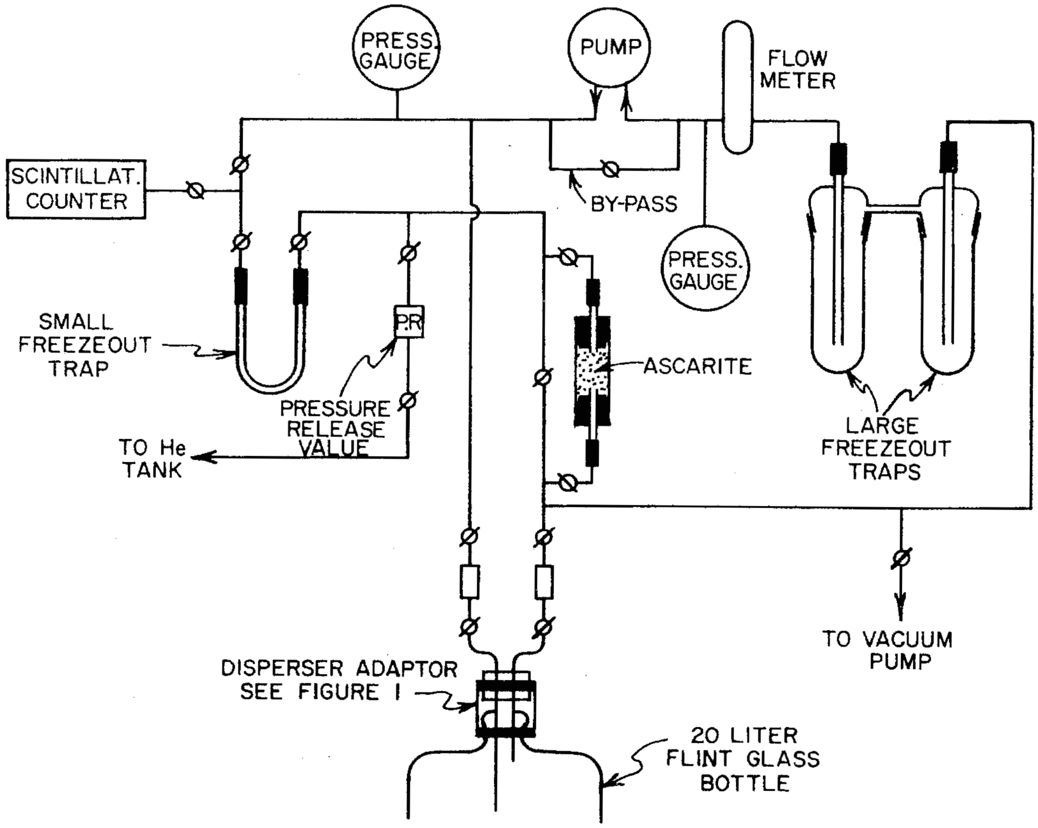

FIGURE 3

139

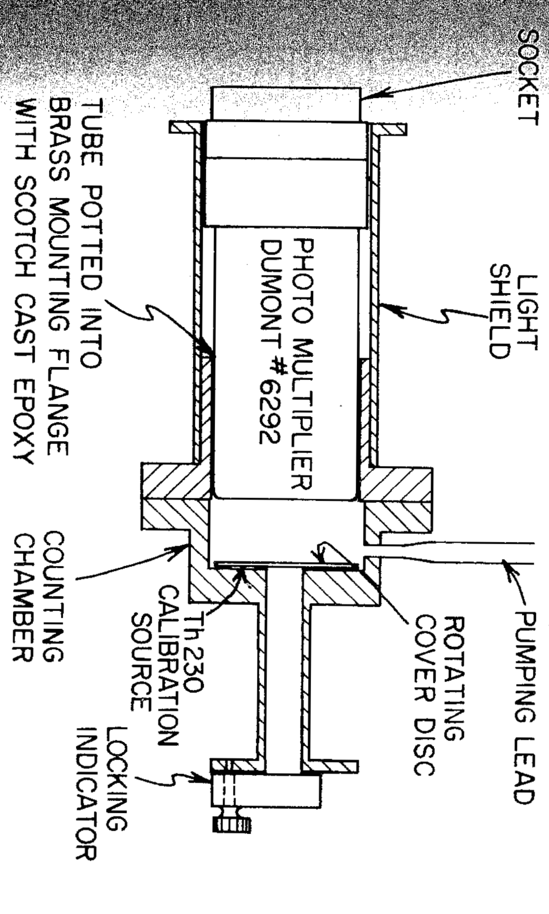

FIGURE 4

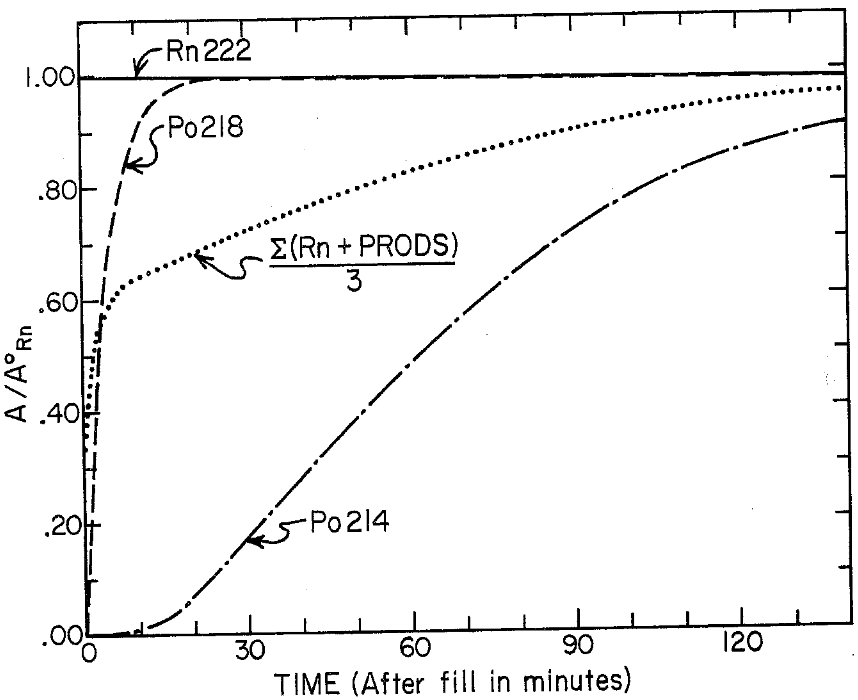

FIGURE 5a

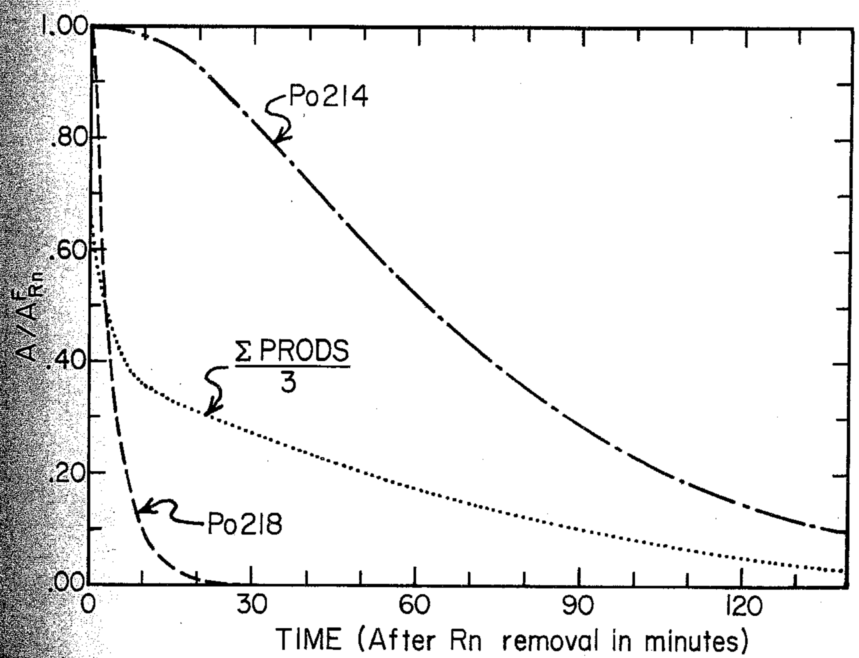

FIGURE 5b

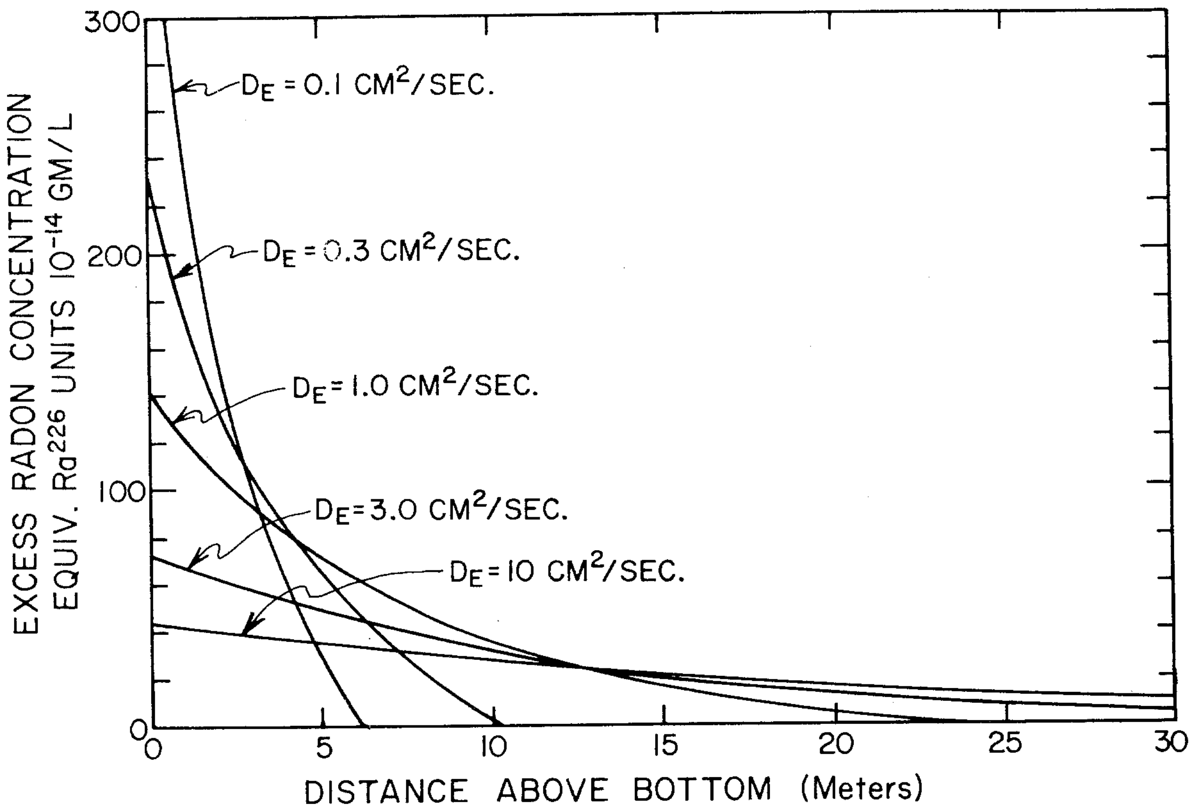

FIGURE 6

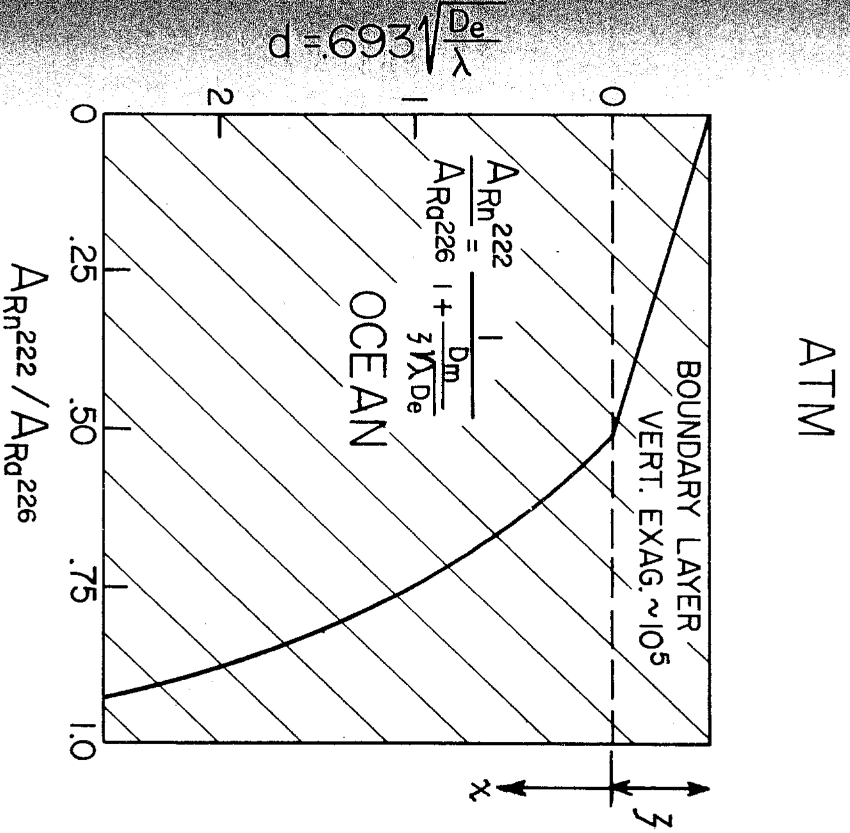

FIGURE 7

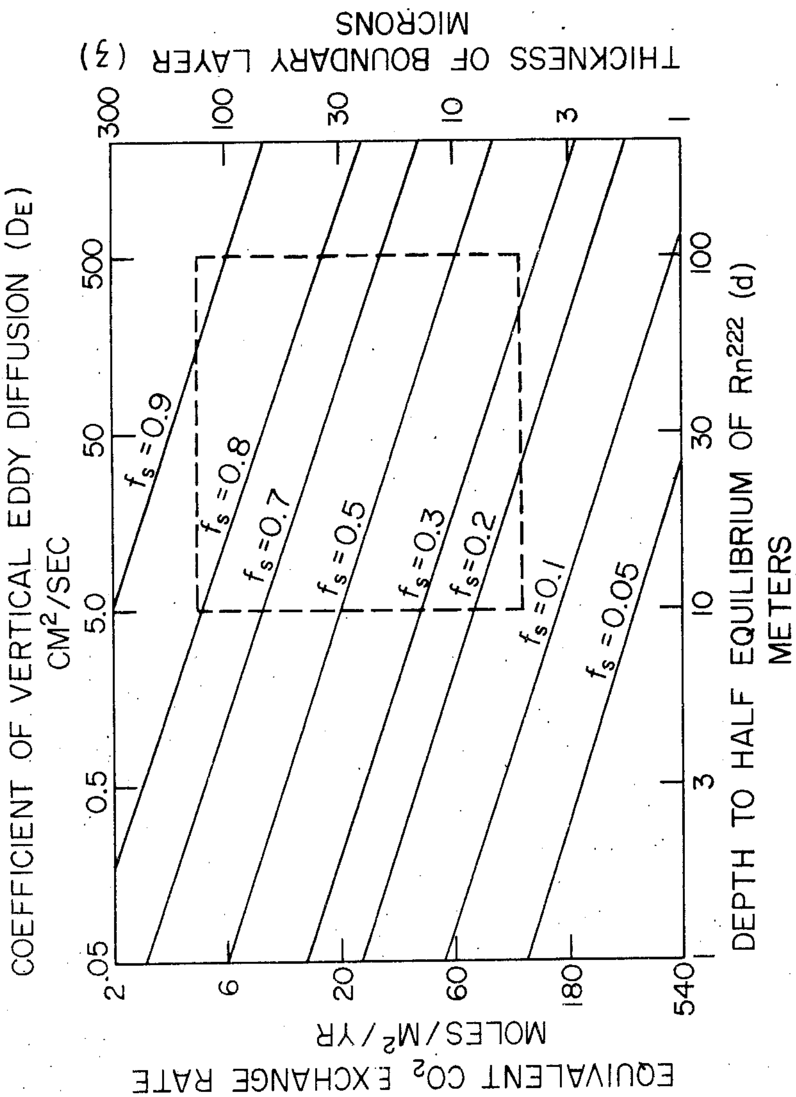

FIGURE 8

Discussion after Broecker's Paper

Question: Are radon profiles applicable to lakes?

Answer: The same complications which plagued the Bahama Bank studies will be present.

Comment: (Pochapsky) It will be advantageous to sample water without disturbing vertical arrangement of water.

Answer: Since twelve gallons of water are needed for one sampling, this would in practice be difficult.

Comment: (Kirwan) The concentration may depend on advective effects as well as diffusion.

Comment: (Ichiye) Physical oceanographers should be aware of the existence of radio-isotope data and learn to apply such data to many problems of ocean circulation. The use of data of isotopes with suitable half-lives will yield accurate determinations of sluggish deep water movement.

ON DYE DIFFUSION TECHNIQUES USED IN CHESAPEAKE BAY INSTITUTE*

D. W. Pritchard
The Johns Hopkins University, Baltimore, Maryland

The proper use and modifications of a Turner Model III fluorometer is discussed. Many workers were often forced to use more dye in fields than necessary, without taking full advantage of this instrument. Some special cares taken by CBI for this instrument are as follows:

1. The instrument has light leaks which must be covered especially for field use.

2. Field power sources need transient current suppressors for which the "sampling switch" is used at CBI as an input shunting switch to provide a zero reference line.

3. CBI makes its own special cuvettes.

The Turner fluorometer can achieve 1/2 ppb sensitivity with special care in "tuning". However, because of background variations, sensitivity of 1/2 to 1 ppb is usually used with 0.7 ppb as optimum on thirty times or full scale readings. Calibration should be made with in-situ water in the fields, with temperatures kept constant during calibration. Rubber, tygon or copper should not be used in the sampling tubing though brass pumps do not harm owing to the short contact time; instead use of glass, polyethylene or stainless steel is recommended.

Relative merits of different kinds of dyes are discussed. Rhodamine B (RB) is widely used, has relatively low cost of five dollars per pound and can use the easily available mercury 546 mμ green line as excitant, although it is somewhat lost by absorption on naturally-suspended particles. Pontacyl Pink, which is RB with the carboxyl group replaced by a sulfonic acid group, costs about three times RB, has poorer sensitivity than RB when used with a standard fluorometer. Rhodamine 5 G has an absorption band near the thorium 535 mμ line which is a narrow band, allowing low backgrounds. Emitted light is more toward the orange than RB. The advantage of this dye is that the sensitivity of a fluorometer is about three times RB yielding a detection capability of one part in 10^{12}. However, it should be used only in a place where suspended particles are small in number, since surface absorption is higher. Rhodamine W T is a new product of Dupont. Its chemical structure is not yet known but is highly sulfonated. It has the same spectral properties as RB with low absorption and good stability but it costs twice RB. Presently, it is available only in solution of density 1.2.

*(Adapted by the Editor from notes taken by G. B. Dowling)

About thirty-seven field experiments have been made by CBI in surface zone estuaries and offshore, using 50 to 100 pounds of dye (and up to 250 pounds offshore) for a tracing period of three to fifteen days. Experiments with continuously released sources were often continued for about thirty days. Experiments in the tidal regime were carried out for many tidal cycles. Some experiments have been designed to simulate sewer outfalls. In some sewerage fields, fluorescence of detergents was used to determine geometrical configuration of the plume. In plume measurements, it is necessary to obtain repeated concentration versus distance curves across the plume and to average the curves after matching the peak of each curve.

Discussion

Question - Can microdensitometry of aerial photographs be used for determining two-dimensional diffusion at the surface?

Answer - The aerial photos are affected by the three-dimensional structure of dye patches. However, when one uses the same orange filter on the camera as is used on the Turner fluorometer, the film responds to emitted light from Rhodamine B excited by sunlight yielding a picture of dye whose concentration is measurable by densitometry against a black background.

Question - What do we know about the input versus output transfer function of the Turner Model III and sampling system?

Answer- There is an averaging process which removes some of the small scale structure.

THE "NAVI-THERM" - A NEW DEVICE MEASURING SUBSURFACE TEMPERATURE UNDERWAY*
(Summary)

E.C. Brainard, III
Braincon Corporation, Marion, Massachusetts

Worthington of Woods Hole Oceanographic Institution found that the "core" or the maximum current zone (with 4.8 knot at the surface) of the Gulf Stream is approximately indicated by the 15° isotherm at 200 m depth. If a ship locates and stays in this maximum current zone by measuring temperature underway, it can save time on a northerly trip. The "Navi-Therm" provides such means. It consists of a V-FIN depressor, a thermistor and depth sensing element towed by a "Haired-Fairing" cable which reduces the drag of a cable of a given diameter by half, and a remote indicator on the bridge giving left-right steering order to the helmsman. Since the underwater unit must be towed at 60 m depth owing to towing drag, the 22.5° C isotherm is used as indicator of the core current. The system has been profitably used by tankers for over a year and Woods Hole Oceanographic Institution is obtaining a system for research purposes. Data obtained with the "Navi-Therm" indicated that the core of the Gulf Stream was about eight miles wide and deviated laterally by about eleven miles per day. Ship courses, temperatures and depth data of the Gulf Stream accumulated by use of this system will be made available to the scientific community.

* (Adapted by the Editor from notes taken by G. B. Dowling)

OCEAN WAVE BOUNDARY LAYERS*

C. E. Grosch and S. J. Lukasik
Stevens Institute of Technology, Hoboken, N.J.

(Summary)

Theoretical Aspects (Grosch) Experimental Aspects (Lukasik)

For the near-shore ocean waves, the bottom boundary layer is about 6 mm. thick. When the ratio of wave amplitude a to the water depth h is small, there is little difference in the bottom shear stress predicted by either linear or non-linear theories. For larger amplitudes, the oscillatory bottom currents can be expressed by

$$u = c\,(a/h) \sum_n A_n \cos(2n\pi/L)(x - ct)$$

where c and L are phase velocity and wave length, respectively, and

$$A_1 = 1, \quad A_2 = (3/16)\,\pi^2 (a/h)(\lambda/h)^2$$

In order that the linear theory may be valid, A_2 must be much less than unity. In the ocean waves studied by the authors, it is found that $A_2 \approx 0.02$.

A Reynolds number for waves can be defined as $R_w = L\,c/\nu$, where ν is kinetic viscosity. This parameter becomes 10^9 to 10^{10} for waves with periods 3 to 20 seconds in coastal waters. However, for the criterion of transition from laminar to turbulence of the bottom boundary layer, a different Reynolds number $R_\delta = (U_p)(38)/\nu$ must be defined, where U_p is the potential flow velocity and R_δ is the boundary layer thickness. The few available experimental data indicate that the transition occurs roughly at $R_\delta = 500$ to 1000. Calculations show that the value of $R_\delta = 10^3$ corresponds to waves of 30 cm amplitudes and 6 second periods or those of 20 cm amplitudes and 12 second period at the depth of 12 m. In the field measurement off Block Island, the value of R_δ is about 190, yielding laminar flow.

Discussions

A problem of how to handle the steady (tidal) velocity components which were included in their records was discussed. There was no direct

*(The major part of this paper was reported in "Pressure-velocity correlations in ocean swell" by S.J. Lukasik and C.E. Grosch in J. Geophys. Res. 68(20), 5189-5199. This summary describing the rest of the paper was adapted by the Editor from a note by G. B. Dowling)

measurement of such currents, although their effects were made minimal by choosing the experiment time near the slack water. Efforts were also made to cause a good agreement between measured and predicted velocity spectra by removing the amount of variances supposed to be due to the steady current.

Lukask added that they have started measurements of directional spectra of waves by use of a triangular array of sensors with one in the center.

References

Grosch, C. E. (1962) Laminar boundary layer under a wave. Physics of Fluids 5 (10), 1163-67

Grosch, C. E., L. W. Wand and S. J. Lukasik (1959) Viscous dissipation of shallow water waves. Physics of Fluids 3(3) 477-78.

Lukasik, S. J. and C. E. Grosch (1963) Laminar damping of oscillatory waves. Proc. Amer. Soc. of Civil Engrs., J. of Hydraulics Div. HYI (3405), 231-239.

Lukasik, S. J. and C. E. Grosch (1963) Pressure-velocity correlations in ocean swell, J. Geophys. Res. 68(20, 5689-99.

ATMOSPHERIC DIFFUSION*

H. E. Cramer
Round Hill Field Station, Dept. of Meteorology, Massachusetts Institute of Technology, S. Portsmouth, Massachusetts

There are a number of similarities in the two fields of research: Diffusion in Atmosphere and in the Oceans. Firstly, there is a healthy feedback between the practical aspects and the theoretical understandings. Secondly, there is heavy reliance on empiricism. Thirdly, actual physical problems are so intractable that one has often to resort to statistics.

One of the important problems is that of sources of turbulent energy. When energy spectrum of the atmospheric turbulence is determined against time scale, a spectral curve has several peaks and gaps over the period range of one second to six or more days. One special domain which is not well understood is that of internal gravity waves. Steady state conditions will be best approximated at gaps or troughs of this energy spectrum and it is necessary to know in which part of the spectrum the measurements are made.

Limitations on use of observed data for determining turbulence arise because averaging time of instruments obliterate small scale spectra features and finite record lengths limit large scale features. These two limitations may be compensated for a certain degree. It is most significant and also fortunate that in the atmosphere Langrangian and Eulerian statistics are almost equivalent.

Another significant result is that an azimuth wind direction instrument provides sensitive measurements of turbulent winds by determining fluctuations of wind directions. The applicability of this method should be tested in the oceans. A wind direction record will yield the directional spectrum and it is often possible to tell whether the wind was blowing overland or water by looking at the wind direction record. It is also possible to predict smoke plume dispersion from directional wind spectrum.

Observed spectra in atmosphere follow $k^{-5/3}$ law. The data on lateral spread of smoke plumes indicate $k^{-7/5}$ law when all such data available are put together on one graph. The structure function widely used by the Russian workers is constructed and is used for estimation of vertical momentum flux.

Discussions: Foxworthy asked about differences of lateral spread experiments

---

*(Adapted by the Editor from notes of G. B. Dowling)

utilizing continuous versus instantaneous puff sources. Cramer answered that there are indications that such experiments may not be equivalent.

Kirwan asked whether energy transfer in atmosphere occurs both to larger and smaller wave number regimes, contrary to concepts of homogeneous, isotropic turbulence. Cramer answered that it might be possible but not certainly supported by data.

References

Cramer, H. E., F. A. Record and H. C. Vaughan (1958) The study of the diffusion of gases or aerosols in the lower atmosphere. Final report under Contract No. AF 19(004)-1058, Dept. of Meteorology, M.I.T.

Cramer, H. E. et al (1962) Studies of the spectra of the vertical fluxes of momentum, heat, and moisture in the atmospheric boundary layer. Final Report under Contract No. DA-36-039-SC-80209, Dept. of Meteorology, M.I.T.

TURBULENT DIFFUSION IN SODIUM VAPOR TRAILS IN THE UPPER ATMOSPHERE*

O. R. Coté, Geophysics Corp. of America, Bedford, Mass.

Rockets were used to provide line sources of sodium vapor which was to be viewed at twilight against a dark background. The purpose was to measure large scale transport and molecular diffusivity in the upper atmosphere. Unexpected phenomena were observed in these experiments: The sodium vapor trails had turbulent appearances below about 100 km altitude but they changed to smooth cylindrical configuration above 100 km suggesting that the flow regime changed from turbulent to laminar at about 100 km height. Vertical profiles of winds showed rapid changes of speed and direction above 100 km. However, since other effects than turbulence could cause the observed effects, it is not yet conclusive whether the atmosphere near 100 km height is turbulent or not.

Also data on luminous clouds obtained by a photographic method can be analyzed quantitatively. This method could be used for photos of dye patches in the ocean with an additional advantage that the direct calibration is possible in the ocean by comparing photos with sampling of dye.

In some cases, the sodium vapor trails enlarged to an extent that outward diffusion at the outside edge become so large that the trails appeared to contract. When the initial distribution of the vapor is assumed to be Gaussian, the variances of the concentration change as the first, second or third power of time thus satisfying different theories. The results of this research have implication for large rockets, which spend relatively longer times in the atmosphere. From these results, it is concluded that horizontal eddy diffusivity is about one hundred times as large as vertical one.

F. C. W. Olson entered two pleas at the end of the session.

1. During the meeting each paper was presented with different units and conversion of units caused some confusion. It is suggested that all authors henceforth express in both English or "engineering" and metric or "scientific" units.

2. It is hoped that aerial photographs of dye experiments cited in reports will contain all pertinent photographic data in the future.

---

* Summary adapted by the Editor from notes taken by G. B. Dowling

Comments by C. G. Worrall (September 23, 1964)

We have been concerned with matching the density of dye solution to that of the water in which it is released, and were surprised to hear little mention of this problem at the meetings. If the dye solution has a density only 0.1% greater than the ambient surface water, it will tend to sink (in our local waters) to the depth of the thermocline. Although the dye may not reach this depth because of dilution, we feel that the initial vertical distribution might invalidate application of the point source condition. On the other hand, dye which is lighter than the ambient surface water in which it is released might significantly alter diffusion in the early stages. Laboratory studies have suggested that the exothermic reaction which occurs when acid rhodamine solution is introduced into the sea may create a mixture significantly less dense. Other preliminary laboratory and field experiments indicate that dyed water may undergo a greater rate of solar heating, even to depths greater than a meter, thus creating an artificial circulation as well as stability field.

There is undoubtedly a significant, but as yet undetermined relationship between stability and the magnitude of diffusion coefficients. The new instruments which continuously trace temperature and salinity as a function of depth show that density may be quite variable over small intervals of depth. Consequently, the stability determined for some level depends on the scale of the depth interval through which it was computed. Although there are regions in the ocean in which the determinations of temperature and salinity would indicate a positive stability, an obscure paper by Stommel (1962) indicates that due to the differing diffusivities of salt and heat, physical instability may exist. It has been found that a significant diurnal variation of stability usually occurs in the upper layers of the ocean. The figure below shows stabilities computed from hydrographic data obtained in July at different hours of the day in the upper ten meters of the California current. We feel such a diurnal variation of stability should be considered before hydrographic and diffusion measurements taken over a limited portion of the day are extrapolated to longer times.

We have tried two methods of introducing dye as an instantaneous point source at the surface: direct release from a ship and remote release from a container. The dye distribution can be greatly distorted by the ship's presence with direct release, and by continued flushing of residual dye with a remote release.

At the conference there appeared to be a distinct dichotomy: interests in the diffusion equations, and interest in the problems of waste disposal. Hopefully, we need not neglect basic oceanographic investigations. Such nearshore phenomena as upwellings, internal waves, rip tides, and plankton distributions may well be studied by diffusion techniques. Offshore investigations may be more amenable to comparison with diffusion theories, and may shed new light on some "classical" observations. Of special interest to us is the salinity minimum quite generally encountered offshore and classically attributed to convergence at high latitudes and advection at intermediate depths. We believe the existence of the salinity minimum may be largely attributed in certain localities to the different diffusivities of heat and salt. (Stommel, 1961 and 1962; Stern, 1960). It is also felt that the salinity minimum is often a region of anomalous instability and may result in significant upwelling when disturbed by topographic features.

References

Stern, M. (1960) The salt fountain and thermohaline convection. Tellus 12 (2), 171-175

Stommel, H. (1961) Thermohaline convection with two stable regimes of flow. Tellus 13(2), 224-230

Stommel, H. (1962) Examples of mixing and self-stimulated convection on the S-T diagram. Okeanologii (Moscow) 2 (2), 205-209.

Comments by C. G. Gunnerson (October 7, 1964)

I concur with Charles Worrall's comments on the necessity of evaluating the effects of stability upon diffusion. I was able to neglect this in the Santa Monica Bay work since we were concerned with predicting mixing rates after the initial dilution period. During this time, the effluent-sea water mixture attains density equilibrium with the surrounding waters. Some thirty-five years of studying the mechanics of initial dilution are reviewed and brought up to date by A. M. Rawn, F. R. Bowerman and N.H. Brooks, "Diffusers for Disposal of Sewage in Sea Water" Proc. Amer. Soc. Civil Engrs., 84 (SA 2) 65-105 (1960). The scale of the stirring or advective phenomena involved in the initial dilution of wastes is probably much greater than that contemplated by Mr. Worrall. Even so, the results of waste-disposal investigations can provide much of oceanographic interest.

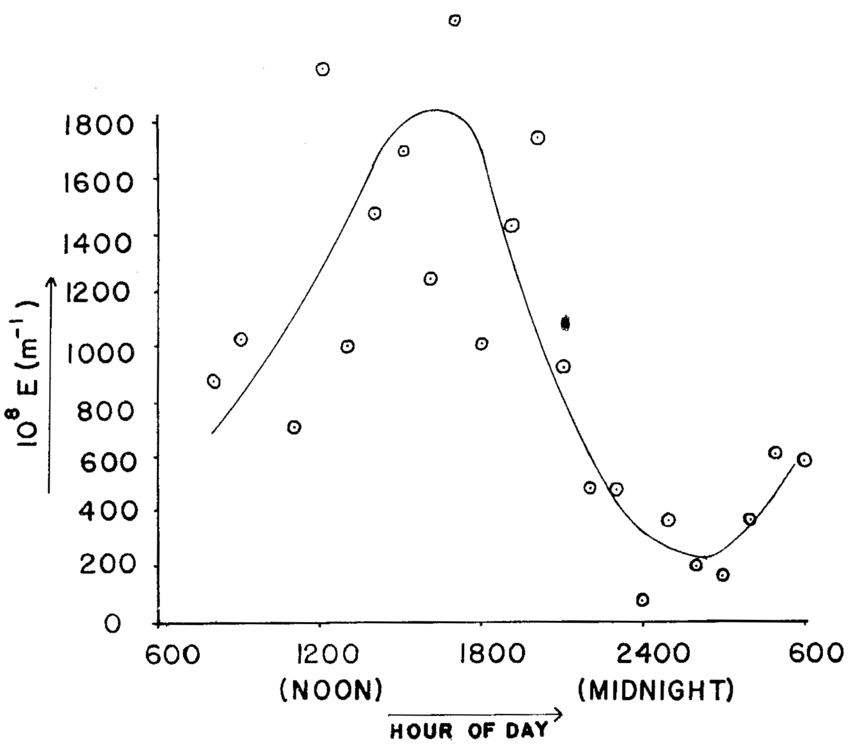

Average Stabilities at Different Hours of the Day in the Upper Ten Meters

(From CALCOFI Data, July, 1959)

Addenda

Since editing these proceedings first started, there have been several changes in the publication plan, particularly in the printing format. Therefore, some authors were asked to rewrite their manuscripts or to revise their illustrations. Minor revisions of most of the papers were made by the editor with the diligent assistance of J. E. Breeding.

A number of papers on diffusion in oceans and fresh waters were published since the inception of this symposium. In order to update these proceedings, an annotated bibliography of some of these papers has been prepared and listed below.

Bowden, K. F. (1965) Horizontal mixing in the sea due to a shearing current. J. Fluid Mech. 21(1). 83-96

The effective coefficient of horizontal diffusion is defined as the ratio of the mean total transport across a vertical section minus the advection by the mean flow to the horizontal gradient averaged vertically. In general, this coefficient is inversely proportional to the vertical eddy diffusivity. This coefficient is determined for several models of horizontal velocities with different vertical profiles including logarithmic, parabolic and Ekman spiral profiles, both in an alternating flow such as tidal current and in a steady flow. Application of the result to dye patches is suggested. The effective coefficients determined from distributions of salinity in the estuaries of the Severn, the Mersey and Liverpool Bay are 10^5 to 10^6 cm^2/sec.

Csanady, G. T. (1963) Turbulent diffusion in Lake Huron. Journ. Fluid Mech. 17(3) 360-384

Diffusion of small floating objects and of Rhodamine B dye from a constant source has been studied in Lake Huron. The dispersal of floating objects was influenced by surface confluences, slicks and windrows. Without these disturbing effects, the rate of diffusion of floating objects and of dye perpendicular to the mean current increases with the size of the diffusing cloud. Vertical diffusivity determined was low and about ten times the molecular constant. Meandering of the dye plume seemed to be a more important agency than relative diffusion in dispersing dye over a large area.

Csanady, G. T. (1965) Hydrodynamic studies on Lake Huron at Baie du Dore, summer, 1964. Diffusion Studies. Report No. PR 19, 85-101. Water Resources Inst., Univ. of Waterloo and Great Lakes Inst., Univ. of Toronto.

Experiments on diffusion of dye plumes in the summer of 1964 in Lake Huron are discussed. The vertical eddy diffusivity ranged from 1 cm^2/sec on a calm day to 20 cm^2/sec on windy days. On windy days turbulence was generated both by shear of the wind-driven currents and by thermal instability due to surface cooling.

Faller, A. J. (1964) The angle of windrows in the ocean. Tellus 16 (3), 363-370

Windrows were observed from lines of foam and from streaks of sheets of paper or of insulation material either with small boats or airplanes. The angle of windrows with respect to the wind direction is about thirteen degrees. From this angle and data of row spacings, it is discussed that the windrows are produced by shear-flow instability in the Ekman boundary layer.

Ichiye, T. (1965) Experiments and hydrographic surveys off Sandy Hook, New Jersey, 1963. Tech. Rept. CU-2663-18 and CU-266(48)-11 of Lamont Geological Observatory, pp 22.

Dye diffusion experiments in summer and fall of 1963 off Sandy Hook are discussed. Spectrum of mean square deviations of concentration in relation to dye diffusion is determined.

Isayeva, L. S. and I. L. Isayev (1964) One of the methods of determining vertical eddy diffusivity in the sea. Trudy Morskovo Gidrofiz. Inst. 30, 41-45 (English Transl. Soviet Oceanog. 1964 No. 2, 31-34).

A solution of the diffusion equation for an instantaneous point source yields the eddy diffusivity (assumed to be constant) as proportional to ratio of the square of a distance between the point considered and the source to the time of appearance of maximum concentration. The rule is applied to determine eddy diffusivity in the ocean by measuring dye concentration continuously with a photo-cell at a fixed distance from a dye source. The whole system including a measuring unit and a dye source can be suspended from a boat or a buoy. The vertical eddy diffusivity measured with this device ranges from 0.7 to 4 cm/sec for protected areas and 15 cm/sec for open seas.

Joseph, J., H. Sendner and H. Weidemann (1964) Untersuchungen über die horizontale Diffusion in der Nordsee. Deutsche Hydrog. Zeits. 17(2), 57-75.

Dye diffusion techniques were utilized at three stations of 40 to

65 m depths in the German Bight. Instrumentation for measurement of dye and field techniques for tracking dye patches only with one ship are explained. The dye patches made of 175 to 450 kg. of Rhodamine B were tracked for three to five days and their radius increased to 3 to 4 km at the end of tracking. Vertical profiles of concentration showed that halocline or a thermocline inhibits vertical diffusion. Diffusion velocities (horizontal) determined by these experiments were 0.2 to 0.4 cm/sec.

Katz, B., R. Gerard and M. Costin (1965) Response of dye tracers to sea surface conditions. J. Geophys. Res. 70 (22). 5505-5514

Aerial photographs of dye patches have revealed features of the surface circulation: elongation and striations of patches nearly parallel to the wind and a spiral pattern similar to a hodograph of the surface Ekman current.

LIST OF PARTICIPANTS

Symposium on Diffusion in Oceans and Fresh Waters
Lamont Geological Observatory, Palisades, New York
August 31 thru Sept. 2, 1964

Bailey, James F., U. S. Geological Survey, Arlington Towers, Va.
Benoit, Dr. R. J., General Dynamics Electric Boat, Groton, Conn.
Bloom, Justin L., U. S. Atomic Energy Commission, Washington, D. C.
Brainard III, Edward C., Braincon Corp., P. O. Box 267, Marion, Mass.
Carter, H. H., Chesapeake Bay Inst., Johns Hopkins Univ., Baltimore, Md.
Clark, R. M., U. S. Public Health Service, Raritan Bay Project, Metuchen, New Jersey.
Cote, Dr. Owen R., Geophysics Corp. of America, Bedford, Mass.
Cramer, Dr. H. E., Mass. Inst. of Ocean., Applied Ocean. Group, San Diego, California
Crew, Henry, Scripps Inst. Of Ocean., Applied Ocean. Group, San Diego, California
Dextrage, R. E., Braincon Corp., P. O. 267, Marion, Mass.
Dowling, George B., U. S. N. Mine Defense Lab., Panama City, Florida
Elder, Robert B., U. S. N. Ocean. Off., Washington 25 D. C.
Farlow, John S., U. S. Public Health Service, 1819 W. Pershing Road, Chicago, Illinois
Forrest, William E., U. S. Geological Survey, P.O. Box 37, College Park, Maryland
Foxworthy Dr. J. E., Hancock Foundation, Univ. of Southern California Los Angeles, California
Gallagher, Brent, Scripps Inst. of Ocean. Applied Ocean. Group, San Diego, California
Grosch, Chester E., Stevens Inst. of Tech., Hoboken, New Jersey
Gunnerson, Charles G., U. S. Public Health Service, 1014 Broadway, Cincinnati, Ohio
Hetling, Leo J., U. S. Public Health Service, Chesapeake Field Station Box 20-A, R R 1, Annapolis, Maryland
Kaulum, Keith, Naval Rad. Def. Lab., San Francisco, California
Kirwan, Jr., Dr. A. D., New York University, Bronx, N.Y.
Kisiel, Prof. Chester C., Univ. of Pittsburgh, Civil Engineering Dept., Pittsburgh, Pennsylvania
Lukasik, Prof. Stepnen, Stevens Institute of Technology, Hoboken, N.J.
Martineau, Donald P., Office of Naval Research, Washington 25, D. C.
Mehr, E., New York University, Bronx , New York
Meyer, Eric H., U. S. Geological Survey, Washington 25 D.C.
Mongovan, H. E. American Cyanamid Company, 111 W 50th Street, N.Y.C.
Neumann, Prof. G., New York University, Bronx 53, N.Y.
Ochinero, Robert V., National Oceanographic Data Center, Washington, D.C.

LIST OF PARTICIPANTS (Cont'd.)

O'Connell, Richard L., U. S. Public Health Service, Chesapeake Field Station, Box 20A RR #1, Annapolis, Maryland
O'Connor, Prof. Donald J., Manhattan College, Riverdale 71, New York
Okubo, Dr. Akira, Chesapeake Bay Inst., Johns Hopkins, Univ. Baltimore, Maryland
Olson, Dr. F. C. W., U. S. N. Mine Defense Lab., Panama City, Florida
Olson, Martha A., Naval Rad. Def. Lab., San Francisco, California
Oshiver, Albert H., U. S. Coast and Geodetic Survey, Washington 25, D.C.
Pagden, I.M.H., Bedford Inst. of Ocean., P.O. Box 1006, Dartmouth, Nova Scotia, Canada
Parke, Dale B., U.S. Public Health Service, Raritan Bay Project, Metuchen, New Jersey
Pochapsky Dr. T. E., Hudson Laboratories, Dobbs Ferry, New York
Pritchard Prof. Donald W., Chesapeake Bay Inst., Johns Hopkins Univ., Baltimore, Maryland
Reinert, Richard, New York University, Bronx, New York
Scholl, William H., G.K. Turner Asso, 2524 Pulgas Ave., Palo Alto, Calif.
Shonting, David H., Naval Underwater Ordnance Stn., Newport, R. I.
Smith, Paul F., Geodyne Corp., 23 Water Street, Woods Hole, Mass.
Stevens, Richard, Office of Naval Research, 207 W. 24th Street, N.Y.C.
Wennekens Dr. Pat M., Office of Naval Research, 1000 Geary Street, San Francisco, California
Wilson, Jr. James F., U. S. Geological Survey, Code 40435402, Washington D. C.
Worrall, Charles, Scripps Institution of Oceanography, La Jolla, Calif.

From Lamont Geological Observatory

Dr. Wallace Broecker (Geochemistry)
J. Michael Costin (Oceanography)
Dr. Charles L. Drake (Oceanography)
Dr. Maurice Ewing (Director)
Dr. Arnold L. Gordon (Oceanography)
Paul Hale
Dr. Kenneth Hunkins (Seismology)
Bernard Katz (Oceanography)
Thomas Pauls (Oceanography)

General Management

Dr. Takashi Ichiye ((Oceanography)
Noel B. Plutchak (Oceanography)

Index of Authors

BARSON, G., 71
BRAINARD, E. C., 148
BROECKER, W. S., 116
COSTIN, J. M., 68
COTE, O. R., 153
CRAMER, H. E., 151
DiTORO, D. M., 80
FORREST, W. E., 1
FOXWORTHY, J. E., 71
GROSCH, C. E., 149
GUNNERSON, C. G., 53
ICHIYE, T., 54
KIRWAN, A. D., 86
KISIEL, C. C., 28
LUKASIK, S. J., 149
McCULLOUGH, C. A., 53
O'CONNOR, D. J., 80
OKUBO, A., 74
POCHAPSKY, T. E., 112
PRITCHARD, D. W., 146
REINERT, R. L., 19
SHONTING, D. H., 93
TIBBY, R. B., 71
WENNEKENS, M. P., 108
WILSON, J. F., 1
WORRALL, C. G., 154

Subject Index

Aerial photograph, 22, 23, 54, 56, 63, 68
Anisotropic mixing, 38
    eddies, 74
Antarctic Intermediate Water, 88
Argentine coast, 58, 63
Atmospheric diffusion, 151
    in upper atmosphere, 153
Bahama Banks, 54, 56, 68, 76, 117, 124
Boundary layers:
    ocean bottom, 149
    ocean surface, 58, 95
Buzzards Bay, 101
Cape Kennedy, (Canaveral) 63, 77
Chesapeake Bay Institute, 146
Cloud of dye, 35, 36
Conservative waste, 29
Continuity equation, 80
Curvature of dye patch, 57, 59
Decay rate of dye, 53
Delaware River model, 85
Densitometer, 60, 143
Density of dye solution, 154
Diffusing particles in the deep oceans, 112
Dilution capacity, 28
Dispersion of small particles, 23,157
Doppler navigator, 20
Ducted current meter, 94
Dye plume, 20, 30, 37, 157
East River, 85
Eddy diffusivity, 29, 74, 76, 92, 153 159
    vertical, 122, 158
    effective horizontal, 157
Eddy viscosity, 58, 59
Ekman spiral, 58, 157, 159
Elongation of dye patch, 56, 159
Estuary, 80, 157
Fickian mathematical model, 29, 37, 56
Floats, neutrally-buoyant, 112
Four-thirds power law, 30, 72, 112, 113
Fluorometer, 4, 21, 31, 53, 68, 146
    deep-towed, 68
    in situ, 69
Friction depth, 58
Gifford's model, 72
Helical vortices, 57
Interleaf, 109
Inertial sub-range, 55, 114
Internal waves, 112, 151
James River, 85
Kolmogoroff's theory, 30
KYMA, 20,
Laboratory flume, 29, 30
Lake Huron, 157
Long Island Sound, 19
    off Long Island, 54
Longitudinal convection, 30
    dispersion, 6, 8, 157
Mixing coefficient, 36, 90
Momentum flux in ocean waves, 93
Multi-dimensional diffusion, 71, 72
Narragansett Bay, 94
Navi-therm, 148
New Jersey coast, 54, 56, 158
New York Bight, 58
North Sea, 158
Oceanic microstructure, 108
Ohio River, 28, 31
Pearson Type III statistical distribution, 6
Point source
    continuous 19, 71, 151
    instantaneous, 20, 74, 80
Pontacyl Brilliant Pink B, 4, 53, 146
Potomac River
    Basin, 2, 7
    Time-travel-measurements, 1
Puerto Rico Trench, 123

Radon
- sampling techniques, 117
- counting of, 118
- Pore water analysis of, 120
- flux, 120
- concentration of, 121

Rayleigh-Ritz method, 86
Reynolds number, 55
- of bottom boundary layers, 149

Reynolds stress, 94, 102
Rhodamine
- B, 1, 21, 31, 53, 54, 146 157, 159
- BA, 4
- 5Q, 146
- WT, 4, 146

Roll-type instability, 57
Sampler for 50-liter water, 117
Sewage discharge, 73, 85
Shearing deformation, 74, 75
Sodium vapor trails, 153
Southern California, 71
Spectra
- auto-covariance, 100
- covariance, 96, 102

Spectral analysis, 94
Statistical theory of turbulence, 31, 60, 151
Stretching deformation, 74, 75
Striations, 22, 56
SVTP (sound velocity, temperature, pressure) instrument, 108
T^3-law, 56
Transport equation, 74
Travel time, 1, 8, 9, 35
Turbulimeter, 60
Two-particle model, 55
U. S. Geological Survey, 1, 9
Variational form of diffusion equation, 86
Vertical stability, 92, 154, 155
Waste disposal, 28
Windrows, 157, 158
Wind stress, 94

Printed by Ruddell-Conte Press, Nyack, N.Y.